Molecular characterization of Ptf1a activity during *Xenopus* embryogenesis

Doctoral Thesis

Dissertation for the award of the degree
"Doctor rerum naturalium (Dr. rer. nat.)"
in the GGNB program "Genes and Development“
at the Georg August University Göttingen
Faculty of Biology

submitted by
Marie Charlotte Hedderich
born in Marburg, Germany

Göttingen, August 2012

Members of the Thesis Committee:

Dr. Kristine A. Henningfeld (Supervisor)
Department of Developmental Biochemistry, University of Göttingen

Prof. Dr. Andreas Wodarz (Reviewer)
Department of Stem Cell Biology, University of Göttingen

Prof. Dr. Anastassia Stoykova
Department of Molecular Cell Biology/Molecular Developmental Neurobiology/Max Planck Institute for Biophysical Chemistry

Prof. Dr. Tomas Pieler (Reviewer)
Department of Developmental Biochemistry, University of Göttingen

Date of the oral examination: 18.10.2012

Affidavit

Herewith, I declare that I prepared the PhD thesis

"Molecular characterization of Ptf1a activity during *Xenopus* embryogenesis"

on my own and with no other sources and aids than quoted.

Submission date
Göttingen, 31.08.2012

Marie Charlotte Hedderich

Table of Contents

Acknowledgements

First of all, I would like to thank Dr. Kristine Henningfeld for her great supervision, her support and advice, which guided me during this thesis.

Furthermore, I would like to thank Prof. Pieler for his support in many ways, including fruitful discussions and helpful suggestions.

In addition, I would like to thank Prof. Wodarz and Prof. Stoykova for being part of my thesis committee and for providing me with advice and ideas. I also thank Prof. Bucher, Prof. Doenecke and Dr. Prpic-Schäper for being part of my extended thesis committee.

Furthermore, I would like to thank Katja Ditter, Patrick Rolf Berndt, Maja Gere and Juliane Melchert for the nice working atmosphere and for the help during all the experiments. I also would like to thank Lennart Opitz and Dr. Gabriela Salinas-Riester for the extensive help with the RNA-sequencing.

My special thanks go to my family, who always supported and encouraged me throughout my life.
Finally, I would like to especially thank Reinhard Spiekermann for his patience, his support and motivation.

Abstract

A balance between inhibitory and excitatory neurons is essential for the establishment of a functional vertebrate nervous system. A key factor in regulating this balance is the bHLH transcription factor Ptf1a, which promotes a GABAergic inhibitory neuronal identity at the expense of a glutamatergic excitatory neuronal identity in the vertebrate retina, hindbrain and spinal cord. In this context, the activity of Ptf1a requires formation of a trimeric complex, in which Ptf1a binds to a commonly expressed bHLH E-protein and to a member of the Su(H) family. Ptf1a has also been shown to promote general neuronal differentiation in *X. laevis* embryos and explants, suggesting that Ptf1a has proneural activity.

In this thesis work, the role of Ptf1a in the context of both general neurogenesis (early function) and neuronal subtype specification (late function) was investigated. Through the temporal expression analysis of known genes, Ptf1a was shown to drive neurogenesis in animal caps (naïve ectoderm) at early time points through the activation of downstream target genes similar to the proneural transcription factor Ngn2. However, at later stages, Ptf1a activated marker gene expression indicative of GABAergic neurons, while glutamatergic neuronal markers were induced by Ngn2. A mutant version of Ptf1a ($Ptf1a^{W224A/W242A}$), that is unable to interact with the cofactor Su(H), maintained the ability to drive general neurogenesis, but was unable to activate GABAergic marker genes. These findings suggest that Ptf1a forms context specific transcription complexes during the development of the nervous system: a Su(H)-independent complex to drive general neurogenesis and Su(H)-dependent complex to specify GABAergic neurons.

As target genes of Ptf1a during the development of the nervous system are not well defined, two independent whole transcriptome analyses were conducted to elucidate the genetic network downstream of Ptf1a. In these assays, a temporal analysis of genes induced by wild-type Ptf1a, $Ptf1a^{W224A/W242A}$ and Ngn2 in *X. laevis* animal caps was performed; direct targets for Ptf1a and Ptf1a/Su(H) were determined by activation of these transcription factors in the presence of an inhibitor of protein synthesis (CHX). Through this approach, many putative

novel early and late Ptf1a target genes were identified. Further analysis of these downstream targets will give insight into how Ptf1a regulates general neurogenesis and neuronal subtype specification.

List of Figures

List of Tables

Abbreviations

A	Alanin
AP	alkaline phosphatase
aa	amino acid
BCIP	5-bromo-4-chloro-3-indolyl-phosphate
bHLH	basic-helix-loop-helix
BMB	Bohringer Mannheim blocking reagent
BMP	bone morphogenetic protein
bp	base pairs
BSA	bovine serum albumin
°C	Celsius degree
cDNA	complementary DNA
CHX	cycloheximide
CIAP	calf intestine alkaline phosphatase
Dex	dexamethasone
Dig	dioxigenine
DNA	desoxyribonucleic acid
DNAse	desoxyribonuclease
DTT	1,4-dithiothreitol
EDTA	ethylendiaminetetraacetic acid
EGTA	ethylenglycole-bis(2-aminoethylether)-N,N'-tetraacetate
et al.	*et alii*
EtOH	ethanol
Gad1	glutamatic acid decarboxylase
h	hour/hours
HCG	human chorionic gonadotropin
H_2O	water
is	injected side
k	kilo
kb	kilobase
l	liter
LB	Luria-Bertani

µ	micro
m	milli
M	molar
MAB	maleic acid buffer
MEM	MOPS-EGTA-$MgSO_4$ buffer
MEMFA	MOPS-EGTA-$MgSO_4$ formaldehyde buffer
min	minutes
mRNA	messenger RNA
n	Nano, number
NaAC	sodium acetate
NBT	nitro-blue-tetrazolium
Ngn	neurogenin
Ngnr	neurogenin-related
nm	nanometer
OD	optic density
PAGE	polyacrylamid gel electrophoresis
PBS	phosphate buffered saline
PCR	polymerase chain reaction
pH	negative decade logarithm of hydrogen ion concentration
%	percentage
PTF1	pancreas transcription factor complex 1
Ptf1a	pancreas transcription factor 1a
RNA	ribonucleic acid
RNase	ribonuclease
rpm	rounds per minute
RT	room temperature, reverse transcriptase
RT-PCR	reverse transcriptase PCR
SDS	sodium dodecyl sulfate
sec	second
SHH	Sonic Hedgehog
SSC	standard saline citrate buffer
st	stage
T_A	annealing temperature

Taq	*Thermus aquaticus*
T_m	melting temperature
U	units
V	voltage
Vol.	volume
W	Tryptophan
wmish	whole mount *in situ* hybridization
X-Gal	5-bromo-4-chloro-3-indolyl-β-d-galactoside

1. Introduction

1.1 Neurogenesis

A primary aim in the field of neurobiology is the development of therapeutic treatments for neurodegenerative and other neurological diseases. Many promising strategies are based on the manipulation of cells *in vitro* and *in vivo*. It is therefore essential to understand the molecular mechanisms by which a progenitor cell acquires a neuronal fate and subsequently obtains a specific neuronal subtype identity.

The African clawed frog *Xenopus laevis (X. laevis)* is an ideal vertebrate model organism to study the development of the vertebrate nervous system. The first primary neurons are born in the open neural plate in a relative simplistic pattern (Hartenstein, 1989; Chitnis et al., 1995). Moreover, owing to the external development, the earliest stages of embryogenesis are easily accessible for manipulations, such as microinjection of DNA, mRNA or antisense morpholino oligonucleotides. In addition, explant and transplantation experiments are easy to perform. The animal caps are pluripotent embryonic cells derived from the ectoderm of blastula stage embryos and are an attractive system to study *in vitro* differentiation (Borchers and Pieler, 2010). As the *X. laevis* genome is partially tetraploid, the closely related species *Xenopus tropicalis (X. tropicalis*) is increasingly being used as it has a sequenced diploid genome (Amaya, 2005; Hellsten et al., 2010; Harland and Grainger, 2011). However, routine use of *X. tropicalis* as a model system is hindered by the faster development of early cleavage stages and the more difficult cultivation of the embryos.

1.2 Neural induction

The development of the nervous system begins with the process of neural induction, during which ectodermal cells become committed to a neural cell fate (Rogers et al., 2009b). *X. laevis* explant experiments demonstrated that the neural fate of ectodermal cells is specified during gastrulation. While ectodermal explants (animal caps) of blastula stage embryos develop into epidermal tissue, those from gastrula stage embryos give rise to neural tissue

(Hamburger, 1969; Sanes, Reh and Harris, 2006). However, upon dissociation of *X. laevis* blastula ectodermal explants, cells obtain a neural instead of an epidermal fate, implicating that in the absence of cell-to-cell signalling a neural fate is specified (Godsave and Slack, 1989; Grunz and Tacke, 1989; Sato and Sargent, 1989; Wilson and Hemmati-Brivanlou, 1995) (Fig. 1.1). This is further supported by the rescue of an epidermal cell fate in dissociated cells when cultivated in the presence of BMP-4 (Wilson and Hemmati-Brivanlou, 1995) (Fig. 1.1). Similarly, upon overexpression of a dominant-negative activin receptor, animal caps also acquire a neural fate, further indicating that inhibition of the TGF-beta signalling-pathway is required for neural cell fate determination (Hemmati-Brivanlou and Melton, 1994) (Fig. 1.1). These initial experiments led to the so called 'default model', suggesting that the neural identity of dorsal ectodermal cells is the 'default' state and that BMP-signalling must actively be inhibited.

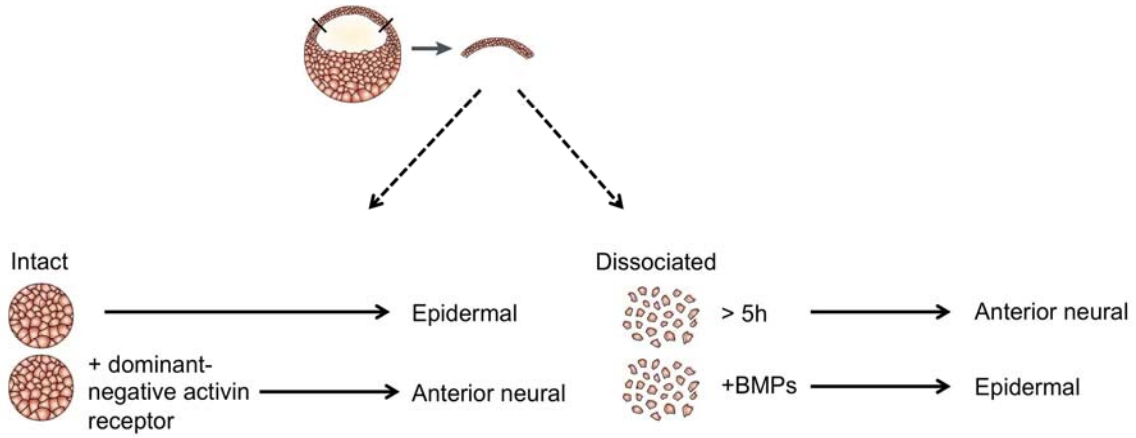

Figure 1.1 Schematic representation of experiments supporting the 'default model' of neural induction.
Ectodermal explants (animal caps) excised from the animal pole of *X. laevis* blastula stage embryos, develop into atypical epidermis. However, upon overexpression of a dominant-negative activin receptor or dissociation of the animal caps, the cells acquire a neural cell fate. An epidermal cell fate can be restored, if dissociated animal caps are cultivated in the presence of BMPs. (Muñoz-Sanjuán and Brivanlou, 2002, modified)

Several BMP-antagonists including *Chordin* (Piccolo et al., 1996; Sasai et al., 1994), *Noggin* (Zimmerman et al., 1996; Lamb et al., 1993) and *Cerberus* (Bouwmeester et al., 1996; Piccolo et al., 1999) have been identified. These factors all have neural inducing activity and are expressed in the Spemann Organizer, which during gastrulation involutes and underlies the prospective neuroectoderm. Moreover, they are all secreted factors that inhibit BMP-signalling by binding BMP-molecules in the extracellular space and prevent

receptor activation (Fig. 1.2). BMP activity is further attenuated by FGF-signalling (Furthauer et al., 1997; Wilson et al., 2000), which inactivates Smad1 (Fig. 1.2), an intracellular effector of the BMP-pathway (Pera et al., 2003).

The 'default model' of neural induction remains controversial as several experimental findings, particularly in higher vertebrates, are inconsistent with this hypothesis. In this regard, individual knock-out mice of the neural inducer molecules *Noggin*, *Chordin* or *Follistatin* show no defect in neural induction (Bachiller et al., 2000; Bachiller et al., 2003; Matzuk et al., 1995; McMahon et al., 1998). However, functional redundancy of the multiple neural inducer molecules cannot be excluded. Furthermore in chick, the BMP-inhibitors are not sufficient to induce neural cells in epidermal or extra-embryonic ectodermal tissue and their temporal expression pattern does not coincide with the ability of the chick organizer to induce neural cells (Wilson and Edlund, 2001; Wilson et al., 2000; Streit et al., 1998; Storey et al., 1992; Levin, 1998). In summary, these data indicate that an inhibition of BMP-signalling alone is not sufficient to induce neural fate.

Several experiments implicate a role for FGF-signalling in neural induction, independently from its function to attenuate BMP-signalling. In *X. laevis*, experiments demonstrated that the induction of neural cell fate in non-neural ectoderm requires both, inhibition of BMP-signalling and active FGF-signalling (Wawersik et al., 2005; Delaune et al., 2005; Linker and Stern, 2004). This notion is further supported by the fact that in *X. laevis* and chick, blockage of FGF-signalling disturbs neural development (Streit et al., 2000; Hongo et al., 1999) and that overexpression of a dominant-negative FGF-receptor renders Noggin and Chordin unable to induce neural cell fate (Launay et al., 1996; Sasai et al., 1996). FGF alone is also able to induce ectopic expression of neural markers in *X. laevis* ectodermal cells as well as in chick epiblast cells (Lamb and Harland, 1995; Kengaku and Okamoto, 1995; Storey et al., 1998; Alvarez et al., 1998).

In addition to FGF-signalling and inhibition of the BMP-pathway, Ca^{2+}-signalling has been implicated in neural induction (Leclerc et al., 2012). Spontaneous elevations of intracellular Ca^{2+} occur in dorsal ectodermal cells at blastula stage and Ca^{2+}-levels increase during gastrulation (Leclerc et al., 2000; Leclerc et al., 1997). Furthermore, blocking Ca^{2+}-signalling abolishes neural

induction (Leclerc et al., 2012), whereas an increase in Ca^{2+} is sufficient to induce neural cells (Moreau et al., 1994) .

Several transcription factors are expressed in the neuroectoderm during neural induction and are involved in neural fate stabilization (Rogers et al., 2009b) (Fig. 1.2). One important group is the Zic family of zinc-finger transcription factors. Both *Zic1* and *Zic3* are activated in the ectoderm through inhibition of the BMP-pathway (Nakata et al., 1997; Mizuseki et al., 1998a; Marchal et al., 2009) and *Zic3* is additionally a target of Ca^{2+}-signalling (Leclerc et al., 2003). Overexpression of both members of the Zic family, as well as any of the three *Iroquois* genes, *Iro1*, *Iro2* and *Iro3,* not only expands the neural plate, but also promotes the onset of neural differentiation factors (Bellefroid et al., 1998; Gomez-Skarmeta et al., 1998). Overexpression of *Zic2*, another member of the Zic family, also expands the neural plate, however, it represses the expression of neural differentiation genes (Brewster et al., 1998). This suggests that *Zic2* expression maintains neural cells in an undifferentiated cell state. Additionally, three members of the Sry-related HMG-box family, *Sox2*, *Sox3* and *SoxD* are involved in neural fate stabilization. Sox2 and Sox3 are thought to be important for neural progenitor maintenance (Hardcastle and Papalopulu, 2000; Ellis et al., 2004; Pevny and Placzek, 2005; Rogers et al., 2009a), whereas SoxD was shown to activate the expression of the neural determination gene *Neurogenin 2* (*Ngn2*) and to promote delayed neural differentiation (Mizuseki et al., 1998b). Further pan-neural genes involved in progenitor maintenance are the forkhead transcription factor *FoxD5* and the coiled-coil protein Geminin (Seo and Kroll, 2006; Kroll, 2007; Kroll et al., 1998; Pitulescu et al., 2005; Sullivan et al., 2001). Several studies indicate a cross-talk between these genes, which thereby regulates the balance between neural fate stabilization and neural differentiation (Rogers et al., 2009b).

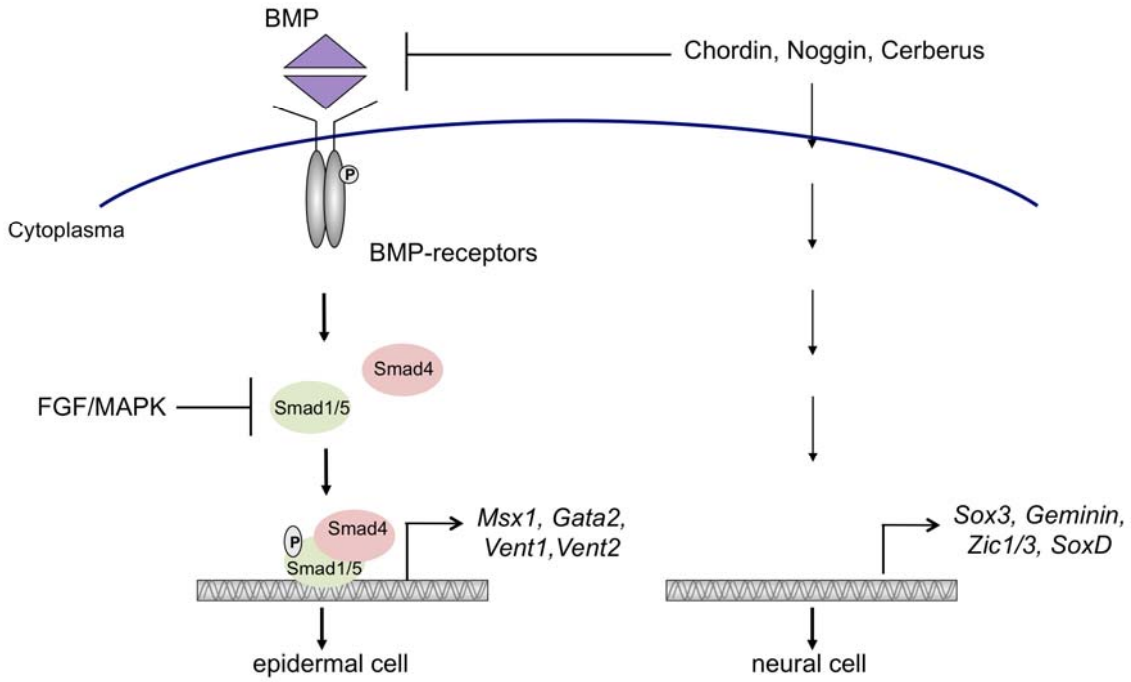

Figure 1.2 Scheme of the molecular mechanism of neural induction in *X. laevis*. Upon BMP binding to the receptors, the BMP-receptors dimerize and undergo autophosphorylation. Through the activation of target genes such as *Gata2*, *Msx1*, *Vent1* and *Vent2*, BMP-signalling induces an epidermal cell fate. However, BMP-signalling can be intracellular inhibited through the FGF/MAPK pathway, as well as extracellular through the secreted molecules Noggin, Cerberus and Chordin. Through the inhibition of BMP-signalling, multiple genes are activated, including *Zic1*, *Zic3* and *SoxD*, which lead to neural differentiation of ectodermal cells. Progenitor pools are maintained by the induction of genes like *Sox3* and *Geminin*. (after Rogers et al., 2009b)

1.3 Neuronal differentiation

In vertebrates, the progenitor cells within the neural plate are highly mitotic (Hartenstein, 1989) and become differentiated due to the expression of proneural genes. The first proneural basic-helix-loop-helix (bHLH) genes discovered were the genes of the *Achaete-scute complex* in *Drosophila* (Murre et al., 1989). These genes, as well as the gene *Atonal* (Jarman et al., 1993), induce neural commitment of ectodermal cells and were therefore termed proneural genes (Ghysen and Dambly-Chaudiere, 1989; Jan and Jan, 1994). Several vertebrate homologues have been identified, including in *X. laevis,* and can be classified into *Atonal* and *Achaete-scute* related genes (Fig. 1.3) (Lee, 1997; Guillemot, 1999). Through the conserved bHLH domain, these factors form dimers, either homo- or heterodimeric complexes with an ubiquitously expressed class A bHLH transcription factor. These complexes bind a

characteristic sequence known as the E-box motif (CANNTG) within regulatory elements of target genes (Murre et al., 1989).

In vertebrates, proneural genes induce neuronal cell fates of neural cells and are key regulators of the neurogenic differentiation program. However, not all members of the *Achaete-scute* and *Atonal* gene family have an endogenous proneural function, as *NeuroD1*, *NeuroD6/Ath2* and *NeuroD4/Ath3* are only expressed in post-mitotic neurons.

Family	Gene	Onset of expression	Expression st. 14	Reference
Achaete-scute	*Ascl1/Xash1*	st. 21	-	Ferreiro *et al.*, 1993
	Ascl3/Xash3	st.11.5	one stripe encompassed by the medial and intermediate stripe of primary neurons, which ends in an anterior transversal stripe	Turner *et al.*, 1994, Bellefroid *et al.*, 1998
Atonal	*Ngn1*	st.11	three stripes of primary neurons, tp	Nieber *et al.*, 2009
	Ngn2/Ngnr1	st.10.5/11	three stripes of primary neurons, tp	Ma *et al.*, 1996, Nieber *et al.*, 2009
	Ngn3	st.11	one stripe between medial and intermediate stripe of primary neurons	Nieber *et al.*, 2009
	Atoh1/Xath1	st.17	-	Kim *et al.*, 1997
	NeuroD6/Xath2	st.32	-	Taelman *et al.*, 2001
	Atoh7/Xath5	st.17	-	Kanekar *et al.*, 1997
	NeuroD4/Xath3	st.12	three stripes of primary neurons, tp	Perron *et al.*, 1999
	NeuroD1	st.14	two stripes representing medial and lateral stripe of primary neurons, tp	Lee *et al.*, 1995

Figure 1.3 *X. laevis* homologues of the proneural *Achaete-scute* and *Atonal* genes of *Drosophila*.
Due to conserved sequences in the bHLH domain, *X. laevis* proneural bHLH transcription factors can be classified into the *Achaete-scute* and the *Atonal* gene family. The table summarizes the onset of gene expression as well as the expression domains of the identified proneural bHLH transcription factors on each side of the midline in *X. laevis* at st. 14 (open neural plate). tp, trigeminal placode

The vertebrate proneural genes include the members of *Neurogenin* family (Sommer et al., 1996; Nieber et al., 2009), *Ascl1/Ash1* (Ferreiro et al., 1993; Talikka et al., 2002) and *Ascl3/Ash3* (Turner and Weintraub, 1994; Chitnis and Kintner, 1996) as well as *Atoh1/Ath1* (Kim et al., 1997) and *Atoh7/Ath5* (Kanekar et al., 1997). During neuronal differentiation, the proneural genes have multiple functions, which induce the process of neuronal differentiation and maturation (Fig. 1.4 A) (Bertrand et al., 2002; Guillemot, 1999; Castro and Guillemot, 2011). To promote neuronal commitment of a cell,

proneural genes activate a cascade of neuronal differentiation factors (Guillemot, 1999; Bertrand, 2002), regulate cell migration (Ge et al., 2006) and cell-cycle withdrawal (Castro et al., 2011; Klisch et al., 2011) (Fig. 1.4 A). In addition, the Notch-signalling pathway is also activated by the proneural bHLH factors, which regulates the balance between neural progenitors and neuronal differentiated cells (see chapter 1.4).

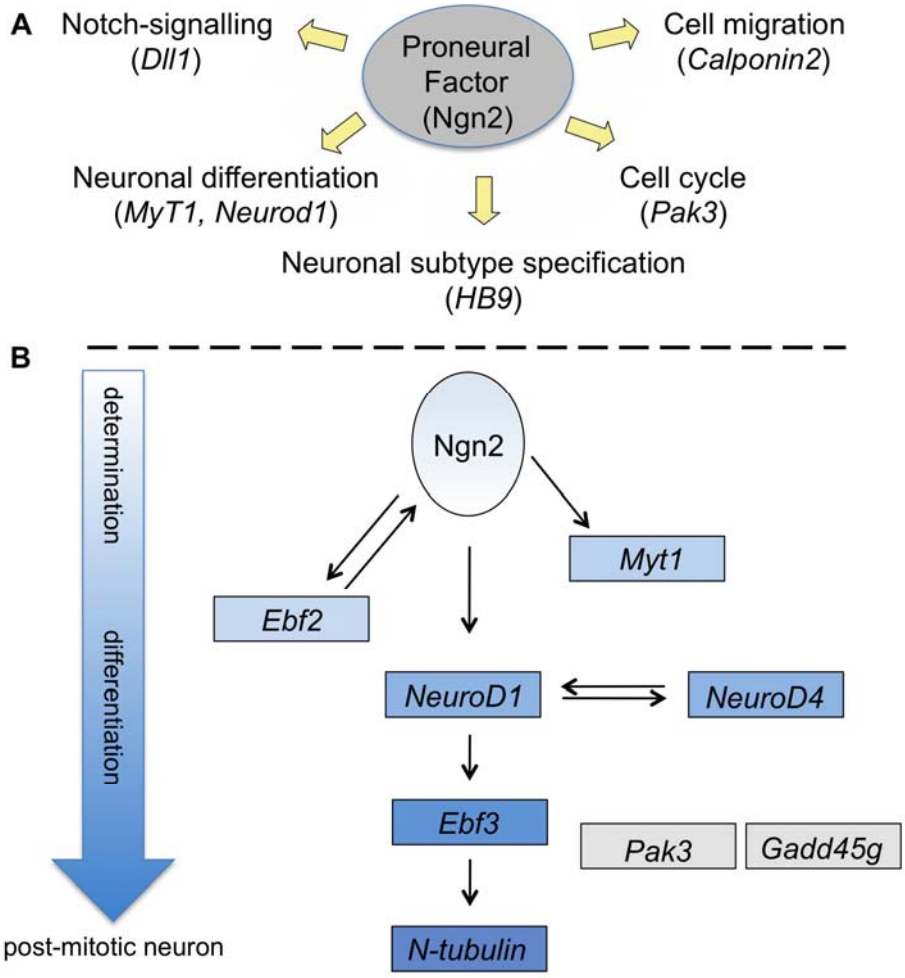

Figure 1.4 Scheme of neuronal differentiation regulated by proneural genes.
(A) Vertebrate proneural genes such as *Ngn2* confer distinct activities to induce neuronal commitment of a cell, including activation of Notch-signalling, promotion of cell migration and neuronal differentiation as well as regulation of the cell cylce. Furthermore, proneural genes are also involved in neuronal subtype specification. **(B)** Due to the onset of proneural gene expression as e.g. *Ngn2*, a neural cell obtains neuronal cell identity. Ngn2 is known to induce a cascade of differentiation factors in *X. laevis*, such as *Myt1*, *Ebf2*, *NeuroD4*, *Ebf3* and *NeuroD1*, which lead to the induction of *N-tubulin*. In addition, Ngn2 activates the cell cycle inhibitors *Pak3* and *Gadd45g*.

In *X. laevis*, the primary nervous system is essential for the movements and responses of the larvae (Roberts, 2000). Prior to morphogenesis, a second round of neurogenesis starts in *X. laevis* and replaces the majority of primary

neurons. Several studies indicate that many factors involved in primary neurogenesis are also expressed during secondary neurogenesis, suggesting that the molecular mechanism between the two processes is conserved (Schlosser et al., 2002; Wullimann et al., 2005).

In *X. laevis*, the first primary neurons differentiate at the open neural plate stage in three longitudinal stripes on each side of the midline, as well as in the trigeminal ganglia (Fig. 1.7 A) (Chitnis et al., 1995). Post-mitotic neurons can be visualized by the expression of *class II beta-tubulin* (*N-tubulin*) (Oschwald et al., 1991). Neuronal differentiation in the anterior neural plate, with exception of the trigeminal ganglia, is delayed until tadpole stages (Papalopulu and Kintner, 1996).

The best-characterised proneural gene during *X. laevis* primary neurogenesis is the *Atonal* ortholog and neuronal determination factor *Neurogenin 2 (Ngn2,* also known as *Ngnr-1*) (Ma et al., 1996). *Ngn2* is expressed already during early gastrula stage (stage 10.5/11) in the prospective neural ectoderm (Ma et al., 1996; Nieber et al., 2009). In the open neural plate, it prefigures the characteristic three longitudinal stripes of primary neurons on each side of the midline (Bellefroid et al., 1996). Ngn2 confers all the above-described activities to be classified as a proneural bHLH transcription factor (Fig. 1.4 A). It induces a cascade of differentiation factors (Fig. 1.4 B.), including the bHLH proteins *NeuroD1* (Ma et al., 1996), *NeuroD4* (*Ath3*) (Perron et al., 1999), the zinc finger HLH transcription factors *Ebf2* (Dubois et al., 1998) and *Ebf3* (Pozzoli et al., 2001) as well as the proneural RNA binding protein *Seb4R* (Boy et al., 2004). In addition, Ngn2 activates the zinc finger transcription factor *Myt1*, which allows the cells fated to become a neuron to escape lateral inhibition (Bellefroid et al., 1996). All these genes downstream of Ngn2 are also expressed in the characteristic stripe-like pattern at the open neural plate and form a synexpression group (Niehrs and Pollet, 1999). Furthermore, genes that regulate cytoskeleton or migratory events in the context of the nervous system development are targets of Ngn2 (Seo et al., 2007) as well as genes that promote cell-cycle withdrawal such as the *growth arrest and DNA-damage-inducible gamma* (*Gadd45g*) *gene* and *Pak3* (Souopgui et al., 2002; de la Calle-Mustienes et al., 2002) (Fig. 1.4 B). Additional proneural bHLH transcription factors are also expressed in the open neural plate, but show expression in

divergent domains (Fig. 1.3). Following neural tube closure, the individual proneural bHLH transcription factors are expressed in discrete domains, suggesting that they are essential for generation of post-mitotic neurons and neuronal subtype identities in distinct domains of the CNS. Indeed several proneural factors such as Ngn2 (Perron et al., 1999) and Ath5 (Kanekar et al., 1997) have been also shown to play a role in neuronal subtype specification.

1.4 Notch-signalling

The Notch-signalling pathway regulates the balance between progenitor maintenance and differentiation (Lewis, 1996). During *X. laevis* primary neurogenesis, the process of lateral inhibition is mediated by the Notch-signalling and generates a salt and pepper like pattern of the neurons at the open neural plate stage (Fig. 1.5 A). The Notch pathway acts through cell-to-cell signalling with cells being defined as either signal-sending or signal-receiving. Proneural genes such as *Ngn2* and *Ascl1* activate the expression of the transmembrane Notch-ligands in the signal-sending cell (Fig. 1.4 B) (Chitnis et al., 1995; Chitnis and Kintner, 1996; Ma et al., 1996; Henke et al., 2009a). In vertebrates, several such ligands are known (Bray, 2006), including *Dll1, 2,* and *4* as well as *Jag1* and *2* in *X. laevis*. The ligands bind one of the four transmembrane Notch-receptors (Bray, 2006) on the neighbouring cell, which induces a series of proteolytic cleavages in the Notch-receptor. As a result, the intracellular domain of the Notch-receptor (Notch-ICD) is released and translocates to the nucleus (Schroeter et al., 1998; Chan and Jan, 1999; Selkoe and Kopan, 2003). In the nucleus, Notch-ICD binds a DNA-binding protein of the CSL family (Su(H)) in *X. laevis* and *Drosophila*, Rbp-j in mouse, Lag-1 in *C. elegans*) (Honjo, 1996), which acts in a complex as a transcriptional repressor. However, after binding of Notch-ICD, the repressor is converted into an activator and together with co-factors activates the transcription of the Notch-target genes (Wettstein et al., 1997).

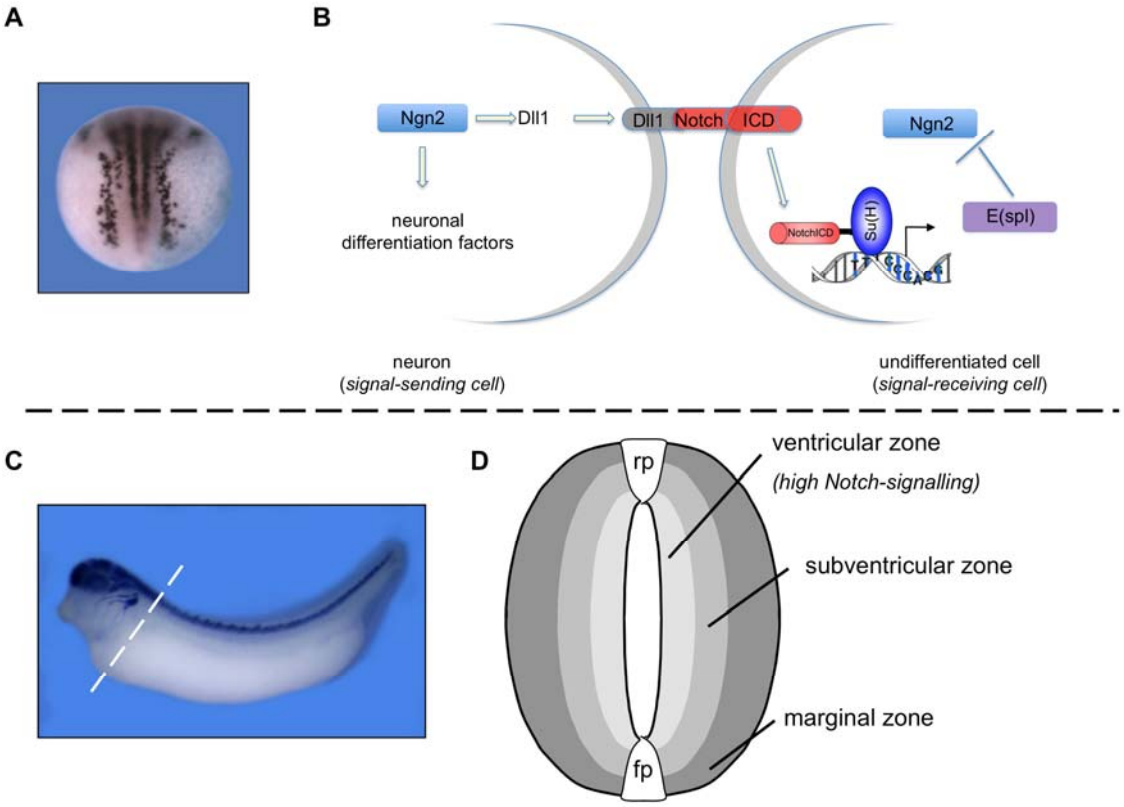

Figure 1.5 Notch-signalling during development.
(A, B) Lateral inhibition. At the open neural plate stage, the primary neurons arise in a salt-and-pepper like pattern, which is mediated by the Notch-signalling pathway. This process allows neuronal differentiation of a cell, whereas its neighboring cells stay in an undifferentiated cell state. Proneural genes such as *Ngn2* activate neuronal differentiation factors as well as the Notch-ligand *Dll1*, which binds to the Notch-receptor at the neighboring cell. Upon binding, the Notch-receptor is proteolytic cleaved and the intracellular domain of the Notch-receptor is released into the nucleus. Notch-ICD binds Su(H) to form an activator complex to induce the transcription of the direct target genes. These transcription factors, in a negative-feedback loop, inhibit the expression of proneural genes. Thus the sending cell differentiates into a neuron, whereas the receiving cell stays in an undifferentiated cell state. (after Louvi and Artavanis-Tsakonas, 2006; Beres et al., 2006, modified) **(C, D) Maintenance of neural progenitor cells.** When the neural tube is closed, Notch-signaling is still essential as it is highly active in the ventricular zone of the neural tube and maintains the pool of progenitor cells. When cells start to differentiate into neurons, they migrate outwards through the subventricular zone into the marginal zone, where the differentiated and post-mitotic neurons are located. rp, roof plate; fp, floor plate

The direct targets of the Notch-signalling include members of the bHLH family that are related to the *Drosophila Hairy and enhancer of split* genes (*E(spl)*) (Sasai et al., 1992; Ohtsuka et al., 1999; Davis and Turner, 2001). In a negative-feedback-loop, the Notch target genes act as repressors and inhibit the expression of the proneural genes (Takke et al., 1999; Schneider et al., 2001; Ishibashi et al., 1995; Cau et al., 2000) in the neighbouring cell (Fig. 1.5 B). Due to this mechanism, the ligand-expressing cell differentiates into a neuron, whereas the neighbouring cells stay in an undifferentiated cell state and

later differentiate into glia-cells (Louvi and Artavanis-Tsakonas, 2006; Wang and Barres, 2000). In this context, overexpression of Notch-ICD in *X. laevis* decreases the number of primary neurons, while inhibition of the Notch-pathway by microinjection of a dominant-negative *Dll1* (*Delta*$_{stu}$) increases the density of primary neurons (Chitnis et al., 1995). After neural tube closure, Notch-signalling is highly active in the ventricular zone of the neural tube and preserves the pool of neural progenitors (Lindsell et al., 1996; Imayoshi and Kageyama, 2011) (Fig. 1.5 C, D).

1.5 Neurulation and Neuronal subtype specification

During neurulation, the neural folds rise and fuse to form the closed neural tube. During this process, neural precursors cells migrate laterally inwards and reside in the ventricular zone (Fig. 1.5 D). After cell cycle exit, these precursor cells migrate outwards through the intermediate zone into the outer marginal zone (Fig. 1.5 D) (Bellefroid et al., 1996) and differentiate into distinct neuronal cell types. Neuronal subtype specification in vertebrates is best-characterised in the chick and mouse neural tube, in which the first neurons are born within the closed neural tube. Dorso-ventral patterning of the neural tube gives rise to specific neuronal subtypes within the neural tube. This is primarily generated through two signalling centers, BMP in the dorsal and Sonic Hedgehog (SHH) in the ventral part of the neural tube (Fig. 1.6) (Dreau and Marti, 2012). These signals act as morphogens, generating gradients along the dorso-ventral axis of the embryo. Thus, the progenitor cells within the neural tube are exposed to different concentrations of these signals. Due to the partly opposing gradients, progenitors domains are generated in the inner ventricular zone of the neural tube. Each progenitor domain expresses distinct transcription factors, including bHLH and homeodomain (HD) transcription factors (Fig. 1.6) (Alaynick et al., 2011). From these progenitor domains, distinct neuronal subtypes arise that express a specific combinatorial code of HD transcription factors (Fig. 1.6) (Alaynick et al., 2011).

The roof plate and the dorsal ectoderm express several members of the TGF-beta-signalling pathway, including *BMP-4*, *BMP-7*, *BMP-5* and *Dsl1* (Liem et al., 1995; Liem et al., 1997). The importance and a concentration-dependent mechanism of the BMP-signals in generating dorsal interneuronal subtypes

could be demonstrated by *in vitro* studies using neural plate explants as well as *in vivo* (Liem et al., 1997; Liem et al., 1995; Timmer et al., 2002; Barth et al., 1999; Nguyen et al., 2000). Furthermore, the *in vitro* experiments suggested that the different BMPs have qualitative distinct functions in generating the dorsal interneuron populations (Liem et al., 1997), which is further supported by *in ovo* electroporations in the chick neural tube (Le Dreau et al., 2012; Dreau and Marti, 2012)

In addition to BMP-signalling, the Wnt-pathway has been implicated in the dorsal patterning of the neural tube (Muroyama et al., 2002; Yu et al., 2008; Alvarez-Medina et al., 2008), which is supported by the expression of multiple Wnts in the roof plate and in the dorsal ectoderm (Parr et al., 1993; Hollyday et al., 1995; Megason and McMahon, 2002). Due to the dorsal extrinsic signalling events, six early (dI1-dI6) and two late (dIL_A and dIL_B) interneuron populations are generated (Fig. 1.6) (Helms and Johnson, 2003).

In the ventral neural tube, the morphogen SHH is expressed by the mesodermal derived notochord as well as by the floor plate induced by it (Echelard et al., 1993; Marti et al., 1995b; Placzek et al., 1991; Yamada et al., 1991). *In vitro* experiments showed a concentration-dependent induction of the ventral neuronal subtypes by SHH (Ericson et al., 1996; Ericson et al., 1997; Marti et al., 1995a; Roelink et al., 1995). However, of the five neuronal subtypes generated (V0-V3, MN) (Ericson et al., 1997; Briscoe et al., 2000), SHH is not sufficient for the specification of V0 and V1 interneurons as in SHH knock-out mice, these neuron types are still present (Litingtung and Chiang, 2000).

The transcription factors in the neural tube can be divided into distinct subgroups. In the dorsal neural tube, genes can be divided into BMP-dependent (Class A) or -independent (Class B). Similarly in the ventral neural tube, Class I transcription factors are independent and in fact repressed by SHH-signalling, whereas class II transcription factors are SHH-dependent (Briscoe and Ericson, 2001; Alaynick et al., 2011; Jessell, 2000). Furthermore, cross-repressive interactions between the distinct classes establish the borders of gene expression and thereby of the progenitor domains (Briscoe et al., 2000; Vallstedt et al., 2001).

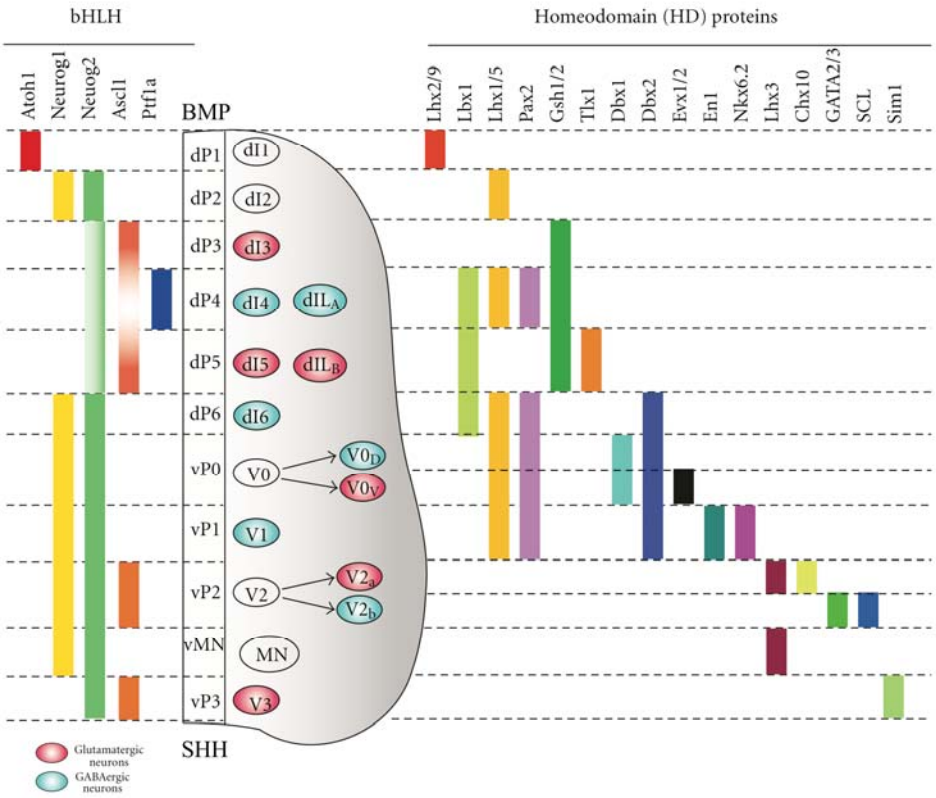

Figure 1.6 Dorso-ventral patterning of the mouse neural tube.
The patterning of the neural tube along the dorso-ventral axis is based on extrinsic signals. In the dorsal part, a gradient of BMP- and Wnt-signalling is generated by the roof plate and is responsible for the formation of the six early (dI1-dI6) and two late (dIL$_A$ and dIL$_B$) dorsal interneuronal subtypes. In the ventral part, the morphogen SHH is expressed from the notochord and the floor plate and is involved in the generation of the five ventral (V0-V3 and motor neurons (MN)) neuronal subtypes. The two ventral neuron populations V0 and V2 can be subdivided into two distinct neuron types (indicated by arrows). Due to the opposing gradients, specific bHLH (left) and HD (right) transcription factors become expressed in the ventricular zone along the dorso-ventral axis, forming distinct neuronal progenitor domains. From these, different neuronal subtypes arise, which express a specific code of HD transcription factors. The neurotransmitter expression of the distinct post-mitotic neuron populations is indicated by red (glutamatergic) and blue (GABAergic) circles. (Hori and Hoshino, 2012, modified)

In *X. laevis*, the first neurons differentiate not within the closed neural tube, but already at the open neural plate stage in the three characteristic stripes on each side of the midline (Fig. 1.7 A). The region of the ectoderm that gives rise to the neural plate is excluded from BMP expression and can be visualized by the expression of *Sox3*, an early marker for neural progenitor cells (Fig. 1.7 A). However, the lateral stripe of primary neurons is located outside the *Sox3* expression domain (Fig. 1.7 A) (Hardcastle and Papalopulu, 2000) and requires intermediate levels of BMP-signalling (Rossi et al., 2008). Furthermore, SHH is expressed in a longitudinal stripe along the dorsal midline (Brewster et

al., 1998). Therefore, neuronal subtype specification in *X. laevis* may already be initiated at the open neural plate stage.

Dependant on their position within the open neural plate and the closed neural tube, the primary neurons obtain a specific neuronal subtype (Fig. 1.7 B). The lateral stripe of the primary neurons will give rise to the dorsal Rohon-Beard sensory neurons, while the intermediate and medial stripe will develop into interneurons and ventral motor neurons, respectively (Fig. 1.7 A and B) (Chitnis and Kintner, 1995; Hartenstein, 1989). The first differentiating neurons in the *X. laevis* spinal cord are the dorsal Rohon-Beard sensory neurons (Hartenstein, 1993) followed with a slight delay by the ventrally located neurons (Hartenstein, 1993), which include motor neurons and Kolmer-Agduhr cells. Interneurons are the last to differentiate and do so in the lateral part of the spinal cord (Hartenstein, 1993). A more detailed analysis considering soma location, axon projection and neurotransmitter expression defined in total ten different types of neurons in the *X. laevis* spinal cord (Roberts et al., 2012). These include the dorsal Rohon-Beard sensory neurons, the ventral motor neurons and Kolmer-Agduhr cells, but also seven distinct interneuronal subtypes (Roberts et al., 2012). In contrast to mouse, the molecular transcription factor codes to discriminate between distinct neuronal subpopulations are not well established. However, there is evidence indicating that these codes actually might be conserved in vertebrates.

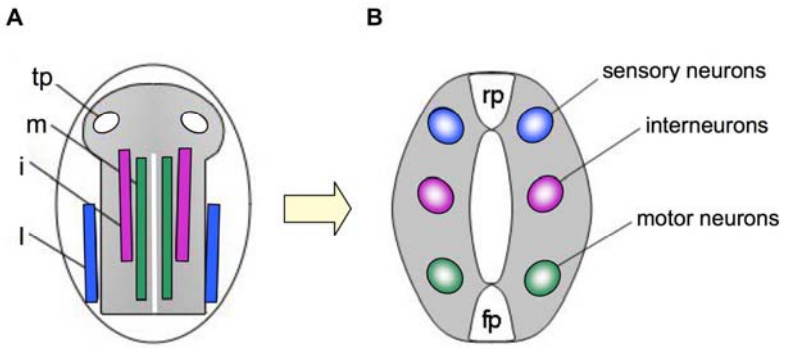

Figure 1.7 Neuronal subtype specification in the *X. laevis* spinal cord.
(A) Scheme of primary neurogenesis domains in *X. laevis*. At the open neural plate stage, primary neurons are born in three longitudinal stripes on each side of the midline (white) and in the trigeminal ganglia. Grey indicates *Sox3* expressing areas, which reflect low BMP-signalling. **(B) Scheme of neuronal subtype identity in the *X. laevis* spinal cord.** When the neural tube is closed, the primary neurons obtain a specific neuronal subtype identity depending on their previous position within the neural plate. The outer stripe of primary neurons will give rise to the sensory Rohon-Beard neurons, while the medial and intermediate stripe will give rise to interneurons and motor neurons, respectively. rp, roof plate, fp, floor plate, m, mediate, i, intermediate, l, lateral, tp, trigeminal placodes

1.6 Ptf1a

The nervous system consists of many different cell types, including distinct neuronal subtypes, astrocytes and oligodendrocytes. Among the different neuronal cell types, most can be classified as excitatory or inhibitory neurons. An imbalance between the two distinct neuronal subtypes impairs functional neural networks, which underlies a number of neurological disorders (McCormick and Contreras, 2001; Rossignol, 2011). GABA and glutamate are the primary neurotransmitters of the inhibitory and excitatory neurons, respectively. The pancreatic transcription factor 1a (Ptf1a), which encodes for a bHLH transcription factor, has a central role in promoting GABAergic inhibitory neurons at the expense of glutamatergic excitatory neurons in the vertebrate CNS (Hori and Hoshino, 2012).

1.6.1 Ptf1a function during development of the pancreas

The importance of *Ptf1a* during embryogenesis is demonstrated by the pancreatic and cerebellar agenesis, as well as diabetes mellitus that occur in individuals with mutations in the *Ptf1a* gene (Sellick et al., 2004; Hoveyda et al., 1999; Tutak et al., 2009; Al-Shammari et al., 2011). A similar phenotype is observed upon loss of *Ptf1a* in the mouse (Kawaguchi et al., 2002; Sellick et al., 2004).

Ptf1a was first identified and characterised in the pancreas and was shown to be essential for the specification of pancreatic precursor cells including both, progenitors for endocrine and exocrine cells (Cockell et al., 1989; Burlison et al., 2008; Kawaguchi et al., 2002). Later in development, Ptf1a plays a central role in exocrine cell differentiation and in the adult exocrine pancreas, Ptf1a activates the transcription of the acinar digestive enzymes (Krapp et al., 1998; Krapp et al., 1996; Kawaguchi et al., 2002; Zecchin et al., 2004; Lin et al., 2004). Microinjection of *Ptf1a* mRNA in *X. laevis* is sufficient to induce ectopic formation of pancreatic tissue within the expression domains of the *Pancreatic and duodenal homeobox 1* (*Pdx1*) gene in the foregut (Afelik et al., 2006). Moreover, a combination of Pdx1 and Ptf1a allows conversion of non-pancreatic endodermal cells into both, endocrine and exocrine pancreatic cell lineages (Afelik et al., 2006).

Pdx1 was shown to be a direct target of Ptf1a in the mouse (Wiebe et al.,

2007; Miyatsuka et al., 2007) and additional Ptf1a downstream targets, including direct targets in early pancreatic progenitors (Thompson et al., 2012), in exocrine cell differentiation (Cockell et al., 1989; Masui et al., 2010) and in *X. laevis* have been identified (Bilogan and Horb, 2012). Additionally, Ptf1a itself has been reported to be a direct target through positive autoregulation (Masui et al., 2008). Experiments in zebrafish and mouse could show that the distinct Ptf1a activities during pancreas development are dosage-dependent. Low levels of Ptf1a expression promote pancreatic endocrine cell fates, whereas high levels specify exocrine cell differentiation (Fukuda et al., 2008; Dong et al., 2008). In addition, recent studies in the mouse showed that Ptf1a molecularly forms context-dependent transcription factor complexes. Ptf1a was originally identified as a subunit of the heterotrimeric pancreas transcription factor complex 1 (PTF1) (Cockell et al., 1989; Roux et al., 1989). In this complex, Ptf1a forms a heterodimer with an ubiquitously expressed class A bHLH factor (E-protein, E2A/p75/HEB/TCF12), which binds to the E-box sequence (CANNTG) at the DNA (Beres et al., 2006; Murre et al., 1989). Additionally, Ptf1a interacts with a member of the CSL family of DNA binding proteins (Su(H), CBF1, Lag-1, Rbp-j and -l) through two conserved C-motifs (C1:HSLSW and C2:WTPEDPR) located in the C-domain of Ptf1a (Beres et al., 2006). The CSL-binding protein binds DNA via a TC-box motif (TTTCCCA) (Beres et al., 2006). Thus, the heterotrimeric PTF1 complex binds a specific bipartite binding site, in which the TC-box must be separated by one or two helix turns from the E-box motif (Cockell et al., 1989). In pancreatic progenitor cells, Ptf1a interacts with Rbp-j, which at the onset of acinar cell development is gradually replaced by its paralogue Rbp-l (Masui et al., 2007). Strong expression of Rbp-l is restricted to adult pancreatic tissue and is so far unknown in *X. laevis* (Beres et al., 2006).

In the mouse, the interaction between Ptf1a and Rbp-j/-l, but not with the class A bHLH protein can be abolished by introducing mutations in the C1 and C2 domain of Ptf1a (Beres et al., 2006). Rbp-j, but not Rbp-l is also involved in Notch-signalling, where it forms a transcriptional complex with Notch-ICD. It could be demonstrated that the binding of Rbp-j to Notch-ICD and Ptf1a is mutually exclusive (Beres et al., 2006). Thus, Ptf1a and Notch-ICD activity could potentially antagonize each other. Furthermore, Notch target genes can

directly bind to Ptf1a (Ghosh and Leach, 2006) and downregulate Ptf1a transcriptional activation and DNA-binding (Esni et al., 2004).

1.6.2 Ptf1a function during development of the nervous system

In the vertebrate nervous system, *Ptf1a* is expressed in the retina, the hindbrain and in the dorsal horn of the spinal cord in precursor cells of GABAergic inhibitory interneurons (Glasgow et al., 2005; Hoshino et al., 2005; Nakhai et al., 2007; Fujitani et al., 2006). *Ptf1a* was shown to act as a selector gene for GABAergic inhibitory interneurons at the expense of glutamatergic excitatory neurons in the vertebrate retina, hindbrain and spinal cord (Glasgow et al., 2005; Hori et al., 2008; Hoshino et al., 2005; Fujitani et al., 2006; Nakhai et al., 2007; Pascual et al., 2007; Dullin et al., 2007). Consistent with the molecular mechanism of gene activation in the pancreas, Ptf1a in neural tissue forms a heterotrimeric PTF1 complex through interaction with Rbp-j and the ubiquitous expressed class A bHLH transcription factor. For its function as a GABAergic selector gene, Ptf1a requires the interaction with Rbp-j (Hori et al., 2008; Lelievre et al., 2011) and Rbp-j function in this context is Notch-independent (Hori et al., 2008).

In contrast to the pancreas, only a few direct downstream targets of Ptf1a in the nervous system have been identified. Similar to the pancreas, Ptf1a regulates its own expression via positive autoregulation (Meredith et al., 2009). In the mouse neural tube and cerebellum, the bHLH transcription factor *Ngn2* is a direct downstream target of the heterotrimeric PTF1 complex (Henke et al., 2009b). Furthermore, the expression of two members of the immunoglobulin superfamily, *Nephrin* and *Neph3* (*Kirrel2* in *X. laevis*) is directly controlled by binding of Ptf1a within the promoter region of these genes (Nishida et al., 2010). *Neph3* is expressed in progenitors of the GABAergic Purkinje cells, suggesting that its activation by Ptf1a plays a role in GABAergic neuronal subtype specification (Mizuhara et al., 2010). In combination with the *oligodendrocyte transcription factor 3* (*Olig3*), Ptf1a induces the expression of the *forkhead box D3* (*FoxD3*) gene to generate the glutamatergic climbing fiber neurons (Yamada et al., 2007; Storm et al., 2009).

1.6.3 Ptf1a also forms context-dependent transcription complexes in the nervous system

In *X. laevis*, *Ptf1a* not only functions as a selector gene for GABAergic inhibitory neuronal cell fates, but also promotes general neurogenesis in naïve ectodermal explants and in the non-neural ectoderm of embryos (Dullin et al., 2007; Hedderich, 2008). Analysis of a limited set of marker genes demonstrated that Ptf1a drives neuronal differentiation similar to the neuronal determination gene *Ngn2* (Hedderich, 2008). However, Ptf1a and Ngn2 have distinct neuronal subtype specificities (Dullin et al., 2007; Hedderich, 2008). Ptf1a activates the expression of *Glutamate decarboxylase 1* (*Gad1*), a marker for GABAergic inhibitory neurons (Li et al., 2006). In contrast, Ngn2 induces the expression of *Hox11L2*, which marks sensory neurons (Patterson and Krieg, 1999; Perron et al., 1999). The murine homolog of *Hox11L2*, *Txl3* functions as a selector gene for glutamatergic excitatory neurons (Cheng et al., 2004; Cheng et al., 2005). Mutations in the *X. laevis* Ptf1a C1- and C2-domain ($Ptf1a^{W224A/W242A}$) reveal that the interaction of Ptf1a with Su(H) is essential for the GABAergic specificity of Ptf1a (Hedderich, 2008), a result congruent to the situation in the murine nervous system (Hori et al., 2008). Surprisingly, the proneural activity of Ptf1a was not impaired by the mutations, as $Ptf1a^{W224A/W242A}$ could still activate neuronal differentiation genes (Hedderich, 2008). Taken together, the data suggest that Ptf1a also forms context-dependent transcription complexes in the nervous system: A Su(H)-independent complex to drive general neurogenesis and a Su(H)-dependent complex to specify GABAergic inhibitory neurons (Hedderich, 2008) (Fig. 1.8).

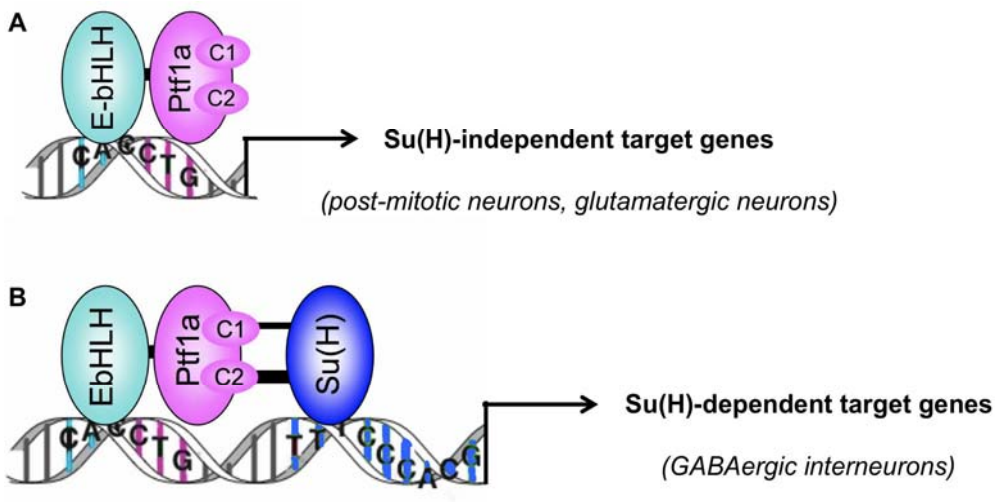

Figure 1.8 Ptf1a forms context-dependend transcription complexes
(A) In the context of general neurogenesis, the dimeric complex, consisting of Ptf1a and the class A bHLH transcription factor is sufficient to drive neuronal differentiation and to induce the formation of glutamatergic/sensory neurons. Thus, this complex activates Su(H)-independent Ptf1a target genes. **(B)** In contrast, the genes involved in GABAergic interneuron formation are Su(H)-dependent as the Su(H)-interaction of Ptf1a is essential for their activation. (Beres et al., 2006, modified)

1.7 Aims

The bHLH transcription factor Ptf1a was identified as an important selector gene for generation of GABAergic inhibitory neurons in the vertebrate CNS. However, previous experiments in *X. laevis* indicated that Ptf1a also functions as a proneural gene and forms context-dependent transcription complexes to drive neuronal differentiation and to promote GABAergic inhibitory interneurons. The goal of the thesis was to further analyse the two distinct Ptf1a specificities, including identification of the genetic network downstream of Ptf1a and providing insight into the regulation of the distinct transcription complexes.

2. Materials and Methods

2.1 Material

2.1.1 Model organism

The African clawed frog *Xenopus laevis* (*X. laevis*) was used as a model organism during this study. Albinos and pigmented frogs were obtained from Nasco (Ft. Atkinosn, USA). The embryos were staged according to Nieuwkoop and Faber (1967).

2.1.2 Bacteria

For molecular biology standard methods, the chemical competent Escherichia coli strain XL1-Blue was used.
XL1-Blue: recA1, endA1, gyrA96, thi-1, hsdR17, supE44, relA1, lac[F'proAB, laclqZDM15, Tn10(Tetr)]c (Stratagene).

2.1.3 Antiobiotics and Media

Antibiotics
Ampicillin
stock: 100 mg/ml in dH_2O, working: 100 µg/ml. Stored at -20 °C.

Media
32 g LB medium (GIBCO) dissolved in 1000 ml dH_2O
The LB Media was autoclaved for 20 min and cooled down to 50 °C. Afterwards the selective antibiotic was added. The agar plates were poured under a steril bench and stored at 4 °C.

2.1.4 Oligonucleotides

Oligonucleotides were purchased from Sigma-Aldrich and dissolved in HPLC H_2O to 100 µM or 500 µM.

Sequencing oligonucleotides

Table 2.1 Summary of Sequencing oligonucleotides and annealing temperature (T_A)

Oligonucleotide	Sequence	T_A °C
SP6	5'-TTAGGTGACACTATAGAATAC-3'	48
T7	5'-TAATACGACTCACTATAGGGCGA-3'	56
T7 pcs2+	5'-TCTACGTAATACGACTCACTATAG-3'	56
GR7	5'-ATCCTGCATATAACACTTC	56
T3	5'-AATTAACCCTCACTAAAGGG-3'	57

RT-PCR oligonucleotides

Table 2.2 Summary of RT-PCR oligonucleotides and working conditions

Oligonucleotide	Orientation	Sequence	T_A °C	Cycles
H4	for	5'-CGGGATAACATTCAGGGTATCACT-3'	56	24
H4	rev	5'-ATCCATGGCGGTAACTGTCTTCCT-3'	56	24
ODC	for	5'-GCCATTGTGAAGACTCTCTCCATTC -3'	56	24
ODC	rev	5'-TTCGGGTGATTCCTTGCCAC-3'	56	24
N-tubulin	for	5'-ACACGGCATTGATCCTACAG-3'	57	30
N-tubulin	rev	5'-AGCTCCTTCGGTGTAATGAC-3'	57	30
Gad1	for	5'-ATGGGCGTCTTACTCCAATG-3'	60	33
Gad1	rev	5'-ATGTCTACATGGCGACCACA-3'	60	33
Hox11L2/Tlx3	for	5'-GCCAACAAGTACAAGTGCACAG-3'	57	30
Hox11L2/Tlx3	rev	5'-CAGGAGCCAGACTCACATTGAC-3'	57	30
Su(H)	for	5'-AGAAGGTTGGAGATGGGTTC-3'	60	33
Su(H)	rev	5'-GATGATGTGACATTGGCTGA-3'	60	33
Ptf1a 3'UTR	for	5'-GTTGTCAGAACGGCCAAAGT-3'	60	33
Ptf1a 3'UTR	rev	5'-GGTACCGAGTGGAACCAAAG-3'	60	33
Ngn2 5'UTR	for	5'-ACTGCAGCATTGTCACTTGC-3'	60	34
Ngn2 5'UTR	rev	5'-CAATGGTTAGCCCCAATGTT-3'	60	34

2.1.5 Overexpression constructs

Ptf1a-GRpCS2+ (Afelik et al., 2006), **Ptf1a-VP16-GRpCS2+** (Dullin et al., 2007), **GR-Ngn2-p3'** (Perron et al., 1999), **ß-Gal-pCS2+** (Chitnis et al., 1995).

Ptf1a$^{W224A/W242A}$-GRpCS2+ (Hedderich, 2008). This construct harbors the open reading frame of Ptf1a (DQ007931.1) with two point mutations at position 224 and 242. The point muations were introduced using the "QuickChange XL Site directed Mutagenesis" kit (Stratagene) and the following primers p48C1mut_up GGA CAT TCT CTC TCA GCG ACT GAT GAG AAG CAA CTG AG and p48C1mut_down CTC AGT TGC TTC TCA TCA GTC GCT GAG AGA GAA TGT CC as well as p48C2mut_up GTT GTC AGA ACG GCC AAA GTG GCG

ACT CCT GAG GAT CC and p48C2mut_down GGA TCC TCA GGA GTC GCC ACT TTG GCC GTT CTG AC AAC, thereby exchanging a tryptophan to an alanine (mutations are red). Ptf1a-GRpCS2+ (Afelik et al., 2006) served as DNA template for the PCR. For preparation of sense mRNA, the construct was linearized with NotI and transcribed with SP6 polymerase.

Chimeric Ptf1a-GRpCS2+ (Hedderich, 2008). To synthesize the chimric Ptf1a-GR, the bHLH domain of Ngn2 was PCR amplified using GR-Ngn2p3' (Perron et al., 1999) as template. The primers contained the surrounding sequences of the bHLH domain of Ptf1a (in italics): Ptf1a/bHLH-Ngnr1_for *CTG AGG TCG GAC GCG GAG ATG CAG CAG* CGG CGC GTT AAA GCT AAC AAC and Ptf1a/bHLH-Ngnr1_rev *GCG GCA GAT CGG ACT GTA CCA TCT CGC* TAA GAG CCC AGA TGT AGT TGT AG. The so called megaprimer was used together with the "QuickChange XL Site Directed Mutagenesis" kit (Stratagene) in a PCR using Ptf1a-GRpCS2+ (Afelik *et al*., 2006) as template. For preparation of sense mRNA, the construct was linearized with NotI and transcribed with SP6 polymerase.

Su(H)-HApCS2+ (Hedderich, 2008)**.** This construct harbors the open reading frame of Su(H) (U60093.1), which was PCR amplified using Su(H)pCS2+ (Wettstein *et al*., 1997) as a template as well as the following primers: 3'HASu(H)_BamHI_for: CTG GAT CCA TGC AAC CTG GC and 3'HASu(H)_XhoI_rev: CAA CTC GAG GGA CAC TAC TGC TGC. Su(H) was subcloned into HA-pCS2+ (Damianitsch, 2008) using the BamHI und XhoI restriction sites. For preparation of sense mRNA, the construct was linearized with NotI and transcribed with SP6 polymerase.

Su(H)-GRpCS2+. The open reading frame of Su(H) (U60093.1) was PCR amplified with the following primers: Su(H)_BamHI_for: CGG GAT CCA TGC AAC CTG GCA TTC and Su(H)_BamHI_rev: CGG GAT CCG GGG ACA CTA CTG CTG and using Su(H)-HApCS2+ as template. Su(H) was subcloned into GRpCS2+ (D. Turner and R. Rupp derivate) using the BamHI restriction sites. For preparation of sense mRNA, the construct was linearized with NotI and transcribed with SP6 polymerase.

MT-Ptf1a-GRpCS2+. The open reading frame of Ptf1a (DQ007931.1) was PCR amplified using the primers: Ptf1a_EcoRI_for: CGG AAT TCC ATG GAA ACG GTC C and Ptf1a_StuI_rev: GAA GGC CTC ATA TCA AGG CAC AAA GT. Ptf1a-GRpCS2+ was used as template in the PCR. The amplified Ptf1a was subcloned into MT-GRpCS2+ (D. Turner and R. Rupp derivate) uisng the EcoRI and StuI restrictions sites. For preparation of sense mRNA, the construct was linearized with NotI and transcribed with SP6 polymerase.

MT-Ptf1a$^{W224A/W242A}$-GRpCS2+. The open reading frame of Ptf1a$^{W224A/W242A}$ was PCR amplified with the following primers: Ptf1a_EcoRI_for: CGG AAT TCC ATG GAA ACG GTC C and Ptf1a_StuI_rev: GAA GGC CTC ATA TCA AGG CAC AAA GT. Ptf1a$^{W224A/W242A}$-GRpCS2+ served as template in the PCR. The amplified Ptf1a$^{W224A/W242A}$ was subcloned into MT-pCS2+GR (D. Turner and R. Rupp derivate) uisng the EcoRI and StuI restrictions sites. For preparation of sense mRNA, the construct was linearized with NotI and transcribed with SP6 polymerase.

2.1.6 Constructs for real-time RT-PCR standard curves

To perform standard curves in the real-time RT-PCR, the amplified RT-PCR products were subcloned into the pGEM-T easy vector (Promega). The amplified region is given with respect to the ATG.

Gad1pGEMT easy (U38225, 1126 to 1289); **ODCpGEMT easy** (X56316, 222 to 441); **N-tubulinpGEMT easy** (X15798, 80 to 329); **Hox11L2/Tlx3pGEMT easy** (AF283693, 9 to 274)

2.1.7 antisense RNA Constructs

Table 2.3 Summary of antisense RNA constructs

Name	Vector	Restriction enzyme	Polymerase	Reference
N-tubulin	pBluescriptst KS	BamHI	T3	Chitnis et al., 1995
Lbx1	pCS107	SalI	T7	Martin and Harland, 2006
Lim1/Lhx1	pBluescriptst-KS	XhoI	T7	Taira et al. 1994
Gad1	pBluescript SK+	BamHI	T7	Li et al., 2006
Hox11L2	BstEII	StuI	T3	Patterson and Krieg, 1999
Pax2	pT7TS	EcoRI	T3	-
Lmx1b	pGEM-T	SalI	T7	Haldin et al., 2003
Ngn1	pCS2P+	EcoRI	T7	Nieber et al., 2009
Ngn2	pBluescript II	BamHI	T3	Ma et al., 1996
Ngn3	pCS2P+	EcoRI	T7	Nieber et al., 2009
Ptf1a	pGEM-T	NotI	T7	Chen et al., 2004
Ptf1a sense	pGEM-T	SpeI	SP6	-

2.2 Methods

2.2.1 DNA standard methods

2.2.1.1 DNA restriction digestion

Restriction digests were performed according to the manufacturer's instruction using restriction enzymes purchased from Fermentas Life Sciences.

2.2.1.2 Agarose gel electrophoresis

TAE (Tris/Acetate/EDTA): 40 mM Tris-Acetate, pH 8.5, 2 mM EDTA

Analytical and preparative restrictions or PCR products were analysed by agarose gel electrophoresis (Sharp et al., 1973). Depending on the size of the DNA fragments, different percentages of agarose gels were used (0.7% to 2%). The gels were made out of agarose and 1x TAE buffer, which was also used as running buffer. To analyse the size of the DNA fragments, Standard DNA ladders (FastRuler DNA Ladder, Fermentas) were used. For visualization of the DNA, ethidium bromide (0.5 µg/ml) was added and for documentation the ChemiDoc video documentation system (EASY view) was used.

2.2.1.3 Purification of DNA fragments and linearized templates

Purification of DNA fragments from agarose gels or restriction digestions were performed with the "Invisorb Fragment Cleanup" kit (Invitek) or the "GFX

PCR DNA und Gel Band Purification" kit (GE Healthcare) according to the manufacturer's instructions.

2.2.1.4 Polymerase chain reaction (PCR)

A standard PCR reaction (Mullis et al., 1986) contained 1x Polymerase buffer, 0.2 mM of each dNTP (Thermo Scientific), 1.15 mM of each oligonucleotide and 0.5-1 U Pfu Polymerase (Stratagene GmbH) as well as 100 ng template DNA. The cycle numbers of the PCR reaction were adapted to the product size and the temperature adapted to the melting temperature of the oligonucleotides. The PCR reaction was performed in thermocyclers (Biometra) with the following program: 95 °C 2 min., 95 °C 45 sec., Tm-2 °C 45 sec., 72 °C 60 sec per 1 kb product, 72 °C 600 sec, 8 °C Pause.

2.2.1.5 DNA ligation

Standard ligation reactions were carried out using the T4 DNA Ligase (10 U/µl) (Fermentas Life Sciences) according to the manufacturer's instructions. The ligation was incubated overnight at room temperature (RT). To prevent self-religation, the linearised vector was treated with 1 U CIAP before ligation.

2.2.1.6 Chemical transformtaion of bacteria cells

For chemical transformation of the ligation reaction, the chemical competent cells XL1-Blue were used. 100 µl to 200 µl thawed cells were added to the ligation and incubated on ice for 30 min. After incubation, a heat shock at 42 °C for 90 sec was performed followed by a further incubation on ice for 3 min. 800 µl LB medium was added and the reaction was incubated for 45 min at 37 °C with mild shaking at 300 rpm. After centrifugation for 30 sec at 10,000 rpm, 800 µl supernatant was discarded and the bacteria pellett was resuspended in the remaining media. The bacteria solution was seeded on LB agar plates supplemented with the appropriate antibiotic for the selection of the transformed cells. Colonies were grown over night at 37 °C (Mandel and Higa 1970).

2.2.1.7 Plasmid DNA preparation

The bacteria were grown in 4 ml LB media together with the selective antibiotic overnight at 37 °C with shaking at 250 rpm. For the plasmid preparation, 3 ml of the bacteria culture was centrifuged for 2 min at 13,000 rpm. Isolation of DNA in analytical amounts was performed using the "GeneJET™ Plasmid Miniprep" kit (Fermentas) according to the manufacturer's protocol. Isolation of DNA in preparative amounts was carried out with the "NucleoBond®Xtra Midi" kit (Macherey-Nagel) following the manufacturer's protocol. The DNA concentration was measured with the NanoDrop-2000c spectrophotometer (Thermo Scientific) using 1 µl of the DNA sample.

2.2.1.8 DNA-sequencing

Sequencing of plasmid DNA (Sanger et al., 1977) was performed with the "Big Dye Terminator Cycle Sequencing" kit (Applied Biosystems) according to the manufacturer's protocol. The reaction was performed in a thermocycler with the following PCR program: 95 °C 2 min, 95 °C 30 sec., 55 °C 30 sec., 60 °C 4 min, 12 °C pause. In total, 26 cycles from step two to four were performed.

To purify the sequencing reaction, 1 µl EDTA (125 mM), 1 µl NaAc (3 M) and 50 µl 100% Ethanol were added and incubated for 5 min at RT. After centrifugation for 20 min at 13,000 rpm, the pellet was washed with 70% ethanol and centrifuged for 5 min with 13,000 rpm. The pellet was air-dried and resuspended in 15 µl HiDi. To sequence the reaction, the ABI 3100 xl Genetic Analyzer (Applied Biosystems) was used.

2.2.2 RNA techniques

2.2.2.1 *In vitro* synthesis of capped sense mRNA

In vitro capped sense mRNA was synthesized using the "SP6/T3 mMESSAGE mMACHINE" kit (Ambion Inc.) according to the manufacturer's protocol. For a 20 µl reaction, 1 µg of linearised plasmid was used. The purification of the synthesized mRNA was performed using the "Illustra RNASpin Mini" kit (GE Healthcare) according to the manufacturer's instructions. The RNA was eluted in 30 µl RNase-free water at 80 °C. The RNA concentration was measured using the NanoDrop 2000c spectrophotometer

(Thermo Scientific). The quality of the mRNA was analysed on a 1% agarose gel. The RNA was aliquoted in 2 µl and stored at -80 °C.

2.2.2.2 *In vitro* synthesis of antisense RNA

Antisense RNA was used in the whole mount *in situ* hybridization as probe to detect *in vivo* transcripts. To synthesize antisense RNA, 1 µg of the linearised plasmid was used in a 25 µl reaction. A standard reaction contained:

5x transcription buffer (Fermentas)	5 µl
ATP, GTP, CTP, UTP, Dig or Flu-UTP (10 mM each)	4 µl
DTT (0.75 M)	1 µl
Ribolock RNase inhibitor (40 U/µl) (Thermo Scientific)	1 µl
RNA polymerase (20 U/µl) (Fermentas)	1,5 µl

The reaction was incubated for two hours at 37 °C. Afterwards, the DNA template was digested by the addition of TURBO DNase™ (2 U/µl, Ambion) for 30 min at 37 °C. The purification of the antisense RNA was performed using the "RNeasy® Mini" kit (Qiagen GmbH) according to the manufacturer's protocol. The RNA was eluted in 100 µl RNase-free water at 80 °C. The quality of the antisense RNA was analysed on a 1% agarose gel. 1 ml of hybridization mix was immediately added to the antisense RNA and stored at -20 °C.

2.2.2.3 RNA isolation from ectodermal explants ("animal caps")

For total RNA isolation, 50 to 100 ectodermal explants were cut, frozen in liquid nitrogen and stored at -80 °C.
Total RNA isolation was performed using the "RNAqueous®-Micro" kit (Ambion) or trizol as described below. After RNA isolation according to both protocols, the RNA quality was evaluated with the 2100 Bioanalyzer (Agilent). To check for genomic DNA contamination, a control PCR with histone H4 (H4) was performed and analysed on a 2% agarose gel.

2.2.2.3.1 Isolation of total RNA with the "RNAqueous®-Micro" kit (Ambion)

The animal caps were lysated in 100 µl lysis buffer by a 29-Gauge syringe and centrifuged for 5 min at 4 °C. Afterwards, total RNA was isolated

according to the manufacturer's protocol. The RNA was eluted in 30 µl elution buffer at 75 °C. For genomic DNA digestion, the RNA was incubated with DNaseI provided within the kit for 1.5 h at 37 °C. The DNAseI activity was inhibited by incubation for 10 min at 70 °C followed by the use of the DNaseI inactivation reagent according to the manufacturer's protocol.

2.2.2.3.2 Isolation of total RNA with trizol

The animal caps were lysated in 400 µl trizol with a 29-Gauge syringe and vortexed for 30 sec. 80 µl chloroform was added, vortexed and centrifuged for 10 min at 4 °C and 13,000 rpm. After centrifugation, the upper phase, containing the total RNA (approximately 200 µl), was transferred to a new eppendorf tube. 200 µl chlorofom was added, vortexed for 30 sec and again centrifuged for 10 min at 4 °C. The supernatant was recovered and transferred into a new eppendorf tube and 500 µl isopropanol was added, mixed well and incubated at -20 °C for at least 2 h. After centrifugation at 4 °C and 13,000 rpm for 30 min, the precipitate was washed with 400 µl of 70% ethanol and centrifuged for 2 min at 4 °C. The pellet was air-dried and resolved in 30 µl RNase-free water. For genomic DNA digestion, the RNA was incubated with DNaseI (1U/µl) (Thermo Scientific) at 37 °C for 1.5 h. The DNAseI activity was inhibited by incubation for 10 min at 70 °C.

2.2.2.4 Reverse transcription and PCR (semi-quantitative and quantitative RT-PCR)

2.2.2.4.1 Reverse transcription

For cDNA sysnthesis, 50 ng to 100 ng total RNA was used per 10 µl reaction mix. A standard reaction mix contained 5 mM $MgCl_2$, 2.5 ng random hexamer, 5 mM dNTP mix, 8 U Ribolock RNase inhibitor (Thermo Scientific) and 20 U MuLV reverse transcriptase (Roche) in 1x Go Taq flexi buffer (Promega). The synthesis was performed in cycler using the following conditions: 20 °C for 20 min, 42 °C for 1 h and 95 °C for 5 min.

2.2.2.4.2 Semi-quantitative RT-PCR

For semi-quantitative RT-PCR analysis, 2.5 µl cDNA was added to a 12.5 µl total reaction volume. The standard reaction mix contained: 1x Go Taq reaction buffer (Promega), 0.2 mM of RT-primer each as well as 0.5 U Go-Taq DNA-Polymerase (Promega). The reaction was performed in a thermocycler with the following program: 2 min at 95 °C, 45 sec at 95 °C, 45 sec at annealingtemperature of the oligonucleotides, 45 sec at 72 °C, 5 min at 72 °C. The cycle number from step 2 to 5 of the PCR was adapted to the oligonucleotides. The RT-PCR was analysed on a 2% agarose gel.

2.2.2.4.3 Quantitative real-time RT-PCR

For quantitative real-time RT-PCR analysis, 5 µl cDNA was added to a 25 µl reaction volume. The standard reaction mix contained: 1x iQ^{TM}SYBRGreen Supermix (Biorad) and 0.2 mM RT-primers each. The real-time RT-PCR was performed with the IQ5 Biorad machine. All measurements were performed in triplicates and normalized to the values of ornithine decarboxylase (ODC). Two independent biological replicates were performed. The copy numbers were based on a standard dilution series.

2.2.2.5 Quantitative Nanostring

In addition for quantitative measurements, the digital multiplexed gene expression analysis system Nanostring was used according to the manufacturer's instructions using 500 ng of total RNA. The genes analysed by Nanostring as well as the target region and sequences of the reporter probes are shown in Appendix 6.3. To process the data, the counts were first normalized with respect to the geometric mean of the positive control counts using the nSolver software program provided by Nanostring. In a second step, the counts were normalized with respect to the geometric mean of ornithine decarboxylase (ODC). Even though additional housekeeping genes were present in the Nanostring set, only ODC was chosen for normalization as the other genes show developmental regulatory effects. Finally, a stringent background correction was performed by subtracting the mean and two standard deviations of the eight negative control counts for each lane. Negative

values were set to 1 as background level. Two independent experiments were performed.

2.2.2.6 RNA-sequencing

2.2.2.6.1 RNA isolation

For RNA-sequencing, total RNA was isolated with trizol as described above with the following modifications:
The ectodermal explants were lysated in 360 µl trizol with a 29-Gauge syringe and incubated for 10 min at RT. 72 µl chloroform was added, mixed and incubated for further 5 min at RT. After centrifugation for 20 min at 4 °C, the upper phase, containing the total RNA, was transferred to a new eppendorf tube. 180 µl isopropanol was added, mixed well and incubated at -20 °C for at least 2 h. After centrifugation at 4 °C for 30 min, the precipitate was washed with 500 µl of 75% ethanol. The pellet was air-dried and dissolved in 20 µl of RNase-free water. For genomic DNA digestion, the RNA was incubated for 1 h at 37 °C in a 50 µl reaction containing 1x DNaseI reaction buffer (Thermo Scientific), 1 µl DNaseI (Thermo Scientific) and 0.5 µl RNAse inhibitor (Thermo Scientific). The DNaseI digest was stopped by the addition of 150 µl RNase-free water and 200 µl Phenol-Chloroform-Isoamylalcohol. After mixing well, the solution was centrifuged for 10 min at 4 °C and the upper phase transferred to a new eppendorf tube. To the upper phase, 1/10 vol. of 5 M ammonium acetate and 1 vol of isopropanol was added and incubated for at least 2 h at -20 °C. After centrifugation for 30 min at 4 °C, the pellet was washed twice with 75% ethanol and air-dried. The pellet was resolved in 25 µl RNase-free water.
To evaluate the RNA quality, an analysis with the 2100 Bioanalyzer (Agilent) was performed. To check for genomic DNA contamination a control PCR with histone H4 was performed and analysed on a 2% agarose gel.

2.2.2.6.2 Sample preparation and sequencing

For sequencing, the RNA-samples were prepared with the "TruSeq RNA Sample Prep Kit v2" according to the manufacturer (Illumina). The sequencing was performed using the HiSeq 2000 (Illumina). Two independent biological replicates were performed.

2.2.2.6.3 Sequencing alignment

After quality control using FastQC (http://h.bioinformatics.babraham.ac.uk/projects/fastqc/), the sequence reads consisting of 2 x 95 base pairs from the paired-end mode were first aligned to the *Xenopus tropicalis* (*X. tropicalis*) using JGI v72b (kindly provided by Michael J. Gilchrist). Additionally, the reads were also aligned to selected sequences of the X. *laevis* transcriptome (UniGene Build #91 X. laevis) representing genes which were not found in the *X. tropicalis* transcriptome to get more information and to avoid redundancies.
The mapping was performed using the software Bowtie2 (version 2.0.0-beta5) in local alignment mode allowing 3 mismatches (Langmead and Salzberg, 2012). Reads aligned greater than 2 times were removed to facilitate the analysis.

2.2.2.6.4 Statistical analysis

First, the reads were counted on transcript level and the gene level expression was calculated as the sum of counts from all associated transcripts. After normalization between library samples, gene models with less than 50 read counts were subtracted from the data set. For the detection of differentially expressed genes, the DESeq package (Anders and Huber, 2010) (version 1.4.1) of bioconductor (http://h.bioconductor.org) was used.

2.2.3 *Xenopus laevis* embryo culture and microinjections

2.2.3.1 Stimulation of eggs

X. laevis female frogs were induced to lay eggs by the injection of 1000 units human chorionic gonadotropin (HCG, Sigma Aldrich) into the dorsal lymph sac the evening before the supposed egg-laying. The frogs were kept at 16 °C overnight. To induce the egg-laying later in the afternoon, the female *X. laevis* frogs were injected with 500 units of HCG into the dorsal lymph sac the evening before and kept at RT over night. The next morning the frogs were injected with 1000 units of HCG.

2.2.3.2 Preparation of *Xenopus laevis* testis

10x MBS: 880 mM NaCl, 10 mM KCl, 10 mM $MgSO_4$, 25 mM $NaHCO_3$, 50 mM HEPES, pH 7.8
1x MBS: 1x MBS, 0.7 mM $CaCl_2$

For *in vitro* fertilization of the eggs, the male *X. laevis* frog was sacrificed and the testis was removed, washed in 1x MBS and stored at 4 °C. For the fertilization, around one third of the testis was cut and diluted in 1x MBS and stored on ice.

2.2.3.3 Fertilization

Cysteine: 2% L-cysteine hydrochloride in 0.1x MBS, pH 8.0
10x MBS: 880 mM NaCl, 10 mM KCl, 10 mM $MgSO_4$, 25 mM $NaHCO_3$, 50 mM HEPES, pH 7.8
Nile Blue: 0.01% (w/v) Nile blue in 0.1x MBS

The layed eggs were *in vitro* fertilized using 50 µl of the testis diluted with 450 µl water. To remove the jelly coat, the eggs were treated with 2% cysteine hydrochloride, pH 8.0 and washed three times with 0.1x MBS. Albino embryos were additionally stained with Nile Blue vital dye for 5 min and washed three times with 0.1x MBS.

2.2.3.4 Microinjections

Injection buffer: 2% Ficoll in 1x MBS

Microinjections were performed on a cooling plate at 12.5 °C. For microinjections, the mRNA was loaded into glass needles, which were prepared on a needle puller (PN-30, Science Products GmbH, Hofheim). The microinjector PV 820 (H. Sauer, Reutlingen) was used. During and after the injections, the embryos were kept in injection buffer. 4 nl of the mRNA were injected either in one or in both blastomeres of two-cell stage embryos. After 1 h incubation in injection buffer, the embryos were transferred into 0.1x MBS and cultured in incubators until the desired developmental stage was reached. The

developmental stage of the embryos was defined according to Nieuwkoop and Faber.

2.2.3.5 *Xenopus laevis* ectodermal explants ("animal caps")

5xMBS AC: 880 mM NaCl, 10 mM KCl, 10 mM $MgSO_4$, 25 mM $NaHCO_3$, 2.05 mM $CaCl_2$, 1.65 mM $Ca(NO_3)_2$, pH 7.8

Animal caps were cut at blastula stage (stage 8 to 9) on a 1% agarose-coated Petri-dish in 0.8x MBS on a cooling plate set at 12.5 °C (Wallingford and Harland 2001). First, the vitelline membrane was carefully removed with foreceps and then the animal caps were excised from the animal hemisphere of the embryo using the gastromaster system (Xenotek Engineering, Bellville, USA). The ectodermal explants were cultivated in 0.8x MBS until control whole embryos reached the desired developmental stage.

2.2.3.6 Treatment of whole embryos and animal caps

2.2.3.6.1 Dexamethasone (Dex) treatment

Dexamethasone
stock: 4 mg/ml in 100% ethanol, working: 10 µM

To control the time point of protein activity, hormone-inducible constructs were used for microinjections. Therefore, the coding regions were fused to the ligand-binding domain of the glucocorticoid receptor (Gammill and Sive, 1997). To induce protein activity, injected embryos or animal caps were cultivated in the dark in the presence of 10 µM dexamethasone in 0.8x MBS until the desired stage was reached (Perron et al., 1999). For the 3 and 6 h time point, the animal caps were incubated at 14 °C. For the 9 h and the 25 h as well as for the 32 h time point, the animal caps were incubated at 16 °C and 18 °C, respectively.

2.2.3.6.2 Cycloheximide (CHX) treatment

Cycloheximide
stock: 100 mg/µl in DMSO (Sigma-Aldrich), working: 10 µg/ml

To block protein synthesis, animal caps were treated with 10 µg/ml CHX in 0.8x MBS (Perron et al., 1999) and incubated at 16 °C.

2.2.4 Whole mount *in situ* hybridization

Whole mount *in situ* hybridization was performed to visualize the spatial and temporally expression of endogenous RNA transcripts. For detection, a Digoxigenin or Fluorescin labeled antisense RNA probe was used, which was visualized using an alkaline phosphatase-coupled anti-Dig antibody or FastRed (Roche) (Harland, 1991; Hollemann and Pieler, 1999; Nieber et al., 2009).

2.2.4.1 Fixation and β-Gal staining

10x MEM: 1 M Mops, 20 mM EGTA, 10 mM $MgSO_4$, pH 7.4, sterile filtered and stored in dark
10x PBS: 1.75 M NaCl, 1 M KCl, 65 mM Na_2HPO_4, 18 mM KH_2PO_4, pH 7.4
$K_3FE(CN)_6$: 0.5 M in H_2O, stored in dark
$K_4FE(CN)_6$: 0.5 M in H_2O stored in dark
MEMFA: 4% (v/v) formaldehyde (37%) in 1x MEM
X-Gal: 40 mg/ml 5-Bromo-4-chloro-3-indolyl-b-D-galactopyranoside in formamide, stored -20 °C in the dark
X-Gal staining solution: 1 mg/ml X-Gal, 5 mM $K_3FE(CN)_6$, 5 mM $K_4FE(CN)_6$, 2 mM $MgCl_2$ in 1x PBS

Embryos were collected in glas vials and fixed in MEMFA at RT. Uninjected-embryos were fixed for 1 h and washed three times with 100% ethanol for 5 min. Injected embryos were fixed for 25 min and washed three times with 1x PBS for 10 min.
LacZ (*β-gal*) mRNA was co-injected as a lineage tracer to discriminate the injected from the uninjected side of the embryo and to analyse the distribution of the injected mRNA. To visualize the β-gal injected side of the embryos, X-Gal staining was performed (Hardcastle et al., 2000). Therefore, the embryos were incubated in the dark in X-gal solution for at least 20 min until the desired level of staining was achieved. Afterwards, the embryos were washed three times for

10 min in 1x PBS and refixed for 25 min in 1x MEMFA. Finally, the embryos were washed three times for 5 min in 100% ethanol and stored at -20 °C.

2.2.4.2 Rehydration

PTW: 0.1% Tween-20 in 1x PBS

The following steps were performed at RT in 4 ml solution with mild agitation. The embryos were rehydrated using an ethanol series (75%, 50%, 25%) and finally incubated 4 times for 5 min in 100% PTW.

2.2.4.3 Proteinase K treatment

Proteinase K: 10 µg/ml proteinase K in 0.1x PBS
PTW: 0.1% Tween-20 in 1x PBS

To make the embryos accesible to the Dioxigenin labeled antisense RNA probe, the embryos were treated with proteinase K (Merck). Therefore, the embryos were incubated in a 2 ml PTW/proteinase K-solution (10 µg/ml PTW) for a defined time depending on the developmental stage. Embryos of developmental stage 28/29 were treated for 17 min in proteinase K solution.

2.2.4.4 Acetylation and refixation

PTW: 0.1% Tween-20 in 1x PBS
0.1 M Triethanolamine: 0.93 g Triethanolamine in H_2O, pH 7.5

To stop the proteinase K treatment, the embryos were washed two times for 5 min in triethanolamine. To avoid unspecific reaction of the Dioxigenin labeled antisense RNA probe, free amino-acid ends were blocked by treating the embryos with 25 µl acetic anhydride in triethanolamine. Afterwards the embryos were washed two times for 5 min with PTW and refixed in 4% formaldehyde (v/v) in PTW for 20 min. Before hybridization, the embryos were washed again 5 times for 5 min in PTW.

2.2.4.5 Hybridization

Hybridization Mix: 50% formamide, 1 mg/ml Torula RNA, 10 µg/ml Heparin, 1x Denhardt's, 0.1% Tween-20, 0.1% CHAPS, 10 mM EDTA in 5x SSC
20X SSC: 3 M NaCl, 0.3 M NaCitrate, pH 7.2-7.4
100x Denhardts solution: 1 g BSA, 1 g Polyvinylpyrollidone (PVP), 1 g Ficoll,

For pre-hybridization, the embryos were first incubated in 1 ml fresh hybridization mix and then after exchanging the hybridization mix, for at least 5 h at 65 °C. Afterwards, the embryos were incubated in 1 ml hybridization mix containing the Dioxigenin labeled antisense RNA probe overnight at 65 °C.

2.2.4.6 Washing

20X SSC: 3 M NaCl, 0.3 M NaCitrate, pH 7.2-7.4
MAB: 100 mM maleic acid, 150 mM NaCl, pH 7.5

The next morning, the hybridization mix conatining the antisense RNA probe was exchanged for fresh hybridization mix for 10 min at 65 °C. Afterwards, the embryos were washed three times with 2x SSC for 15 min at 65 °C. To remove unspecific and unbound RNA probes, the embryos were washed and treated for 1 h at 37 °C with RNAse A (10 µg/ml, Fermentas) and RNAse T1 (10 U/ml, Fermentas) in 2x SSC. After a short washing step with 2x SCC for 5 min, the embryos were incubated two times in 0.2x SSC at 65 °C. Finally, the embryos were transferred into MAB and incubated two times for 15 min.

2.2.4.7 Blocking and antibody reaction

MAB: 100 mM maleic acid, 150 mM NaCl, pH 7.5
MAB/BMB: 2% BMB in 1x MAB
MAB/BMB/HS: 2% BMB, 20% heat-treated horse serum in 1x MAB

To avoid additionally unspecific binding, the embryos were treated with blocking buffer containing MAB and the Boehringer Mannheim Blocking reagent (BMB) as well as horse serum (Gibco). First, the embryos were washed 15 min in MAB/BMB, which was exchanged for MAB/BMB/HS for 40 min. For detection,

the Sheep alkaline phosphatase-coupled anti-Dig antibody (1:5000, Sigma) was used and the embryos were incubated for 4 h at RT. Afterwards, the embryos were washed 3 times for 10 min and then overnight at 4 °C with MAB.

2.2.4.8 Staining reaction

APB: 100 mM Tris-HCl, pH 9.0, 50 mM $MgCl_2$, 100 mM NaCl, 0.1% Tween-20, pH 9.0
NBT: 100 mg/ml in 70% Dimethylformamide, stored in dark
BCIP: 50 mg/ml in 100% Dimethylformamide, stored in dark

The next day, the embryos were washed 5 times for 5 min with MAB, followed by two times for 5 min with ABP at 4 °C. The staining reaction was performed in the dark until the desired staining was reached using a mixture of BCIP/NBT, a substrate of the alkaline phosphatase.

2.2.4.9 Destaining and refixation

To remove background staining, the embryos were treated stepwise with methanol of different perncentage (100%, 75%, 50%, 25%). Finally, the embryos were refixed with MEMFA for 15 min at RT. The MEMFA was replaced by fresh MEMFA for long storage of the embryos at 4 °C.

2.2.4.10 Bleaching

20X SSC: 3 M NaCl, 0.3 M NaCitrate, pH 7.2-7.4
MEMFA: 4% (v/v) formaldehyde (37%) in 1x MEM

Pigmented embryos were bleached using one of two different methods and afterwards fixed with MEMFA for long storage.
To reduce the background, the embryos were first destained with 100% methanol. For a more sensitive bleaching, the embryos were incubated in a mixture of 75% methanol/H_2O_2 for up to three days, followed by treatments with 50% and 25% methanol. More time efficient, the embryos were incubated for 1 to 2 h in the following solution at RT: 5x SSC, 50% formamide and 1-2% H_2O_2. Finally, two washing steps with 5x SSC for 5 min were performed before fixation.

2.2.5 Vibratome sectioning

Gelatin/Albumin: 4.88 mg/ml gelatin was dissolved in PBS. Afterwards, 0.3 g/ml bovine serum albumin and 0.2 mg/ml sucrose were added and dissolved. The solution was sterile filtered and stored at -20 °C.
Mowiol: 5 g Mowiol was dissolved in 20 ml PBS by stirring for more than 16 h. Afterwards, 10 ml glycerol was added and stirred for 16 h. The supernatant was recovered and a pH of 7.0 was adjusted. The solution was stored at -20 °C.

For vibratome sectioning, the whole embryos were embedded in a mixture of gelatin and albumin by adding gluturylaldehyde. The embryos were vibratome sectioned at 30 µM using a vibratome (Leica VT1000M). The sections were collected on glass slides and covered with a cover slip using mowiol.

2.2.6 Protein standard techniques

2.2.6.1 Protein-protein interaction *in vivo* (Co-immunoprecipitation)

Table 2.4. Summary of antibodies and working dilutions

	Name	Company	dilution WB	dilution IP
Primary antibody	Mouse monoclonal HA.11	Covance	1:1000	1:150
	Goat polyclonal MT	Abcam	1:10 000	1:250
Secondary antibody	anti-mouse-HRP	Santa Cruz	1:5000	
	anti-goat-HRP	Santa Cruz	1:10 000	

Co-IP buffer: 10 mM Tris-HCl, pH 7.5, 100 mM NaCl, 2 mM EDTA, 1 mM EGTA, 0.5 % (v/v) NP-40, 10 % (v/v) glycerol, 1mM Sodium-Orthovanadate, 1mM b-Glycerolphosphate, 1mM NaF, protease inhibitor cocktail (1 tablet per 50 ml Co-IP buffer, Roche)
6x SDS sample buffer: 125 mM Tris pH 6.8, 30% glycerol, 10% SDS, 0.6 M DTT, 0.012% Bromphenol blue

For a Co-immunoprecipitation assay, 25 injected embryos were harvested at gastrula stage. The embryos were lysated with a 27-gauge-syringe in 500 µl Co-IP buffer. The lysates were centrifuged for 15 min at 4 °C and the

supernatant was transferred to a new eppendorf tube. 50 µl of the lysates were transferred to a new eppendorf tube and served later as input control (10%). To the input samples, 10 µl 6x SDS loading buffer was added and heated for 3 min at 95 °C before storing at -20 °C. The Co-IP samples were adjusted to 500 µl with the Co-IP buffer. For pre-clearing, 30 µl of Y-bind sepharose immunopellets (GE Healthcare) were added. The Co-IP samples were incubated for 30 min at 4 °C on a rotating wheel and then centrifuged for 20 sec at 2,000 rpm. Afterwards, the supernatants were transferred to a new eppendorf tube and split in 250 µl each. To the Co-IP samples the specific antibodies were added. The samples were incubated for 2 h at 4 °C on a rotating wheel. Afterwards 20 µl of the Y-bind sepharose immunopellets was added. The Co-IP samples were incubated for another 2 h at 4 °C on a rotating wheel. Finally, the samples were centrifuged for 30 sec at 2,000 rpm and the pellets were washed 5 times with 1 ml Co-IP buffer. The supernatant was removed and 10 µl of 6x loading buffer were added. The Co-IP samples were incubated for 3 min at 95 °C and stored at -20 °C.

2.2.6.2 SDS-Polyacrylamide gel electrophoresis

10x Laemmli buffer: 250 mM Tris-base, 2.5 M Glycine, 0.1% SDS

To separate denatured proteins according to their molecular weight in an electric field, SDS-polyacrylamide gel electrophoresis was performed (Laemmli, 1970). To denaturate the proteins, the samples were diluted with 6x SDS loading buffer and boiled for 3 min at 95 °C in a water bath. For separation of the denatured proteins, a 12% SDS gel was used and prepared according to standard protocols (Sambrook and Russel, 2001). To visualize the size of the proteins molecular weight, a standard protein marker was used (Page Ruler^{TM} prestained protein ladder, Thermo Scientific). The gel electrophoresis was performed using 1x Laemmli buffer as running buffer. First, a voltage of 100 V was applied and when the bromphenol-blue front reached the separating gel, the voltage was raised to 250 V.

2.2.6.3 Western blot

Blocking Buffer: 5% (w/v) dry, non fat-milk powder in PBS-T

PBS-T: 1x PBS, 0.5% (v/v) Tween 20
Anode blotting buffer 1: 0.3 M Tris, 10% methanol, pH 10.4
Anode blotting buffer 2: 25 mM Tris, 10% methanol, pH 10.4
Cathode blotting buffer: 25 mM Tris, 40 mM glycine, 10% methanol, pH 9.4

After separation, the proteins were transferred from the polyacrylamide gel to a nitrocellulose membrane using the semi-dried blotting method for 1 h (Sambrook and Russel, 2001; Towbin et al., 1979). To minimize unspecific binding, the nitrocellulose membrane was blocked for 1 h at RT using 5% (w/v) milk powder in PBS-T buffer. Afterwards, the nitrocellulose membrane was incubated overnight at 4 °C in milk buffer containing the first antibody. The following morning, the membrane was washed with 1x PBS-T for 30 min at RT thereby exchanging the buffer every ten minutes. Afterwards, the second antibody in milk buffer was added. After 1 h incubation at RT, the nitrocellulose membrane was again washed for 30 min with 1x PBS-T. For detection, the membrane was incubated with the chemiluminescent substrate "Super Signal West Dura" (Thermo Scientific) according to the manufacturer's protocol and then exposed to X-ray detection films (Amersham).

3. Results

3.1 Ptf1a promotes general neurogenesis and specifies GABAergic inhibitory interneurons at the expense of other neuronal cell types

The bHLH transcription factor Ptf1a functions in the nervous system to promote generation of GABAergic inhibitory interneurons at the expense of glutamatergic excitatory neurons in the spinal cord, cerebellum and retina (Glasgow et al., 2005; Hoshino et al., 2005; Fujitani et al., 2006; Nakhai et al., 2007; Pascual et al., 2007; Dullin et al., 2007). Microinjection of *Ptf1a-GR* mRNA is sufficient to induce ectopic neurons in animal caps and in the non-neural ectoderm of *X. laevis* embryos and these neurons have a GABAergic identity (Dullin et al., 2007; Hedderich, 2008). Thus, Ptf1a not only acts as a GABAergic selector gene in the post-mitotic neurons, but also drives neuronal cell commitment of progenitor cells.

In the mouse, *Ptf1a* is expressed in the dorsal horn of the spinal cord in the progenitor domain of the dI4 and later dIL_A neurons, which give rise to GABAergic inhibitory interneurons (Glasgow et al., 2005); the dI4 and dIL_A neurons can be molecularly identified by a specific code of HD transcription factors consisting of *Pax2*, *Lbx1*, *Lhx1* and *Lhx5* (Glasgow et al., 2005; Helms and Johnson, 2003). In *X. laevis,* the domains and combinatorial codes of transcription factors that characterise distinct neuronal subtype domains are not well defined. Therefore, to evaluate Ptf1a activity during the development of the *X. laevis* nervous system, gain-of-function experiments analysing marker genes indicative of specific neuronal subtype identities in embryos were performed. To control the onset of protein activity, the ligand-binding domain of the glucocorticoid receptor was fused to the C-terminus of Ptf1a (Ptf1a-GR) (Afelik et al., 2006). In the absence of the ligand dexamethasone (Dex), the fusion proteins are bound by heat shock proteins and remain transcriptionally inactive in the cytoplasm. Upon addition of dexamethasone, the fusion proteins translocate into the nucleus and regulate transcription of target genes (Gammill and Sive, 1997).

Ptf1a-GR mRNA was injected into one blastomere of two-cell stage embryos together with *LacZ* mRNA, in order to localize the distribution of the

injected mRNA. At early gastrula stage (stage 10), the injected embryos were treated with dexamethasone to induce Ptf1a-GR protein activity. In agreement with previous reports (Dullin et al., 2007; Hedderich, 2008), overexpression of *Ptf1a-GR* mRNA in the *X. laevis* hindbrain and spinal cord promoted a dramatic increase in expression of the post-mitotic neuronal marker *N-tubulin* and of *Glutamic acid decarboxylase* (*Gad1*), an enzyme that catalyses the synthesis of GABA and is indicative of GABAergic inhibitory neurons (Li et al., 2006) (Fig. 3.1 B, B' and C, C'). In line with studies in the murine nervous system (Glasgow et al., 2005), overexpression of *Ptf1a-GR* mRNA also promoted the activation of *Pax2* and *Lhx1*, which mark dorsal interneuron populations (Fig. 3.1 E, E' and F, F'). Additionally, *Lbx1* expression was induced, which also encodes for a transcription factor required in the post-mitotic neurons to specify a GABAergic interneuronal subtype (Fig. 3.1 D, D') (Cheng et al., 2005). In contrast, transcription factors expressed in neuronal domains more ventral to the endogenous *Ptf1a* progenitor domain, such as *Hox11L2* or *Lmx1b* (Fig. 3.1 G, G' and H, H) were inhibited by Ptf1a. Similar results were reported for Ptf1a in the murine spinal cord (Glasgow et al., 2005).

While Ptf1a is thought to function as a transcriptional activator (Cockell et al., 1989; Krapp et al., 1996), many transcription factors have been shown to act both as transcriptional activators or repressors in a context-dependent fashion (Iype et al., 2004; Yu et al., 2005; Sakabe et al., 2012). The expression of the above marker genes was therefore evaluated upon microinjection of a hormone-inducible version of Ptf1a that was fused to a heterologous strong activator domain derived from VP16 (Ptf1a-VP16-GR) (Sadowski et al., 1988; Dullin et al., 2007). Similar to *Ptf1a-GR*, overexpression of *Ptf1a-VP16-GR* mRNA induced strong expression of the GABAergic interneuronal markers *Gad1*, *Pax2*, *Lhx1* and *Lbx1* (Fig. 3.1 J, J'; K, K'; L, L' and M, M') as well as of the general neuronal marker *N-tubulin* (Fig. 3.1 I, I'). Moreover, the expression of *Hox11L2* and *Lmx1b* was still inhibited (Fig. 3.1 N, N' and O, O'), suggesting that the repression by Ptf1a is indirect.

The ability of Ptf1a to induce general neurogenesis in the non-neural ectoderm of *X. laevis* embryos and in animal caps is similar to that of the proneural bHLH transcription factor Neurogenin 2 (Ngn2, also known as X-ngnr-1) (Ma et al., 1996). However, while Ptf1a induces *Gad1*, a GABAergic marker

in such assays (Dullin et al., 2007; Hedderich, 2008), Ngn2 promotes the expression of *Hox11L2*, a marker for cranial sensory ganglia and Rohon-Beard sensory neurons (Perron et al., 1999; Dullin et al., 2007; Hedderich, 2008). *Hox11L2* is the *X. laevis* ortholog of *Tlx3*, which has been shown in mouse to act as a selector gene promoting a glutamatergic excitatory at the expense of a GABAergic inhibitory cell fate (Cheng et al., 2004; Cheng et al., 2005). In the *X. laevis* neural tube, overexpression of *Ngn2-GR* mRNA strongly activated the expression of *N-tubulin* (Fig. 3.1 P, P'), similar to *Ptf1a-GR* and *Ptf1a-VP16-GR* mRNA. In contrast, *Ngn2-GR* mRNA did not influence *Gad1*, *Pax2*, *Lbx1* or *Lhx1* expression (Fig. 3.1 Q, Q'; R, R'; S, S'; T, T'), but instead led to ectopic activation of *Hox11L2/Tlx3* (Fig. 3.1 V, V'). Moreover, *Ngn2-GR* mRNA had no effect on the expression of *Lmx1b* (Fig. 3.1 U, U'), which was repressed by injection of *Ptf1a-GR* and *Ptf1a-VP16-GR* mRNA.

Interestingly, overexpression of *Ptf1a-GR* and *Ptf1a-VP16-GR* mRNA not only led to an induction or suppression of the described marker genes, but additionally resulted in a strong increase in tissue formation on the injected side of the embryo (Fig. 3.1 B, B' - O, O'). It can be excluded that the extra tissue formation is a general consequence of mRNA overexpression, as the effect was not upon microinjection of *Ngn2-GR* mRNA (Fig. 3.1 P, P' - V, V'). However, the identity of the extra tissue promoted by *Ptf1a-GR* and *Ptf1a-VP16-GR* mRNA overexpression could not be elucidated so far.

Taken together, these findings demonstrate that Ptf1a like Ngn2 promotes general neurogenesis and that Ptf1a confers GABAergic interneuron subtype specification at the expense of other neuronal subtypes. In contrast, Ngn2 induces a glutamatergic excitatory cell fate.

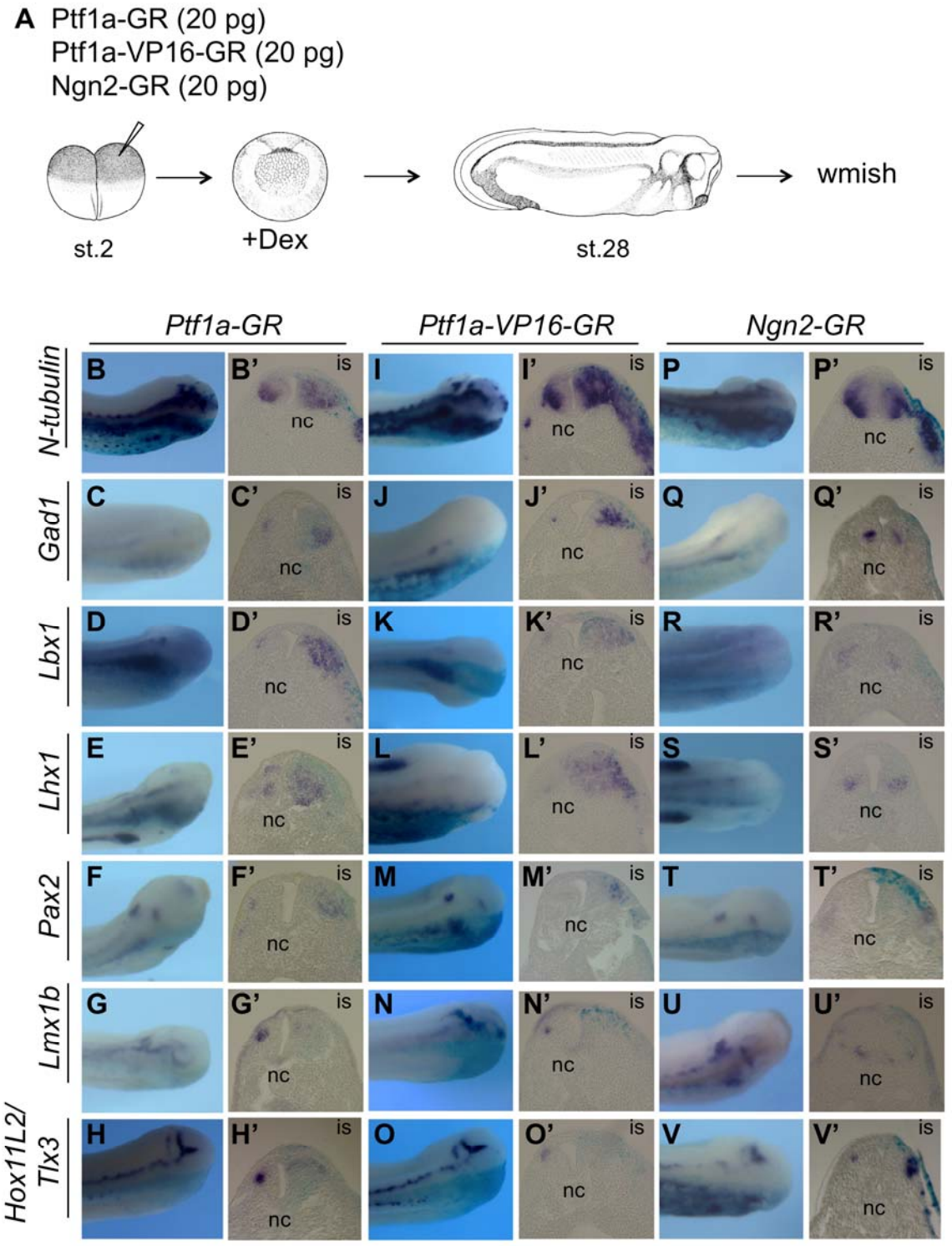

Figure 3.1 Ptf1a promotes general neurogenesis and specifies GABAergic inhibitory interneurons at the expense of other neuronal cell types.
(A) The mRNAs indicated above (20 pg each) were co-injected with *LacZ* mRNA (75 pg) into one blastomere at the two-cell stage. Protein activity was induced by dexamethasone (Dex) at the equivalent of stage 10. (**B-V)** Gene expression was analysed by whole mount *in situ* hybridization (wmish) using markers indicated on the left side. (B-V) Dorsal view of the head region and (B'-V') the corresponding transversal section through the hindbrain at the level of the otic vesicle of stage 28 *X. laevis* embryos. The injected side is always at the bottom of the whole head view and to the right on the sections. nc, notochord, is, injected side.

3.2 Ptf1a and Ngn2 promote general neurogenesis via activation of the same gene network

The ability of Ptf1a to induce general neuronal differentiation in *X. laevis* embryos is similar to the activity of the bHLH transcription factor Ngn2. However, both transcription factors confer distinct neuronal subtype identities (Fig. 3.1). This raises the question, if Ptf1a and Ngn2 activate the same or a different gene network, to achieve general neurogenesis. Previous results in whole embryos analysing only a limited set of marker genes suggested that Ptf1a and Ngn2 drive general neurogenesis in progenitors through the same cascade of neuronal differentiation factors (Hedderich, 2008). To obtain a higher resolution comparison, a temporal expression analysis of genes induced by *Ptf1a-GR* and *Ngn2-GR* mRNA overexpression was performed utilizing the animal cap assay. Animal caps are embryonic pluripotent cells excised from the animal pole of *X. laevis* embryos of the blastula stage. Untreated animal caps will give rise to atypical epidermal tissue. However upon treatment or injection of various factors, the animal caps can obtain cell fates of all three germ layers (Borchers and Pieler, 2010).

Ptf1a-GR or *Ngn2-GR* mRNA were injected into both blastomeres of two-cell stage *X. laevis* embryos, animal caps were excised at blastula stage and treated with dexamethasone to induce protein activity (Fig. 3.2 A). The animal caps were collected 3, 6 and 25 h after addition of dexamethasone. Total RNA was isolated and the levels of specific mRNAs digitally quantified without amplification using Nanostring nCounter multiplex analysis, which employs target-specific fluorescent barcodes and single molecule imaging (Geiss et al., 2008; Kulkarni, 2011) (Fig. 3.2 and Appendix 6.1.1). The analysis of a selected set of genes is represented in Figure 3.2. Animal caps that were injected, but not treated with dexamethasone served as a negative control and did not significantly express any of the analysed marker genes (Fig. 3.2 B-M). Both *Ptf1a-GR* and *Ngn2-GR* mRNA overexpression was sufficient to induce the expression of the Notch-ligand *Dll1* (Fig. 3.2 B), the cell-cycle inhibitor *Cdknx* (Fig. 3.2 C) as well as of the zinc-finger transcription factor *Myt1* (Fig. 3.2 D) 3 h after dexamethasone induction. Other neuronal differentiation genes such as *Ebf2* (Fig. 3.2 E), *Ebf3* (Appendix 6.1.1), *NeuroD1* (Fig. 3.2 F) and *NeuroD4* (Appendix 6.1.1) were also strongly induced by *Ptf1a-GR* and *Ngn2-GR* mRNA

after 25 h of protein induction. Similarly, overexpression of *Ptf1a-GR* and *Ngn2-GR* mRNA led to a high induction of the post-mitotic marker *N-tubulin* (Fig. 3.2 G) and the cell cycle regulator *Pak3* (Appendix 6.1.1) after 25 h of protein induction. In regard to GABAergic neuronal subtype specification, *Ptf1a-GR* but not *Ngn2-GR* mRNA strongly induced *Gad1* (Fig. 3.2 H) expression as well as the expression of *Pax2* (Fig. 3.2 J), *Lhx5* (Fig. 3.2 I), *Lbx1* (Appendix 6.1.1) and *Lhx1* (Appendix 6.1.1) after 25 h. In contrast, *Ngn2-GR* mRNA robustly induced the marker genes for glutamatergic excitatory neurons such as *Hox11L2/Tlx3* (Fig. 3.2 L) and *Vglut1* (Fig. 3.2 M). Furthermore, Ngn2-GR induced the expression of the PR domain containing zinc finger transcription factor *Prdm14* more than a 1000-fold (Fig. 3.2 K), however, the function of which in the nervous system is still unknown (Fog et al., 2012). Interestingly, *Ptf1a-GR* mRNA overexpression in animal caps also led to an increase in *Lmx1b* expression (Appendix 6.1.1), a transcription factor involved in glutamatergic excitatory neuron formation and normally suppressed by Ptf1a in the spinal cord (Fig. 3.1 G, G') (Glasgow et al., 2005).

In summary, both Ptf1a and Ngn2 drive early steps of general neurogenesis through activation of an overlapping set of downstream target genes in a similar temporal order. However, later in development, Ptf1a and Ngn2 induce unique sets of downstream genes to confer specific neuronal subtype identities in post-mitotic neurons.

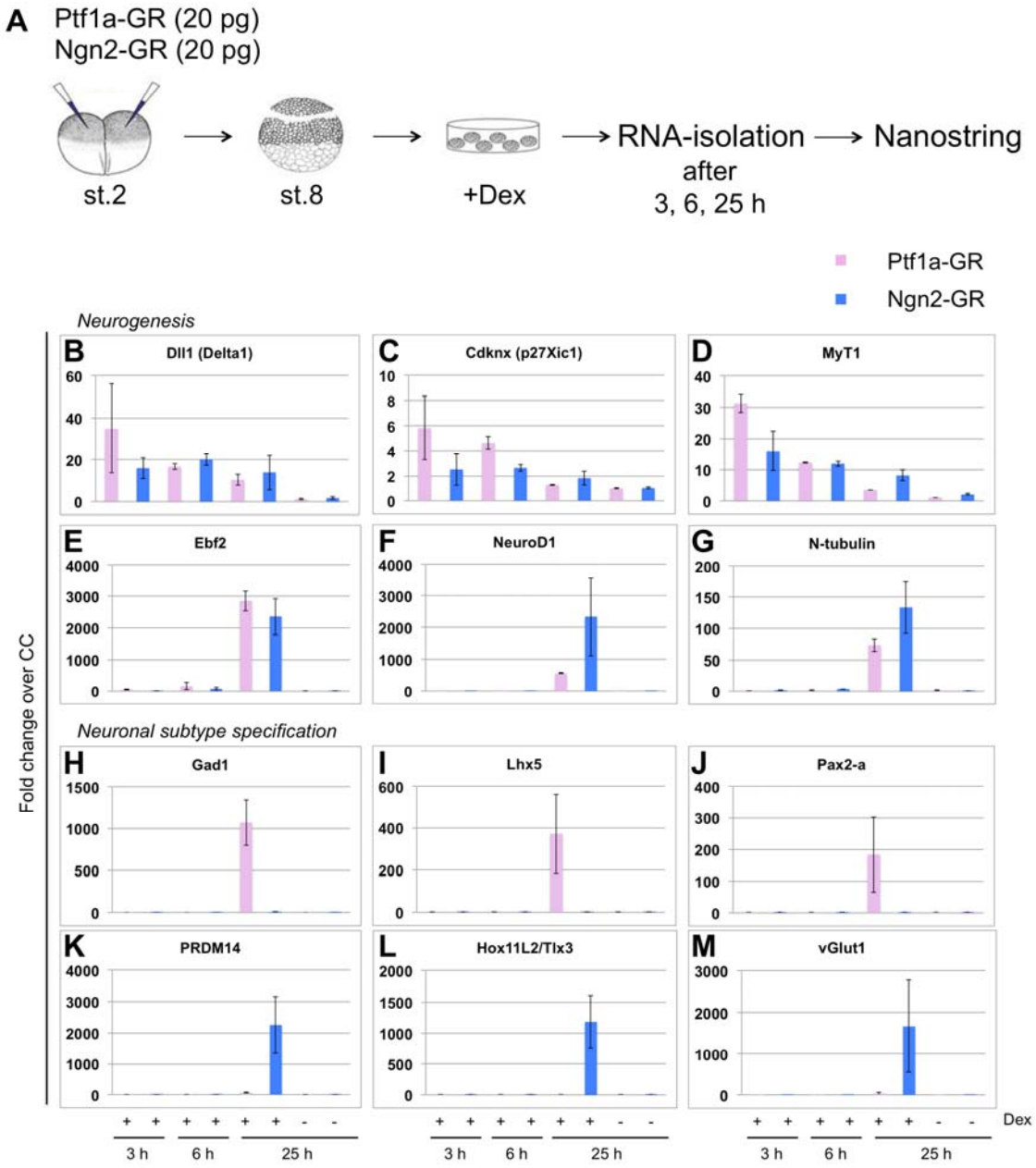

Figure 3.2 Ptf1a and Ngn2 promote general neurogenesis via activation of the same gene network.
Comparative temporal analysis of genes induced by *Ptf1a-GR* and *Ngn2-GR* mRNA in animal cap assays. **(A)** The indicated mRNAs (20 pg each) were injected into both blastomeres of two-cell stage embryos, animal caps excised at the blastula stage and treated with dexamethasone (Dex). Animal caps were cultured for 3, 6 or 25 h, which corresponds to stage 9, 10 and 23 of sibling embryos. Total RNA was isolated and marker gene expression analysed by the Nanostring nCounter system. **(B-M)** Shown is the averaged fold change over uninjected control caps (CC) of two independent experiments. Error bars represent the standard error of the mean (+/-SEM). Note the different scales in each diagram. Shown are graphs of selected genes, for a full list see Appendix 6.1.1.

3.3 Ptf1a is able to drive both general neurogenesis and neuronal subtype specification when induced after neural tube closure

Multiple proneural bHLH genes have been identified in vertebrates, including *X. laevis* (Lee, 1997). Analysis of the expression pattern of the *X. laevis* proneural genes reveals expression in overlapping and distinct domains in the CNS (Fig. 1.3) (Nieber et al., 2009; Kim et al., 1997; Kanekar et al., 1997; Ferreiro et al., 1993; Turner and Weintraub, 1994), suggesting that the proneural genes may have discrete activities in generating specific neuronal identities. By whole mount *in situ* hybridization, the earliest specific expression of Ptf1a is detected at stage 19 in a single longitudinal domain within the neural folds (Afelik et al., 2006). At late tadpole stages, *Ptf1a* is specifically expressed in the hindbrain, the spinal cord and the retina as well as in the ventral and dorsal pancreatic bud (Afelik et al., 2006). Previous experiments had shown that Ptf1a-GR, when activated at gastrula stage, is able to drive general neurogenesis (Dullin et al., 2007; Hedderich, 2008). To analyse, if the expression of Ptf1a at stage 19 may indicate an early physiological function in inducing general neurogenesis, *Ptf1a-GR* mRNA was injected into one blastomere of two-cell stage embryos and protein activity induced at stage 19 (Fig. 3.3 A).

Gene expression analysis by *in situ* hybridization showed that in contrast to induction of Ptf1a-GR activity during early gastrula stages, induction at stage 19, when the ectoderm has obtained an epidermal fate, did not lead to ectopic *N-tubulin* or *Gad1* expression (Fig. 3.3 B and C). However, the corresponding sections through the hindbrain revealed increased expression of both marker genes on the injected side (Fig. 3.3 B' and C'). This result demonstrates that Ptf1a-GR, when induced at a time when endogenous Ptf1a is present, is still able to promote general neurogenesis and a GABAergic interneuronal identity within the neural tube. Moreover, Ptf1a-GR activated at stage 19 was still able to inhibit *Hox11L2/Tlx3* expression on the injected side of the embryo (Fig. 3.3 D, D').

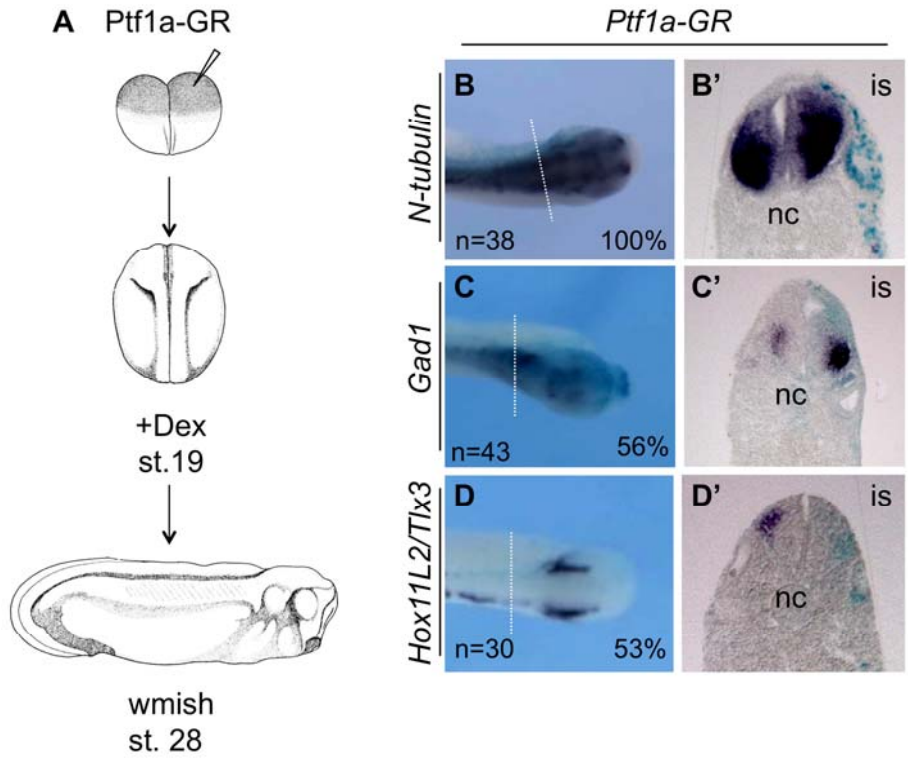

Figure 3.3 Ptf1a is able to drive general neurogenesis and neuronal subtype specification when induced after neural tube closure. (A) *Ptf1a-GR* mRNA (20 pg) was injected into one blastomere of two-cell stage embryos and induced at stage 19 with dexamethasone (Dex). **(B-D)** Gene expression was analysed by whole mount *in situ* hybridization (wmish) of stage 28 *X. laevis* embryos using markers indicated on the left side. (B-D) Dorsal view of the head region with the injected side at the top and (B'-D') the corresponding transversal sections through the hindbrain at the level of the otic vesicle are shown with the injected side to the right. nc, notochord; is, injected side

3.4 Ptf1a is maternally expressed in *X. laevis*

The ability of Ptf1a to induce general neurogenesis before neural tube closure might reflect an early physiological activity. To evaluate if *Ptf1a* might be expressed earlier than detected by *in situ* hybridization, a semi-quantitative RT-PCR of different developmentally staged *X. laevis* embryos analysed for *Ptf1a* transcripts was performed, surprisingly revealing maternal expression of *Ptf1a* (Fig. 3.4 A). *Ptf1a* transcripts were maintained at constant levels until late gastrula stage (stage 11), demonstrating that *Ptf1a* is actually expressed when the first neurons are being born. From early neurula stages (stage 13) onwards, the level of *Ptf1a* expression decreased and increased again after neural tube closure (stage 20). Gene expression analysis by *in situ* hybridization revealed that the maternal *Ptf1a* transcripts are restricted to the animal half of the embryo at early cleavage stages (stage 2 and stage 6) (Fig. 3.4 B and C). At early

gastrula stage (stage 10.5), *Ptf1a* transcripts were excluded from the blastoporus (Fig. 3.4 D). Consistent with previous reports (Afelik et al., 2006), at later neurula stages, weak and diffuse *Ptf1a* expression was detectable in a single longitudinal domain within the neural folds, which became stronger after neural tube closure (Fig. 3.4 E and F). To exclude unspecific background staining, particularly at the early stages, *in situ* hybridization with a Ptf1a sense RNA probe was performed (Fig. 3.4 G - K). In all stages, no specific signal was detected, demonstrating that staining with the Ptf1a antisense RNA probe was specific.

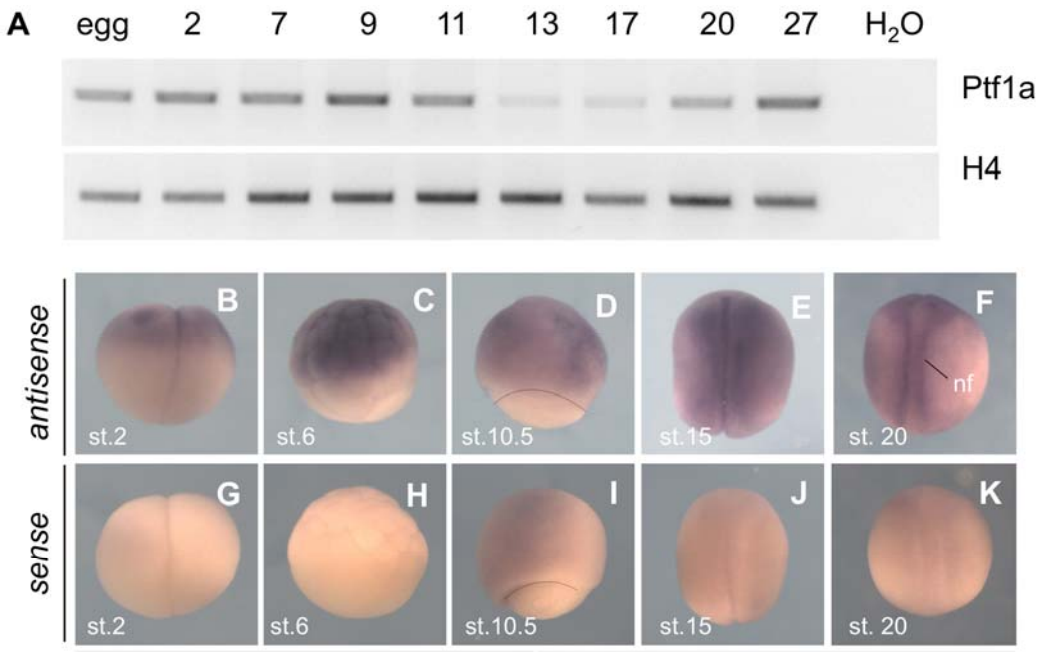

Figure 3.4 Spatial and temporal *Ptf1a* expression in *X. laevis*.
(A) Temporal *Ptf1a* expression. *Ptf1a* expression was analysed by semi-quantitative RT-PCR. Expression levels were shown by histone 4 (H4) expression. **(B-M)** Spatial *Ptf1a* expression. *Ptf1a* expression pattern was analysed by whole mount *in situ* hybridization using (B-F) antisense RNA or (G-K) sense RNA. Shown is the lateral view of the embryo in B, C, D, G, H, I and the dorsal view in E, F, J and K. Dotted line in D and I marks the blastoporus. nf, neural folds

3.5 Ptf1a is expressed in the inner ventricular zone of the hindbrain and neural tube

To further determine if Ptf1a endogenously might be involved in general neurogenesis in the developing embryo, it was evaluated, if *Ptf1a* is expressed in neural progenitor cells that do not express members of the well-characterised neuronal determination factor family *Neurogenin* (Fig. 3.5 A-C). Therefore, a

double *in situ* hybridization of stage 29 *X. laevis* embryos for *Ptf1a* and the three *Neurogenins* (*Ngn1*, *Ngn2* and *Ngn3*) (Ma et al., 1996; Nieber et al., 2009) was performed. The gene expression analysis revealed that *Ptf1a* and *Ngn1* (Fig. 3.5 B, B´) and *Ngn3* (Fig. 3.5 C, C´) were expressed in non-overlapping territories of the hindbrain. In contrast, *Ptf1a* and *Ngn2* (Fig. 3.5 A, A´) were co-expressed in a restricted domain of the hindbrain that will give rise to GABAergic interneurons, which is consistent with findings in the mouse (Henke et al., 2009b). However, only *Ptf1a* transcripts were detected in the inner ventricular zone where the proliferating precursor cells are located, whereas the expression domain of *Ngn2* is found more lateral in the intermediate zone (Fig. 3.5 A, A'), being compatible with the idea, that Ptf1a functions as a proneural factor activating general neurogenesis in the inner ventricular zone of the hindbrain.

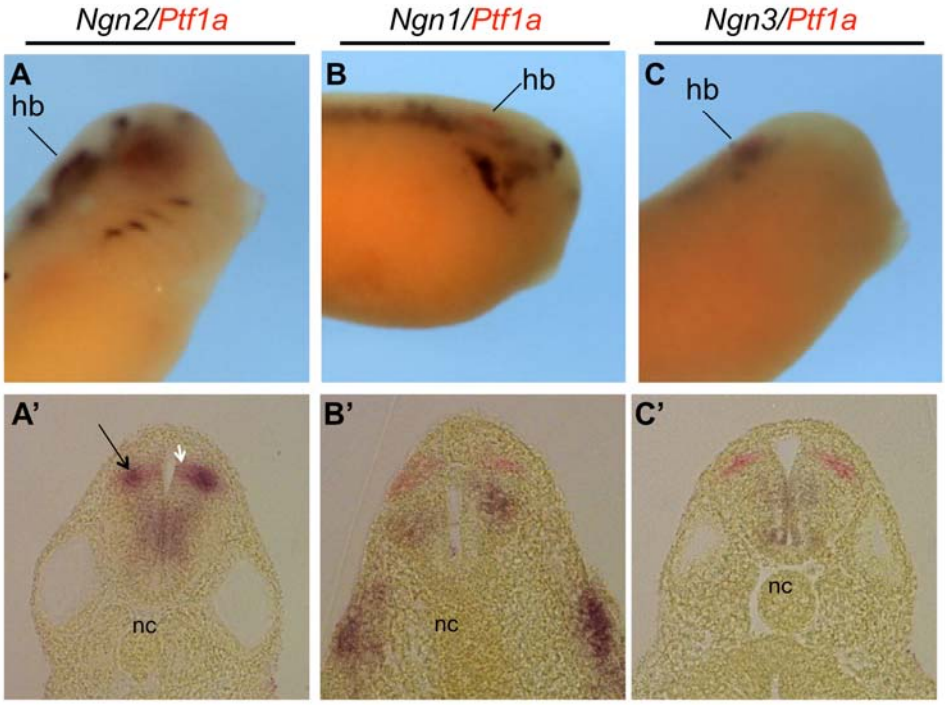

Figure 3.5 *Ptf1a* is expressed in the inner ventricular zone of the hindbrain.
(A-C) Double whole mount *in situ* hybridization of stage 29 *X. laevis* embryos for *Ptf1a* (red) and *Ngn1*, *Ngn2* and *Ngn3* (purple). (A-C) Lateral view of the head region and (A'-C') the corresponding transversal section through the hindbrain at the level of the otic vesicle. Black arrow indicates the region, where *Ptf1a* and *Ngn2* are co-expressed. The ventricular zone of the hindbrain expressing *Ptf1a* is indicated by the white arrow head. nc, notochord, hb, hindbrain

3.6 The neuronal subtype-inducing activity of Ptf1a is dominant over Ngn2

The previous result (Fig. 3.5) shows that Ptf1a and Ngn2 are co-expressed in the region of the hindbrain that gives rise to GABAergic inhibitory neurons. However, Ngn2 and Ptf1a promote distinct neuronal subtype identities in post-mitotic neurons (Fig. 3.1) (Dullin et al., 2007; Hedderich, 2008). To analyse the neuronal subtype inducing-activity of Ptf1a and Ngn2 when co-expressed, *Ptf1a-GR* and *Ngn2-GR* mRNA were injected alone or together into both blastomeres of two-cell stage embryos. Animal caps were excised at blastula stage and the GR fusion proteins induced by dexamethasone (Fig. 3.6 A). When the control embryos reached stage 23, total RNA was isolated and marker gene expression analysed by quantitative real-time RT-PCR (Fig. 3.6 A).

Overexpression of *Ptf1a-GR* and *Ngn2-GR* mRNA alone or in combination induced *N-tubulin* expression compared to uninjected control caps (Fig. 3.6 B). Consistent with previous results, Ptf1a-GR but not Ngn2-GR, strongly induced the expression of *Gad1* (Fig. 3.6 C), whereas Ngn2-GR activated the marker expression of *Hox11L2/Tlx3* (Fig. 3.6 D). Upon co-expression of both bHLH transcription factors, *Ptf1a-GR* mRNA was still sufficient to activate *Gad1* expression (Fig. 3.6 C). In fact, the induction of *Gad1* by *Ptf1a-GR* in combination with *Ngn2-GR* mRNA was even stronger than compared to *Ptf1a-GR* alone (Fig. 3.6 C). In contrast, the induction of *Hox11L2/Tlx3* by Ngn2-GR upon co-injection of *Ptf1a-GR* mRNA was abolished (Fig. 3.6 D). These results suggest that the GABAergic neuronal subtype-inducing activity of Ptf1a is dominant over that from Ngn2.

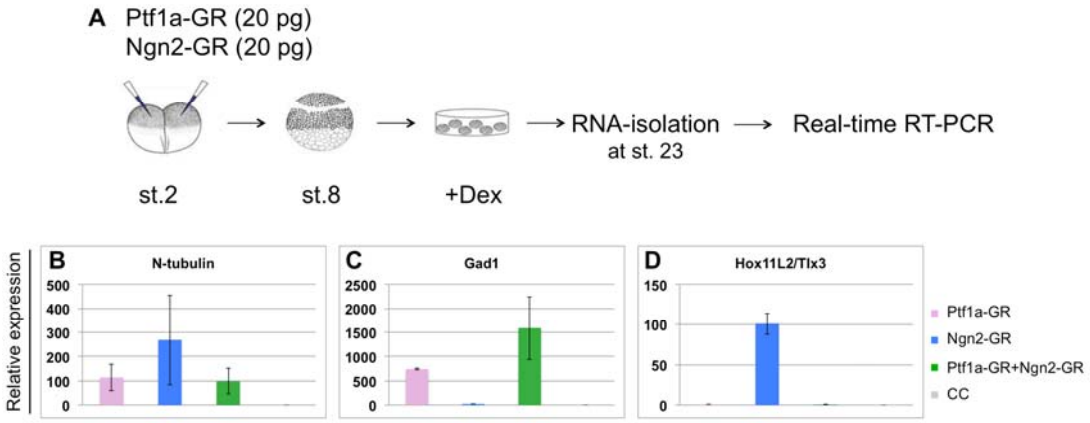

Figure 3.6 The neuronal subtype-inducing activity of Ptf1a is dominant over Ngn2.
The ability of Ngn2 together with Ptf1a to induce general neurogenesis and neuronal subtype identity was analysed in animal cap assays. **(A)** The indicated mRNAs (20 pg each) were injected into both blastomeres of two-cell stage embryos, animal caps excised at the blastula stage and treated with dexamethasone (Dex) until sibling embryos reached stage 23. Total RNA was isolated and marker gene expression analysed by quantitative real-time RT-PCR. **(B-D)** Shown is the average of two independent experiments. Error bars represent the standard error of the mean (+/- SEM).

3.7 The bHLH domain of Ptf1a is not essential for GABAergic interneuronal subtype specification

As shown above, Ngn2 and Ptf1a drive general neurogenesis of neural progenitors through the same cascade of target genes, however, they confer distinct neuronal subtype identities in the post-mitotic neurons. In order to analyse if the shared and unique activities of Ptf1a and Ngn2 are regulated by sequences within their bHLH domains, a chimeric construct was created by swapping the Ptf1a bHLH domain for that of Ngn2 (chimeric Ptf1a-GR, Fig. 3.7 B) (Hedderich, 2008). Previous analysis of a restricted set of marker genes implicated that the bHLH domain of Ptf1a might not be sufficient to impart specificity during the induction of GABAergic interneurons (Hedderich, 2008). To analyse the ability of the chimeric Ptf1a-GR to drive general neurogenesis and to specify a GABAergic interneuronal subtype in detail, quantitative digital multiplexed gene expression analysis using the NanoString nCounter system was performed (Fig. 3.7 and Appendix 6.1.2). *Ptf1a-GR*, *Ngn2-GR* or *chimeric Ptf1a-GR* mRNA were injected into both blastomeres of two-cell stage embryos. Animal caps were excised at blastula stage, proteins induced and cultivated until sibling embryos reached stage 23. Total RNA was isolated and quantitative Nanostring analysis performed (Fig. 3.7 and Appendix 6.1.2).

To first evaluate the role of the bHLH domain in promoting general neurogenesis, genes involved in general neuronal differentiation were analysed. Similar to *Ptf1a-GR* and *Ngn2-GR*, overexpression of the *chimeric Ptf1a-GR* mRNA was sufficient to induce neuronal differentiation factors such as *Ebf2* (Fig. 3.7 C), *NeuroD1* (Fig. 3.7 D), *Ebf3* (Appendix 6.1.2) and *NeuroD4* (Appendix 6.1.2) as well as *N-tubulin* expression (Fig. 3.7 E). Furthermore, the chimeric Ptf1a-GR was also able to induce the expression of the cell-cycle inhibitor *Pak3* (Appendix 6.1.2). In respect to neuronal subtype specificity, the chimeric Ptf1a-GR induced a robust expression of *Gad1* (Fig. 3.7 F), a marker indicative of GABAergic neurons. However, the induction compared to wild-type Ptf1a-GR was reduced about 2.5-fold. Overexpression of the *chimeric Ptf1a-GR* mRNA also activated the expression of transcription factors involved in GABAergic interneuronal subtype specification such as *Pax2* (Fig. 3.7 H), *Lhx5* (Fig. 3.7 G), *Lhx1* (Appendix 6.1.2) and *Lbx1* (Appendix 6.1.2), but compared to wild-type *Ptf1a-GR* the induction was strongly reduced, in particular for *Pax2* and *Lbx1*. However, chimeric Ptf1a-GR-mediated induction of gene expression was considerably stronger than background expression levels observed upon *Ngn2-GR* mRNA overexpression. Interestingly like *Ngn2-GR*, microinjection of the *chimeric Ptf1a-GR* mRNA was sufficient to activate the expression of *Prdm14* (Fig. 3.7 I), *Hox11L2/Tlx3* (Fig. 3.7 J) and *Vglut1* (Fig. 3.7 K), albeit compared to Ngn2-GR the induction was also greatly reduced.

Taken together, the quantitative Nanostring analysis demonstrated that the specificity of Ptf1a to drive general neurogenesis is not based on the function of its individual bHLH domain. Furthermore, the bHLH domain of Ptf1a is not essential for the determination of a GABAergic interneuronal subtype as the chimeric Ptf1a was still sufficient to activate marker gene expression indicative of a GABAergic interneuronal identity, even though the induction was greatly reduced. This suggests that the specification of GABAergic interneurons by Ptf1a is not only conferred through the DNA binding domain via the bHLH domain but likely also due to flanking sequences, which may impart specificity through interaction with other proteins.

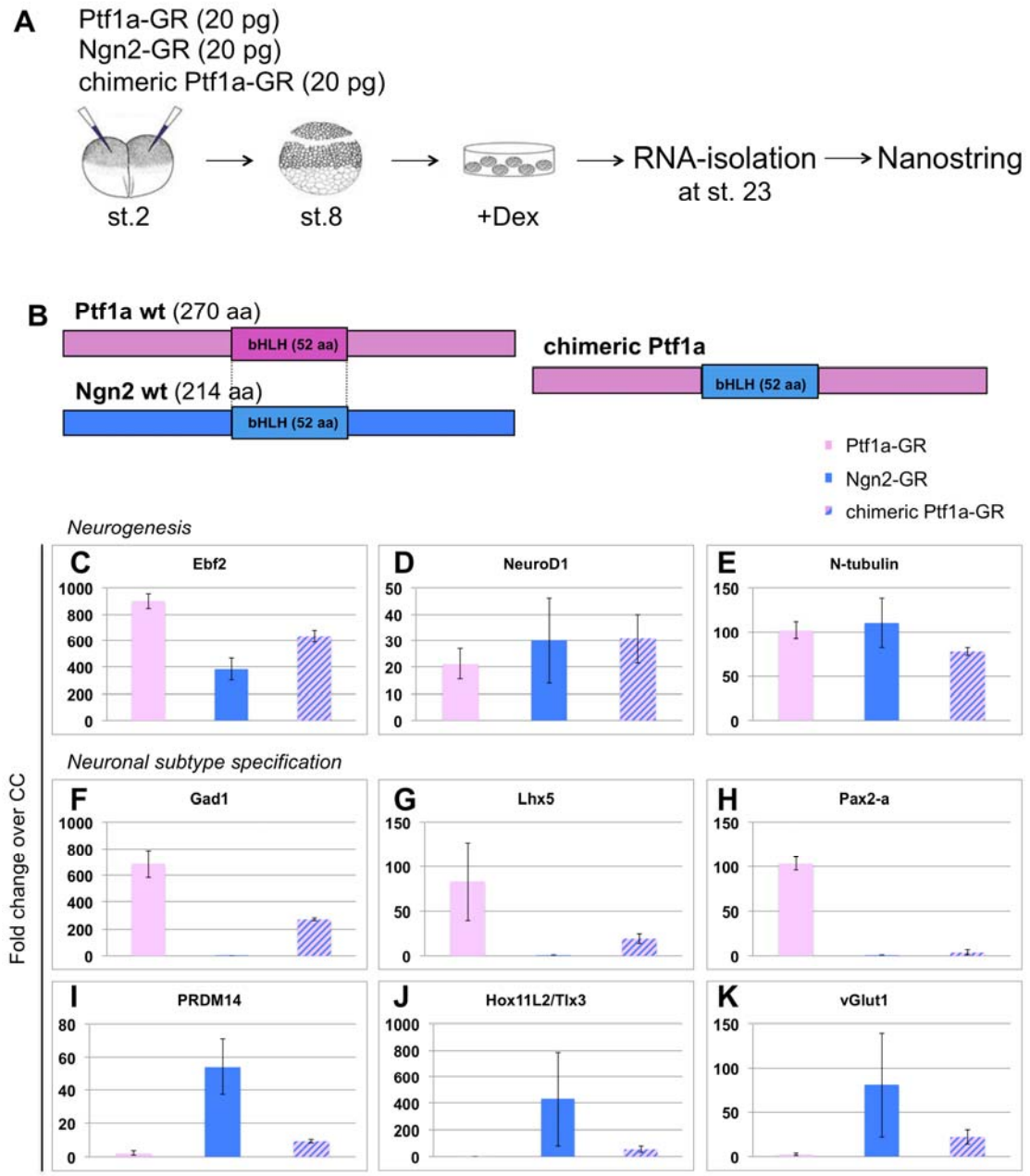

Figure 3.7 The bHLH domain of Ptf1a is not essential for GABAergic interneuron subtype specification.
The ability of Ngn2, Ptf1a or a chimeric construct of Ptf1a (chimeric Ptf1a) to induce general neurogenesis and neuronal subtype identity was analysed in animal cap assays. **(A)** The indicated mRNAs (20 pg each) were injected into both blastomeres of two-cell stage embryos, animal caps excised at the blastula stage and treated with dexamethasone (Dex) until sibling embryos reached stage 23. Total RNA was isolated and marker gene expression analysed by Nanostring. **(B)** Scheme of the chimeric Ptf1a construct, in which the bHLH of Ptf1a was swapped with that of Ngn2. **(C-K)** Shown is the averaged fold change over uninjected control caps (CC) of two independent experiments. Error bars represent the standard error of the mean (+/- SEM). Note the different scales in each diagram. Shown are graphs of selected genes, for a full list see Appendix 6.1.2.

3.8 Interaction of Ptf1a with Su(H) is not required for the general neurogenesis-inducing activity of Ptf1a

The previous result suggested that also sequences outside the bHLH domain of Ptf1a are responsible for its specificity in neuronal subtype specification. Studies in mouse and chick demonstrated that the C-terminus of Ptf1a is essential for Ptf1a to promote GABAergic interneuronal subtype identity (Hori et al., 2008). The Ptf1a C-terminus contains a C1- and C2-domain, which were shown to be required for the interaction with Rbp-j (Su(H) in *X. laevis*) or its paralogue Rbp-l (Beres et al., 2006). The interaction with Rbp-j can be abolished through a point mutation in the C2-domain. In the mouse and chick neural tube, this mutant Ptf1a lost the ability to promote GABAergic inhibitory interneurons (Hori et al., 2008). Previous studies in *X. laevis* investigating the effect of the interaction between Ptf1a and Su(H) on Ptf1a function, revealed that both C-domains must be mutated by an exchange of one amino acid (Ptf1a$^{W224A/W242A}$, Hedderich, 2008) (Fig. 3.8 B) to abolish the ability of Ptf1a to induce a GABAergic interneuronal identity (Hedderich, 2008). To further analyse the importance of these mutations on Ptf1a activity, the animal cap assay coupled with quantitative Nanostring analysis was utilized. *Ptf1a-GR* or *Ptf1a$^{W224A/W242A}$-GR* mRNA were injected into both blastomeres of two-cell stage embryos, animal caps excised and protein activity induced at blastula stage (Fig. 3.8 A). The explants were collected 6 h and 32 h after dexamethasone induction, total mRNA was isolated and analysed by Nanostring (Fig. 3.8 and Appendix 6.1.3).

Similar to *Ptf1a-GR* wild-type, microinjection of *Ptf1a$^{W224A/W242A}$-GR* mRNA activated genes involved in general neurogenesis. The genes *Dll1* (Fig. 3.8 C), *Cdknx* (Fig. 3.8 D) and *Myt1* (Fig. 3.8 E) were already induced after 6 h, while the other neuronal differentiation factors such as *NeuroD1* (Fig. 3.8 F), *Ebf2* (Appendix 6.1.3), *Ebf3* (Appendix 6.1.3), *NeuroD4* (Appendix 6.1.3) as well as *N-tubulin* (Fig. 3.8 G) were activated after 32 h of protein activity initiation. However, in regard to neuronal subtype specificity, only the wild-type *Ptf1a-GR* but not the *Ptf1a$^{W224A/W242A}$-GR* mRNA induced a robust activation of the GABAergic interneuronal marker genes *Gad1* (Fig. 3.8 I), *Pax2* (Fig. 3.8 J), *Lhx1* (Appendix 6.1.3), *Lhx5* (Fig. 3.8 K) and *Lbx1* (Appendix 6.1.3) after 32 h of protein induction. In contrast, *Ptf1a$^{W224A/W242A}$-GR* but not *Ptf1a-GR* wild-type

activated marker genes indicative of a glutamatergic excitatory phenotype such as *Hox11L2/Tlx3* (Fig. 3.8 M) and *Vglut1* (Fig. 3.8 N) as well as *Prdm14* (Fig. 3.8 L). As Ngn2, but not Ptf1a wild-type was shown in similar assays to promote such marker gene expression (Fig. 3.2), the expression of *Ngn2* was evaluated. After 32 h, the wild-type Ptf1a-GR, but not Ptf1a$^{W224A/W242A}$-GR induced *Ngn2* (Fig. 3.8 H) expression, which is consistent with the finding that *Ngn2* is a direct target of the heterotrimeric Ptf1a complex in mouse (Henke et al., 2009b). In contrast, the other members of the *Neurogenin* family*, Ngn1* and *Ngn3*, were differentially regulated. Both, *Ptf1a-GR* as well as *Ptf1a$^{W224A/W242A}$-GR* mRNA was able to induce *Ngn1* (Appendix 6.1.3) but not *Ngn3* (Appendix 6.1.3) expression.

In summary, the experiment supports the hypothesis that Ptf1a forms two distinct transcription complexes during *X. laevis* neurogenesis: a Su(H)-independent one to drive general neurogenesis and to specify glutamatergic excitatory neurons and a Su(H)-dependent one to specify GABAergic inhibitory interneurons.

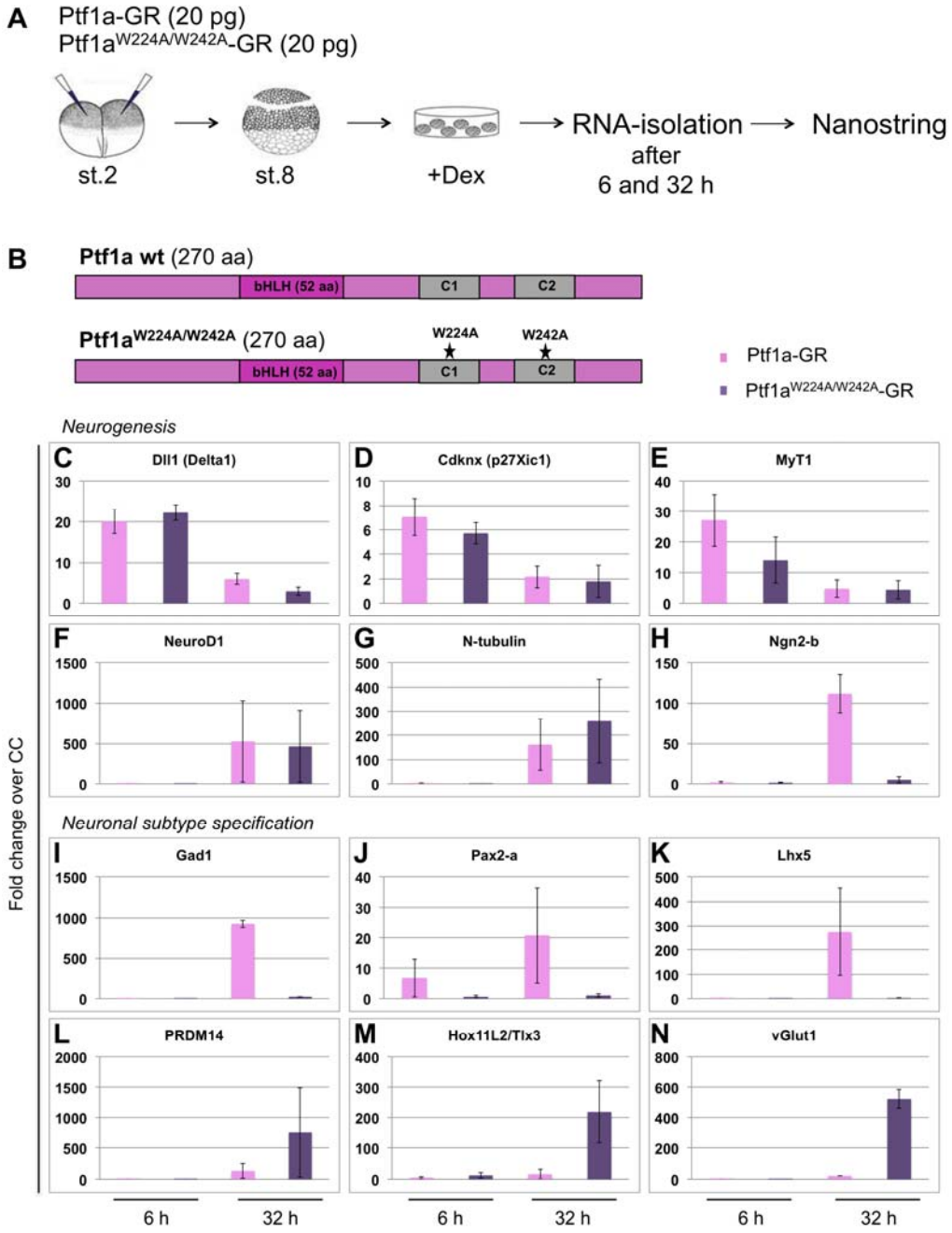

Figure 3.8 Interaction of Ptf1a with Su(H) is not required for the general neurogenesis-inducing activity of Ptf1a.
Comparative temporal analysis of wild-type Ptf1a and a mutant Ptf1a (Ptf1a$^{W224A/W242A}$), containing two point mutations that disrupt the association with Su(H), to induce markers of general neurogenesis and neuronal subtype identity was analysed in animal cap assays. **(A)** The indicated mRNAs (20 pg each) were injected into both blastomeres of two-cell stage embryos, animal caps excised at the blastula stage and treated with dexamethasone (Dex) for 6 and 32 h. Total RNA was isolated and marker gene expression analysed by Nanostring. **(B)** Scheme of the Ptf1a mutant (Ptf1a$^{W224A/W242A}$) construct. At position 224 in the C1 domain and at position 242 in the C2 domain a tryptophan residue was exchanged for an alanine, which disrupts the interaction with Su(H). **(C-N)** Marker gene expression analysed by Nanostring. Shown is the averaged fold change over uninjected control caps (CC) of two independent experiments. Error bars represent the standard error of the mean (+/-SEM). Note the different scales in each diagram. Shown are graphs of selected genes, for a full list see Appendix 6.1.3.

3.9 Ptf1a is capable of interacting with Su(H) at early embryogenesis

In mouse, the proneural gene *Ngn2* was identified as a direct target gene that requires the heterotrimeric complex of Ptf1a (Henke et al., 2009b). It is likely that also in *X. laevis*, *Ngn2* is a direct downstream target of Ptf1a. This is further supported by the co-expression of *Ngn2* with *Ptf1a* in *X. laevis* in the intermediate layer of the hindbrain progenitor domain (Fig. 3.5) that gives rise to GABAergic interneurons. Interestingly, in the quantitative temporal expression analysis shown in Figure 3.8 (and Appendix 6.1.3), *Ngn2* and other Ptf1a Su(H)-dependent genes were activated only after Su(H)-independent genes.

This raises the question as to what prevents the activation of Ngn2 and other trimeric complex target genes from being activated in an immediate early fashion by the Ptf1a heterotrimeric complex that contains Su(H)? One possibility could be that the heterotrimeric Ptf1a complex only forms when cells obtain their neuronal subtype identity, because Su(H) is not present or is at low levels during the phase of general neurogenesis. Therefore, the temporal expression of *Su(H)* transcripts during *X. laevis* development was analysed using total RNA from staged embryos (Fig. 3.9 A). Semi-quantitative RT-PCR analysis revealed that *Su(H)* is maternally expressed and that *Su(H)* transcripts were present at equal levels throughout all development stages tested.

The ability of *in vitro* synthesized Ptf1a to bind Su(H) (Hedderich, 2008; Beres et al., 2006) suggests that the interaction is direct and not dependant on post-translational modification. However, post-translational modifications may prevent their association. Therefore, *in vivo* co-immunoprecipitation (Co-IP) experiments were done using lysates of embryos injected with Myc-tagged wild-type (*MT-Ptf1a-GR*) or mutated *Ptf1a* (*MT-Ptf1a*$^{W224A/W242A}$*-GR*) mRNA together with HA-tagged *Su(H)* mRNA (*Su(H)-HA*) (Fig. 3.9 B and C) to analyse if the heterotrimeric Ptf1a complex is capable of forming at early gastrula stages, when only Su(H)-independent Ptf1a target genes are activated. MT-Ptf1a-GR, but not MT-Ptf1a$^{W224A/W242A}$-GR, which served as a negative control, was co-immunoprecipitated with Su(H)-HA (Fig. 3.9 C). To confirm the result, the Co-IP was also performed in the reverse direction (Fig. 3.9 B), showing that Su(H)-HA was co-immunoprecipitated with MT-Ptf1a-GR, but not with MT-Ptf1a$^{W224A/W242A}$-GR. The Co-IP results demonstrated that MT-Ptf1a-GR, but not MT-

Ptf1a$^{W224A/W242A}$-GR is capable of interacting already at gastrula stages with Su(H)-HA. Thus, at least when co-expressed, the heterotrimeric Ptf1a complex can form.

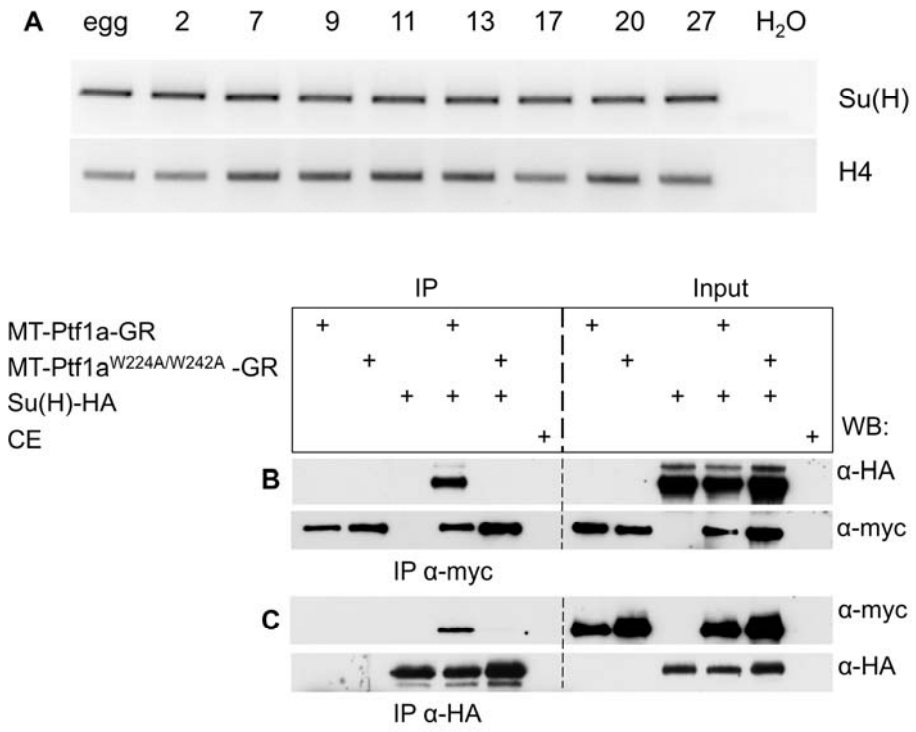

Figure 3.9 Ptf1a is capable of interacting with Su(H) at early embryogenesis.
(A) Temporal expression of *Su(H). Su(H)* expression levels were analysed by semi-quantitative RT-PCR in whole *X. laevis* embryos. Expression levels were shown by histone H4. **(B-C)** Co-immunoprecipitation (Co-IP) of MT-Ptf1a-GR, MT-Ptf1a$^{W224A/W242A}$-GR and Su(H)-HA in *X. laevis* lysates. The mRNAs (250 pg each) were injected into both blastomeres of two-cell stage embryos. Co-IP was performed using embryo lysates from gastrula stage. (B-C) Co-IP experiments showing precipitation of Su(H)-HA via MT-Ptf1a-GR (B) and precipitation of MT-Ptf1a-GR via Su(H)-HA (C).

3.10 Co-expression of Ptf1a and Su(H) influences expression levels of Ptf1a Su(H)-dependent target genes

Even though at early stages *Su(H)* transcripts are present and upon co-injection of *Ptf1a* and *Su(H)* mRNAs in *X. laevis* embryos, Ptf1a can bind Su(H), Su(H)-dependent target gene activation is delayed following injection of *Ptf1a-GR* mRNA. One possibility could be that Su(H) protein availability might be limiting. This could occur for example through a competition between Notch-ICD and Ptf1a for Su(H)-binding, which is mutually exclusive (Beres et al., 2006). The levels of Su(H) in the embryo were therefore increased by co-expression of *Su(H)-GR* mRNA together with *Ptf1a-GR* mRNA and the influence on marker

gene expression determined and compared with injection of *Ptf1a-GR* mRNA alone. *Su(H)-GR* and *Ptf1a-GR* mRNA were injected alone or in combination into both blastomeres of two-cell stage embryos, animal caps excised at blastula stage and proteins activated for 3, 6, 9 and 25 h. Total RNA was isolated and quantitative analysis performed with the Nanostring nCounter system (Fig. 3.10 A). Overexpression of *Su(H)-GR* mRNA alone did not significantly increase the expression of any of the evaluated marker genes (Fig. 3.10 B-M). As shown previously, microinjection of *Ptf1a-GR* mRNA led to an early induction of the genes *Myt1, Dll1 and Cdknx* at 3 h, which was not significantly altered by co-injection of *Su(H)-GR* mRNA (Fig. 3.10 B-D). Also similar to the previous analysis, the expression of the late neuronal differentiation markers such as *NeuroD1* (Fig. 3.10 E), *NeuroD4* (Appendix 6.1.4) and *Ebf3* (Appendix 6.1.4) were strongly activated by Ptf1a-GR after 25 h of dexamethasone induction. However, co-injection of *Su(H)-GR* mRNA led to a reduction in the expression of late neuronal differentiation markers, suggesting that neuronal differentiation is attenuated. This was further supported by the reduced expression of the post-mitotic marker *N-tubulin* (Fig. 3.10 F) upon co-injection of *Su(H)-GR* and *Ptf1a-GR* mRNA and an increase in the expression of *Sox3* (Fig. 3.10 G), a marker for neural progenitor cells. *Ptf1a-GR* mRNA overexpression alone activated the genes *Pax2*, *Lbx1, Lhx5, Lhx1 and Gad1* (Fig. 3.10 H-K and Appendix 6.1.4), which are indicative of a GABAergic interneurons in higher vertebrates (Helms and Johnson, 2003; Glasgow et al., 2005; Cheng et al., 2005), as well as *Ngn2* expression (Fig. 3.10 L) after 25 h after dexamethasone induction. Co-injection of *Su(H)-GR* mRNA did not alter the onset of expression, however, the increase in Su(H) levels quantitatively influenced the induction of these genes. The induction of *Gad1* (Fig. 3.10 H) and *Pax2* (Fig. 3.10 I) was reduced upon co-injection of *Su(H)-GR* mRNA, while the expression of *Lhx5* (Fig. 3.10 J) and *Lmx1b* (Appendix 6.1.4) was unaffected. In contrast, co-expression of *Su(H)-GR* mRNA led to a strong increase in expression of *Lhx1* (Fig. 3.10 K), *Ngn2* (Fig. 3.10 L) and *Lbx1* (Appendix 6.1.4). Moreover, the expression of the *pancreatic protein disulfide protein isomerase* (*Pdia2)* was analysed (Fig. 3.10 M), which is a direct Su(H)-dependent target gene of Ptf1a in the murine pancreas. Microinjection of *Ptf1a-GR* mRNA alone was not sufficient to induce the expression of *Pdia2*, whereas

together with *Su(H)-GR* mRNA *Pdia2* expression was already activated (20-fold) after 6 h of dexamethasone induction (Fig. 3.10), a time point at which *Pdia2* normally is not present in the developing embryo. In summary, elevated Su(H) levels together with Ptf1a inhibited neuronal differentiation of progenitor cells, while the induction of Su(H)-dependent target genes was either increased, decreased or not altered.

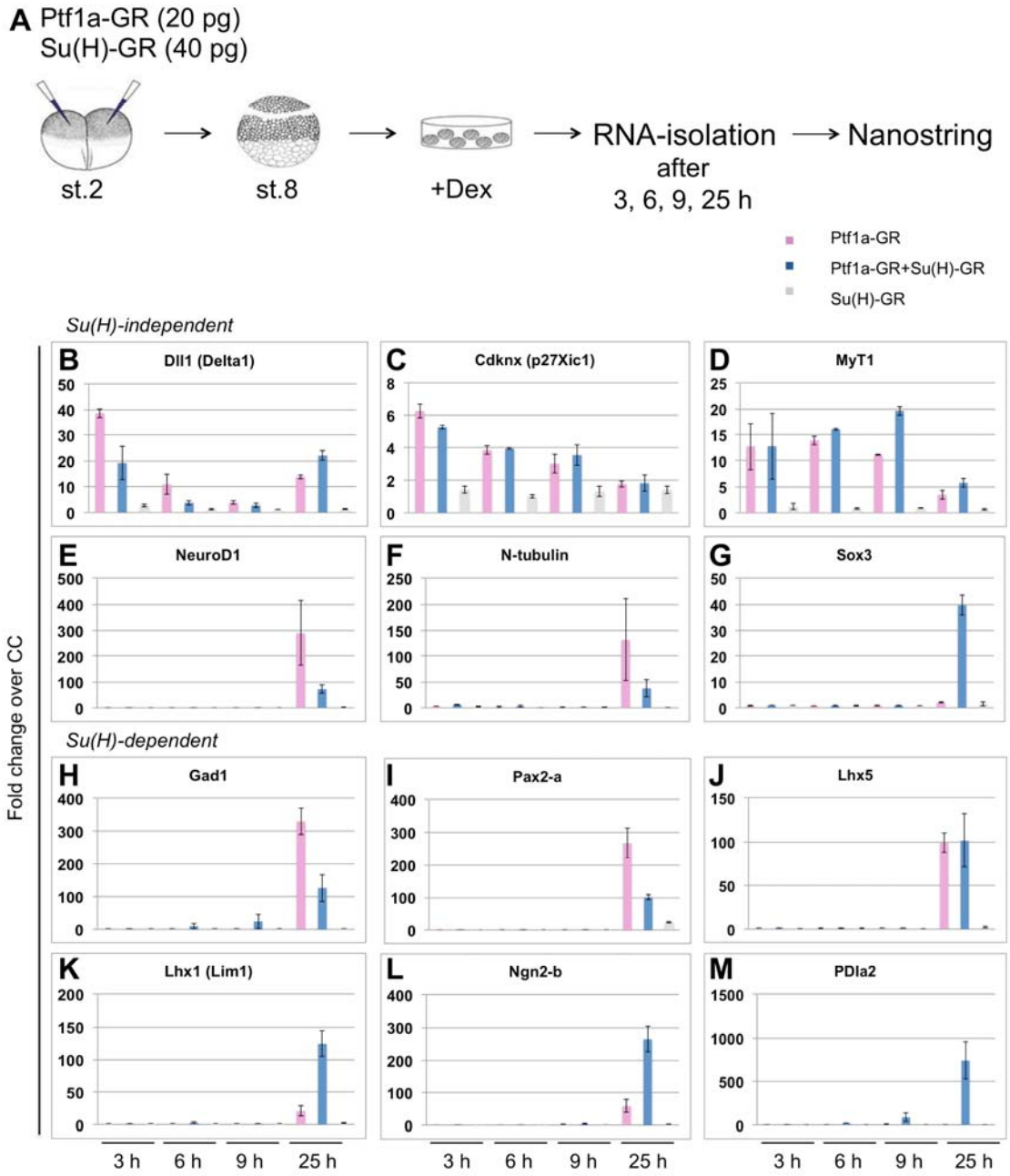

Figure 3.10 Co-expression of Ptf1a and Su(H) influences expression levels of Ptf1a Su(H)-dependent target genes.
Comparative analysis of the activity of Ptf1a-GR alone and together with Su(H)-GR. **(A)** *Ptf1a-GR* (20 pg) and *Su(H)-GR* (40 pg) mRNAs were injected into both blastomeres of two-cell stage embryos, animal caps excised at the blastula stage and treated with dexamethasone (Dex). Animal caps were cultured for 3, 6, 9 or 25 h, which

corresponds to stage 9, 10, 10.5 and 23 of sibling embryos. RNA was isolated and gene expression analysed by Nanostring. **(B-M)** Shown is the averaged fold change over uninjected control caps (CC) of two independent experiments. Error bars represent the standard error of the mean (+/-SEM). Note the different scales in each diagram. Shown are graphs of selected genes, for a full list see Appendix 6.1.4.

3.11 Temporal expression analysis of genes induced by Ptf1a, Ptf1a$^{W224A/W242A}$ and Ngn2 by RNA-sequencing

To gain insight into the genetic network downstream of Ptf1a during general neurogenesis and neuronal subtype specification, a comparative temporal expression analysis of gene induction was performed in animal caps using whole transcriptome RNA-sequencing. To discriminate between Su(H)-dependent and Su(H)-independent targets, both Ptf1a-GR and Ptf1a$^{W224A/W242A}$-GR were used. Ngn2-GR was also included in this study to identify common proneural and unique neuronal subtype inducing activities.

For the whole transcriptome approach, *Ptf1a-GR*, *Ptf1a$^{W224A/W242A}$-GR* or *Ngn2-GR* mRNA were injected into both blastomeres of two-cell stage embryos, animal caps excised and treated with dexamethasone for 6 or 25 h. After total RNA isolation, complementary DNA was prepared and paired-end deep sequencing was performed using an Illumina HiSeq 2000 sequencing system (more than 15 million reads per sample) to evaluate the transcriptome of the different explants (Fig. 3.12 A). To align the sequencing reads, the transcript reads were first mapped to the *X. tropicalis* (*Xt*) transcriptome as the genome is sequenced using the Bowtie2 program allowing three mismatches. Additionally, the transcript reads were also aligned to selected sequences of the *X. laevis* (*Xl*) unigene database, representing genes that were not found in the *X. tropicalis* transcriptome. In total, 74.7% of the sequencing-reads could be assigned using this approach (Fig. 3.11).

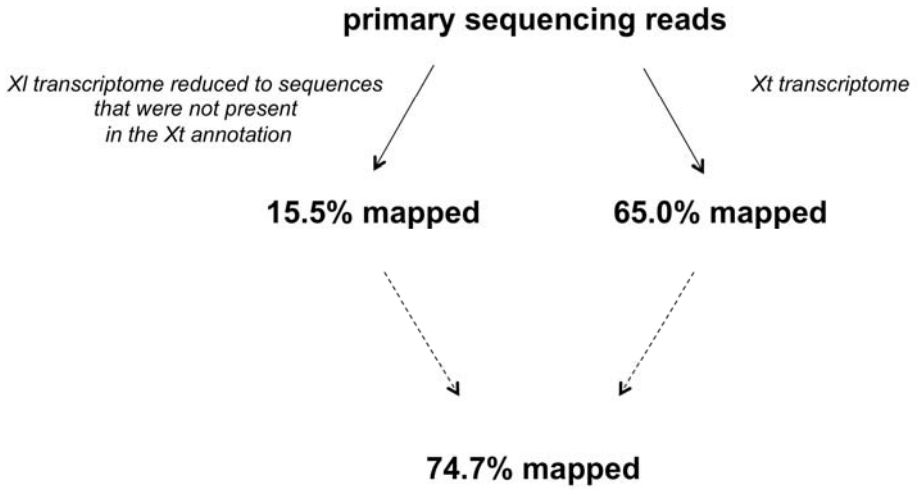

Figure 3.11 Scheme of the alignment process of the sequencing reads to identify new downstream targets of Ptf1a, Ngn2 and Ptf1a$^{W224A/W242A}$
To align the sequencing reads, the transcript reads were first mapped to the *X. tropicalis* (*Xt*) transcriptome, which resulted in 65.0% mapped sequencing reads. Furthermore, the transcript reads were aligned to the *X. laevis* (*Xl*) unigene database allowing further mapping of 15.5% of the sequencing reads. Through this procedure, in total 74.7% of the sequencing reads could be mapped.The dashed arrows indicate that the percentages are not additive as sequences map to both transcriptome libraries.

Applying a minimum two-fold change compared to control caps, Ptf1a-GR, Ptf1a$^{W224A/W242A}$-GR and Ngn2-GR induced 144, 155 and 88 genes, respectively after 6 h of protein induction (Fig. 3.12 B). Increasing this threshold revealed that a significant number of genes was activated more than 10-fold, but not over 50-fold (Fig. 3.12 B).

As expected, after 25 h of protein induction, the number of induced genes was increased. Ptf1a-GR, Ptf1a$^{W224A/W242A}$-GR and Ngn2-GR induced 1636, 369 and 762 genes, respectively, by more than two-fold (Fig. 3.12 C). In contrast to the 6 h time point, application of different thresholds indicated that a high number of genes was still upregulated more than 50-fold and even more than 100-fold (Fig. 3.12 C).

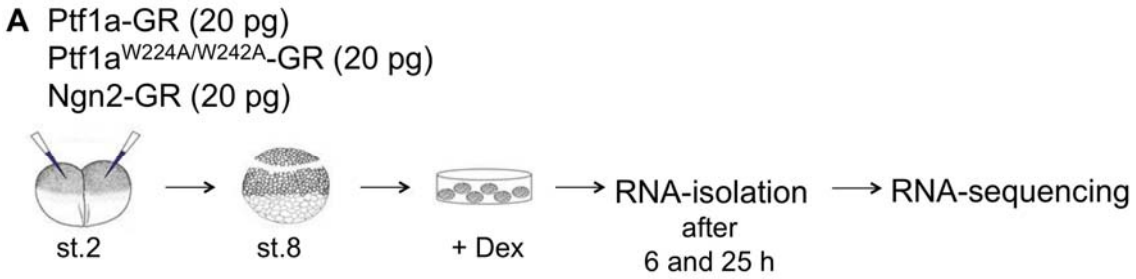

B

	6 h		
fold change	Ptf1a	Ptf1a W224A/W242A	Ngn2
> 2	144	155	88
> 10	50	40	22
> 50	4	2	3
> 100	1	0	0
> 1000	0	0	0

C

	25 h		
fold change	Ptf1a	Ptf1a W224A/W242A	Ngn2
> 2	1636	369	762
> 10	448	120	286
> 50	122	23	92
> 100	44	10	46
> 1000	0	0	2

Figure 3.12 Temporal expression analysis of Ptf1a-GR, Ngn2-GR and Ptf1a$^{W224A/W242A}$-GR target genes by whole transcriptome RNA-sequencing.
(A) The indicated mRNAs (20 pg each) were injected into both blastomeres of two-cell stage embryos, animal caps excised at blastula stage and treated with dexamethasone for 6 and 25 h. Total RNA was isolated and subjected to RNA-sequencing. **(B-C)** Summary of identified target genes of Ptf1a, Ngn2 and Ptf1a$^{W224A/W242A}$ after 6 h (B) and 25 h (C) after application of different fold-change categories. Given is the number of target genes with a two-, 10-, 50-, 100- or 1000-fold change compared to uninjected control caps (CC).

3.12 Analysis of identified downstream targets of Ptf1a, Ngn2 and Ptf1a$^{W224A/W242A}$

The two-fold cutoff was chosen for the more detailed analysis of the downstream targets of Ptf1a, Ngn2 and Ptf1a$^{W224A/W242A}$, to identify gene functions that are regulated by Ptf1a and Ptf1a$^{W224A/W242A}$. The analysis revealed that a similar number of genes were induced by Ptf1a-GR (144 genes) and Ptf1a$^{W224A/W242A}$-GR (155 genes) after 6 h of dexamethasone induction (Table 3.1), while for Ngn2-GR the number was much lower (88 genes) (Table 3.1). A total of 48 genes were shared between Ptf1a-GR, Ngn2-GR and Ptf1a$^{W224A/W242A}$-GR, which represents more than one third of the genes identified for Ptf1a-GR and Ptf1a$^{W224A/W242A}$-GR (33% and 31%, respectively) and more than the half of the genes downstream of Ngn2-GR (55%) (Table 3.1).

The number of genes induced by Ptf1a-GR strongly increased over time, with 1636 genes being identified after 25 h (Table 3.1). However, for Ptf1a$^{W224A/W242A}$-GR, which induced at the early time point approximately the

same number of genes compared to the wild-type Ptf1a-GR, only 369 genes were activated after 25 h (Table 3.1). The number of genes for Ngn2-GR was also lower, with 762 genes being identified (Table 3.1). A total of 276 genes were shared between the three transcription factors, which comprised more than 70% of total genes induced by Ptf1a$^{W224A/W242A}$-GR, but only 17% of the genes downstream of Ptf1a-GR (Table 3.1).

6 h				25 h			
Ptf1a	*Ptf1a* $^{W224A/W242A}$	*Ngn2*	shared and individual genes (2-fold CC)	*Ptf1a*	*Ptf1a* $^{W224A/W242A}$	*Ngn2*	shared and individual genes (2-fold CC)
33%	31%	55%	48	17%	75%	36%	276
23%	21%		33	2%	9%		34
	3%	6%	5		8%	4%	28
6%		10%	9	16%		34	257
38%			54	65%			1069
	45%		69		8%		31
		29%	26			26%	201
144	155	88	Total	1636	369	762	Total

Table 3.1 Comparison of the number of genes that were induced by Ptf1a-GR, Ngn2-GR and Ptf1a$^{W224A/W242A}$-GR after 6 and 25 h.
Represented is the number of shared and unique target genes of Ptf1a-GR, Ngn2-GR and Ptf1a$^{W224A/W242A}$-GR (right side) and the percentage of these compared to the total number of genes (yellow) identified with a two-fold or more increase compared to uninjected control caps (CC) for each transcription factor.

To gain functional insight into the genes identified in the screen, gene ontology was performed using DAVID (Database for Annotation, Visualization and Integrated Discovery, http://david.abcc.ncifcrf.gov/). In a first step, the shared target genes between Ptf1a-GR, Ptf1a$^{W224A/W242A}$-GR and Ngn2-GR were investigated. Most of the 48 downstream target genes shared after 6 h of protein induction were significantly involved in transcriptional regulation and regulation of RNA metabolic processes (Fig. 3.13 A). A more detailed analysis showed that 16 genes present in this group have been previously associated with general neurogenesis in *X. laevis*, including neuronal differentiation (*Ebf2*, *MyT1*), lateral inhibition (*Dll1, Notch1)* and cell cycle exit (*Cdknx*) (Dubois et al., 1998; Coffman et al., 1990; Bellefroid et al., 1996; Chitnis et al., 1995; Vernon et al., 2003).

Gene ontology analysis of the 276 shared target genes after 25 h showed significant enrichment of multiple processes and several could be associated with general neuron development such as axogenesis, cell morphogenesis involved in neuron differentiation, cell motion and transmission of nerve impulse (Fig. 3.13 B). However, the majority of the common target

genes are involved in cell adhesion, neuron differentiation and neuron projection (Fig. 3.13 B). In summary, the group of shared target genes by Ptf1a-GR, Ngn2-GR and Ptf1a$^{W224A/W242A}$-GR is suggested to reflect the general ability of proneural bHLH transcription factors to drive neurogenesis.

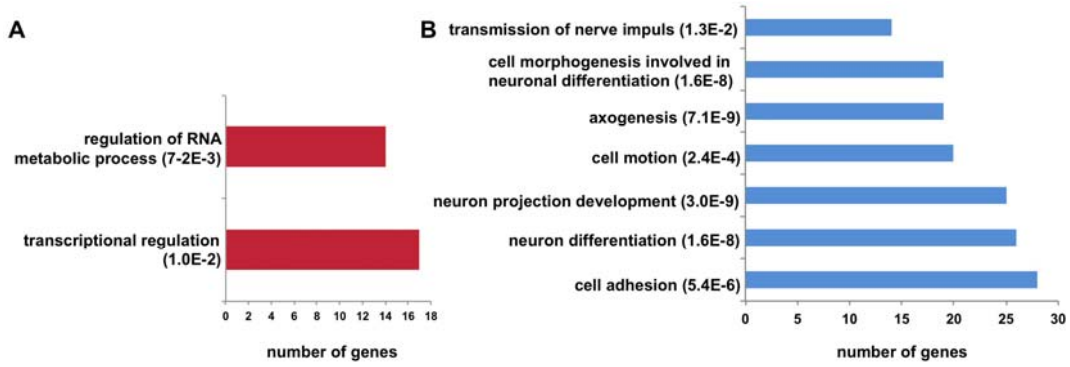

Figure 3.13 Overview of the biological processes enriched in the shared target genes by Ptf1a, Ptf1a$^{W224A/W242A}$ and Ngn2 after 6 h (A) and 25 h (B).
The number of genes in each category is shown as well as the P value at false discovery rate.

To identify the downstream network specific for the two distinct Ptf1a transcription complexes, the sets of induced candidates by Ptf1a-GR and Ptf1a$^{W224A/W242A}$-GR were compared. The analysis revealed that already 6 h after dexamethasone induction, Ptf1a-GR induced 54 target genes (38% of total) that were not activated by Ptf1a$^{W224A/W242A}$-GR (Table 3.1), suggesting that some Su(H)-dependent target genes are activated early. In order to gain insight into the function of the early Su(H)-dependent target genes, gene ontology analysis was performed. This analysis associated the identified genes with tissue and embryonic morphogenesis as well as neural tube closure (Fig. 3.14 A). However, the majority of the identified early Su(H)-dependent candidates are involved in transcription. Congruent to the Nanostring analyses (Fig. 3.2 and Fig. 3.8), none of the known genes involved in the later phase of GABAergic neuronal subtype specification such as *Pax2*, *Lbx1* and *Lhx1/5* were among the early Su(H)-dependent candidate genes.

The number of Su(H)-dependent target genes highly increased at the 25 h time point, with Ptf1a-GR activating 1069 unique genes (65% of total) that were not activated by Ptf1a$^{W224A/W242A}$-GR (Table 3.1). The list of the late Su(H)-dependent Ptf1a target genes is associated with many different biological activities that are not only associated with the development of the nervous

system. The majority of the Su(H)-dependent Ptf1a target genes could be linked to transcriptional regulation, regulation of RNA metabolic processes and cell cycle regulation (Fig. 3.14 B). However, further processes were highly enriched in this data set such as chromosome organization, neuron differentiation, regulation of cell proliferation and DNA metabolic process (Fig. 3.14 B). In terms of molecular function, the Su(H)-dependent target genes had not only a function in DNA binding (161 genes, P value = 1.6E-11), but also in binding chromatin (27 genes, P value = 3.0E-8) and calcium ions (56 genes, P value = 7.1E-2). A more detailed analysis showed that consistent with the previous Nanostring data, the transcription factors involved in GABAergic interneuronal subtype specification *Lbx1, Lhx1/5* and *Pax2* as well as *Gad1* were among the late Su(H)-dependent Ptf1a-GR target genes.

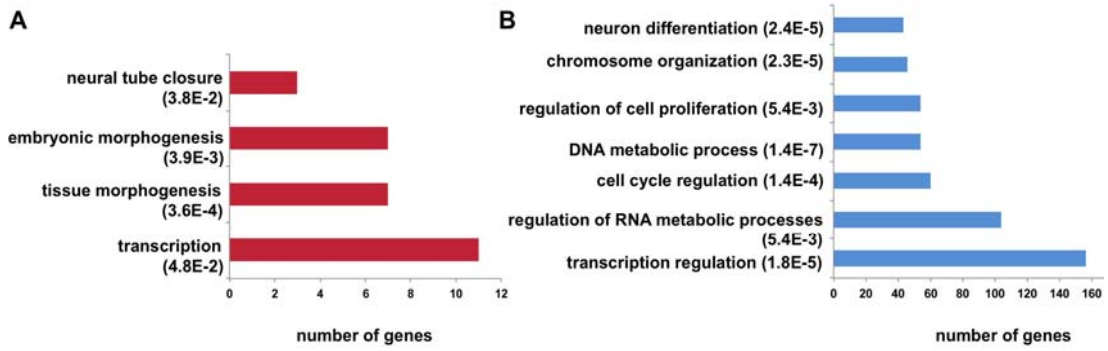

Figure 3.14 Overview of the biological processes enriched in the Su(H)-dependent Ptf1a target genes after 6 h (A) and 25 h (B).
The number of genes in each category is shown as well as the P value at false discovery rate.

Interestingly, Ptf1a$^{W224A/W242A}$-GR mRNA overexpression induced 69 unique genes (45% of total) after 6 h and 31 (8% of total) after 25 h (Table 3.1). This suggests that especially early, Ptf1a$^{W224A/W242A}$-GR does not simply mimic the activity of Ngn2 as would have been suggested by the Nanostring analysis using known genes involved in this process. However, gene ontology analysis revealed no significant enrichment of any biological processes. While most of the genes activated by Ptf1a$^{W224A/W242A}$-GR and Ngn2-GR were also induced by Ptf1a-GR, in total 28 genes were not activated by wild-type Ptf1a-GR (Table 3.1). Included in these target genes was *Tlx3*, which is a marker of glutamatergic excitatory neurons.

3.13 The majority of genes induced after 6 and 25 h by Ptf1a, Ngn2 and Ptf1a$^{W224A/W242A}$ are not shared

Comparison of the genes induced by Ngn2-GR, Ptf1a-GR and Ptf1a$^{W224A/W242A}$-GR after 6 and 25 h, reveals that most transcripts are not shared between these two time points (Fig. 3.15). While many of the genes induced after 25 h are most likely indirect downstream targets of Ptf1a-GR, Ngn2-GR and Ptf1a$^{W224A/W242A}$-GR, some of these genes are direct target genes representing the later neuronal subtype inducing-activity such as *Kirrel2* for Ptf1a.

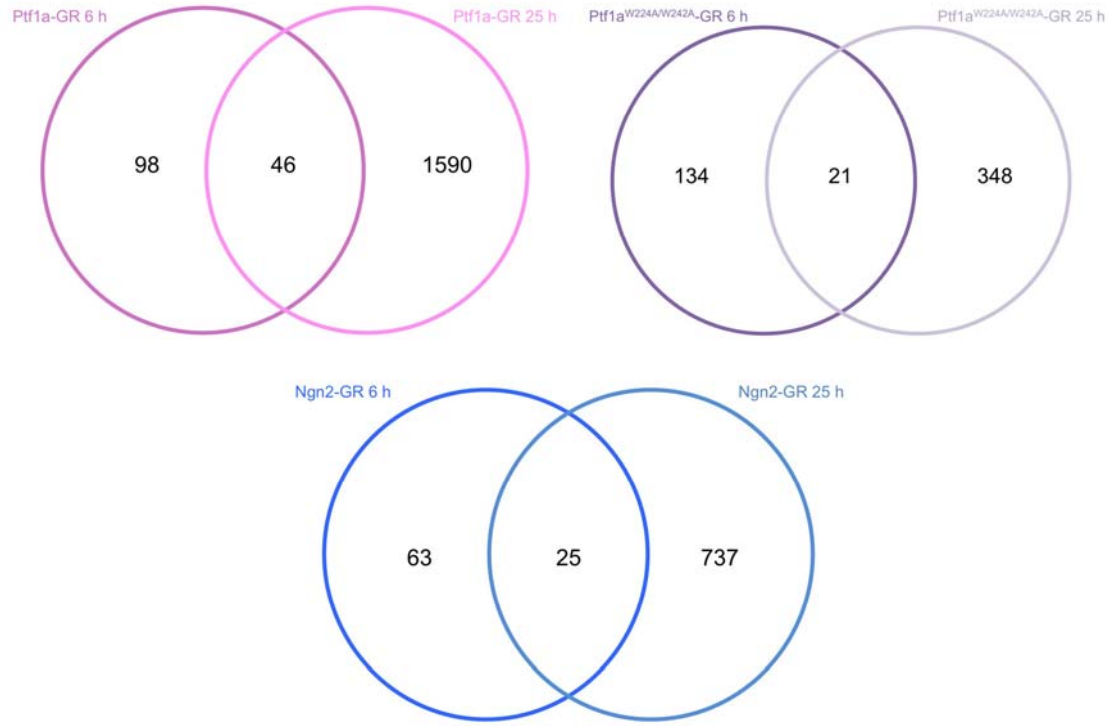

Figure 3.15 Distinct transcripts are present after 6 and 25 h of Ptf1a-GR, Ngn2-GR and Ptf1a$^{W224A/W242A}$-GR induction.
Venn diagrams show unique and shared target genes at 6 and 25 h for Ptf1a-GR, Ngn2-GR and Ptf1a$^{W224A/W242A}$-GR, respectively.

3.14 Inhibition of protein synthesis allows earlier activation of *Ngn2* expression

It is rather surprising that known murine direct Ptf1a Su(H)-dependent target genes such as *Ngn2* and *Kirrel2* are activated only after 25 h, but not after 6 h as it would be anticipated. In fact, as shown by Nanostring (Fig. 3.2 and Fig. 3.8) and RNA-sequencing (Table 3.1) analyses, most of the Su(H)-dependent genes are activated later than the Su(H)-independent genes. There

are many mechanisms that may explain this result. For example, the dimeric Ptf1a complex may activate expression of factors that repress expression of the Su(H)-dependent target genes.

To determine, if Ptf1a directly activates Ngn2, its induction by Ptf1a and Su(H) was analysed in the presence of the protein synthesis inhibitor cycloheximide (CHX). *Ptf1a-GR* or *Su(H)-GR* mRNA were injected alone or in combination into two-cell stage embryos, animal caps excised and treated for 1 h with or without CHX to block translation (Fig. 3.16 A). Afterwards, the animal caps were cultivated for 8.5 h in the presence or absence of CHX and dexamethasone (Fig. 3.16 A). As a control, injected and control caps were treated only with CHX and did not express *Ngn2*. Consistent with previous results (Fig. 3.10), microinjection of *Ptf1a-GR* mRNA together with *Su(H)-GR* mRNA, but not of either one alone, led to a strong induction of *Ngn2* (Fig. 3.16 B). However, in the presence of CHX, *Ptf1a-GR* mRNA alone was sufficient to induce *Ngn2* to a level similar to when *Ptf1a-GR* and *Su(H)-GR mRNA* were co-injected in the absence of CHX (Fig. 3.16 B). The level of Ngn2 induction through co-expression of *Ptf1a-GR* and *Su(H)-GR* mRNAs was increased in the presence of CHX (Fig. 3.16 B). This finding is compatible with the idea that a mechanism, which is dependent on protein synthesis, prevents the early activation of the late Su(H)-dependent target genes.

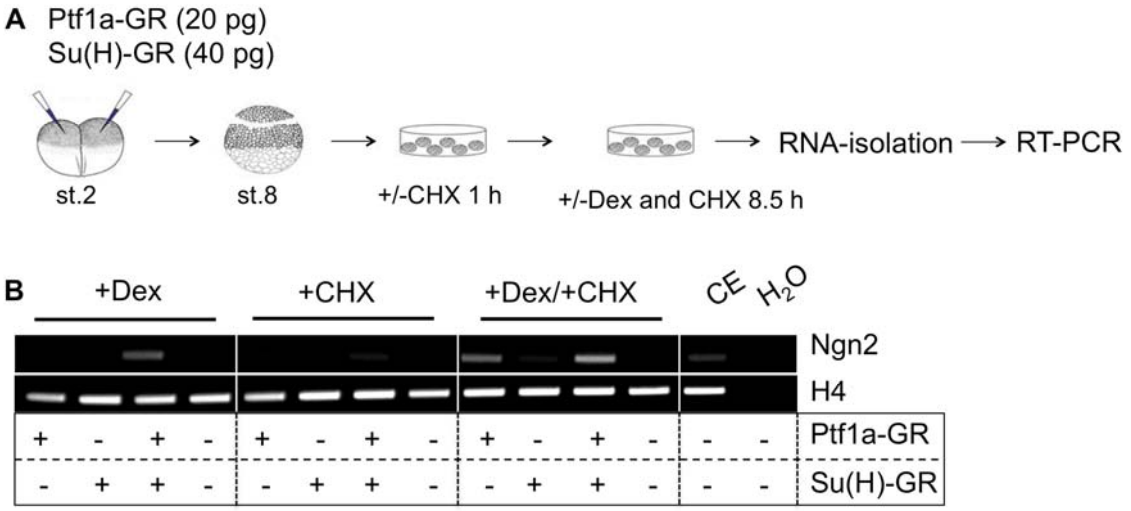

Figure 3.16 Inhibition of protein synthesis allows earlier activation of *Ngn2* expression.
Comparative analysis of the activity of Ptf1a-GR alone and together with Su(H)-GR in the presence of cycloheximide (CHX). **(A)** *Ptf1a-GR* and *Su(H)-GR* mRNA were injected alone or in combination into two-cell stage embryos. Animal caps were excised at the blastula stage and treated with our without CHX for 1 h to block protein synthesis. Afterwards, the animal caps were treated with or without dexamethasone (Dex)/CHX to induce protein activity. **(B)** Gene expression was analysed by semi-quantitative RT-PCR. Expression levels were shown by H4 expression. CE, control embryos

3.15 Identification of direct Ptf1a target genes

In the previous RNA-sequencing experiment (Fig. 3.12), *Ptf1a-GR* mRNA induced more than 100 genes (two-fold or more) after 6 h. Most likely not all of these early-induced genes are direct targets of Ptf1a. Moreover, it could be shown that Ptf1a Su(H)-dependent genes, such as *Ngn2*, are delayed in their activation, but either co-injection with *Su(H)* or treatment with CHX allows early activation (Fig. 3.16). On the basis of these findings, RNA-sequencing analysis was performed with the aim of identifying both, Su(H)-dependent and -independent Ptf1a direct target genes.

Ptf1a-GR and *Su(H)-GR* mRNA alone or in combination were microinjected into both blastomeres of two-cell stage embryos and animal caps were isolated from control and injected embryos (Fig. 3.18 A). After one hour of treatment with CHX, the animal caps were cultivated for additional 8.5 h in dexamethasone and CHX (Fig. 3.18 A). After total RNA isolation, the samples were subjected to RNA-sequencing and sequences mapped as described previously (section 3.11, Fig. 3.11). In total, 67.3% of the sequencing reads could be mapped (Fig. 3.17).

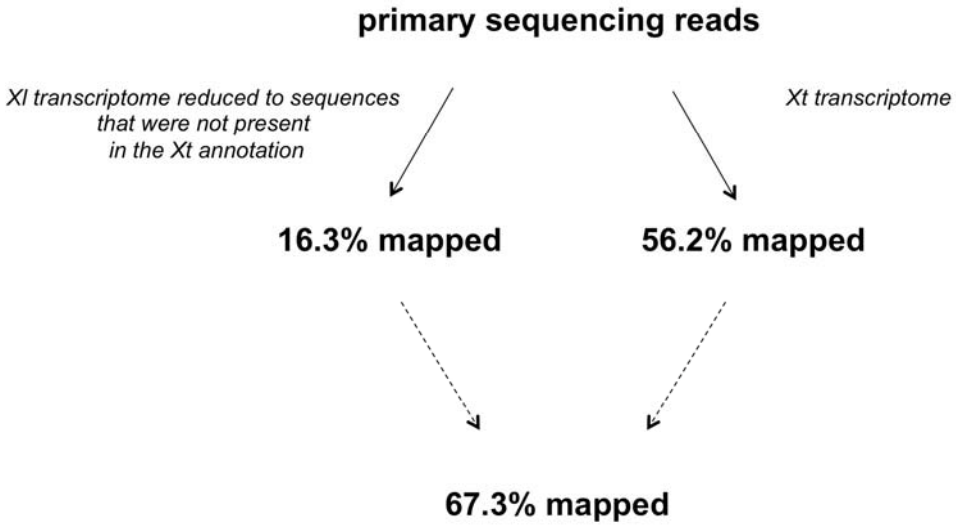

Figure 3.17 Scheme of the alignment process of the sequencing reads to identify new direct downstream targets of Ptf1a.
To align the sequencing reads, the transcript reads were first mapped to the *X. tropicalis* (*Xt*) transcriptome, which resulted in 56.2% mapped sequencing reads. Furthermore, the transcript reads were aligned to the *X. laevis* (*Xl*) unigene database allowing further mapping of 16.3% of the sequencing reads. Through this procedure, in total 67.3% of the sequencing reads could be mapped. The dashed arrows indicate that the percentages are not additive as sequences map to both transcriptome libraries.

In animal caps injected with *Ptf1a-GR* mRNA alone or together with *Su(H)-GR* mRNA, 258 and 638 genes, respectively, were activated more than two-fold compared to uninjected control caps (Fig. 3.18 B). In contrast, only two genes were induced in animal caps by *Su(H)-GR* alone. Different thresholds were applied to investigate the strength of gene induction. By applying a minimum fold change of 10, Su(H)-GR alone did not induce any genes, while Ptf1a-GR and Ptf1a-GR together with Su(H)-GR activated 87 and 222 genes, respectively (Fig. 3.18 B). Increasing the cutoff to a 50 fold-activation, stronlgy decreased the number of candidate genes for Ptf1a-GR alone but not for Ptf1a-GR together with Su(H)-GR.

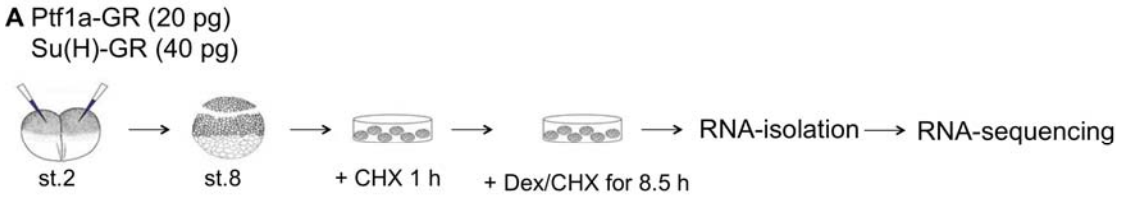

B

	CHX		
fold change	*Ptf1a*	*Ptf1a+Su(H)*	*Su(H)*
> 2	258	638	2
> 10	87	222	0
> 50	15	65	0
> 100	9	19	0
> 1000	0	2	0

Figure 3.18 Identification of direct target genes induced by Ptf1a-GR and Su(H)-GR alone and in combination by whole transcriptome RNA-sequencing.
(A) The indicated mRNAs were injected alone or together into both blastomeres of two-cell stage embryos, animal caps excised at blastula stage and treated with CHX for 1 h to block protein synthesis. Afterwards, the animal caps were treated with dexamethasone/CHX for 8.5 h to induce protein activity. Total RNA was isolated and subjected to RNA-sequencing. **(B)** Summary of identified direct target genes of Ptf1a and Su(H) alone and in combination after application of different fold-change categories. Given is the number of target genes with a two-, 10-, 50-, 100 or 1000-fold change compared to uninjected control caps (CC).

3.16 Identification of direct target genes induced in the previous temporal expression analysis by RNA-sequencing

First, it was determined, which of the Ptf1a candidate genes induced in the earlier RNA-sequencing experiment analysing the temporal expression of Ptf1a target genes (Fig. 3.12), are indeed direct Ptf1a target genes. From the 144 candidate genes that were activated after 6 h, 86 genes (60%) were also induced by Ptf1a-GR in the presence of CHX (Table 3.2). In contrast, from the 1636 target genes that were induced after 25 h, only 63 genes (4%) were induced by Ptf1a-GR in the presence of CHX (Table 3.2). When *Ptf1a-GR* and *Su(H)-GR* mRNA were co-injected, the number of candidate genes increased compared to *Ptf1a-GR* mRNA alone. From the 144 candidate genes induced after 6 h, 106 genes (74%) were identified as direct targets (Table 3.2), while from the 1636 genes activated at the late time point, 171 genes (10%) were identified (Table 3.2).

Identification of direct Ptf1a targets activated after 6 and 25 h				
Ptf1a 6 h	*Ptf1a* 25 h	*Ptf1a* CHX	*Ptf1a+Su(H)* CHX	shared genes (2-fold CC)
60%		33%		86
	4%	24%		63
74%			17%	106
	10%		27%	171
144	**1636**	**258**	**638**	**Total**

Table 3.2 Identification of direct Ptf1a targets activated after 6 and 25 h.
Comparison of the identified genes of the two-independent transcriptome RNA-sequencing approaches to identify bona fide Ptf1a downstream targets during *X. laevis* neurogenesis. Represented is the number of genes that are activated by Ptf1a-GR after 6 and 25 h and by Ptf1a-GR and Ptf1a-GR together with Su(H) in the presence of CHX as well as the percentage of these compared to the total number of genes (yellow) identified with a two-fold or more increase compared to uninjected control caps (CC) for each condition alone.

To identify the biological processes enriched in the direct target genes of Ptf1a-GR during the time course, gene ontology analysis was performed using DAVID for genes activated by Ptf1a-GR in combination with Su(H)-GR. At the 6 h time point, most of the 106 candidates were linked to transcriptional regulation and regulation of RNA metabolic processes (Fig. 3.19 A). Further biological processes significantly enriched in this data set were e.g. cell fate commitment, neuron differentiation and Notch-signalling (Fig. 3.19 A). Similar, most of the 171 direct target genes at 25 h are involved in transcriptional regulation and regulation of RNA metabolic processes (Fig. 3.19 B). However, other processes were also present, including cell motion, cell projection organization, neuronal differentiation, cell adhesion and hindbrain development (Fig. 3.19 B). Interestingly, eye development as well as endocrine system development were also enriched (Fig. 3.19 B), reflecting two known developmental functions of Ptf1a during development. Interestingly, none of the transcription factors known to be involved in GABAergic interneuronal subtype determination such as *Pax2* (Cheng et al., 2004), *Lhx1/5* (Pillai et al., 2007) and *Lbx1* (Cheng et al., 2005) were among the Ptf1a direct target genes, suggesting that their activation by Ptf1a is indirect.

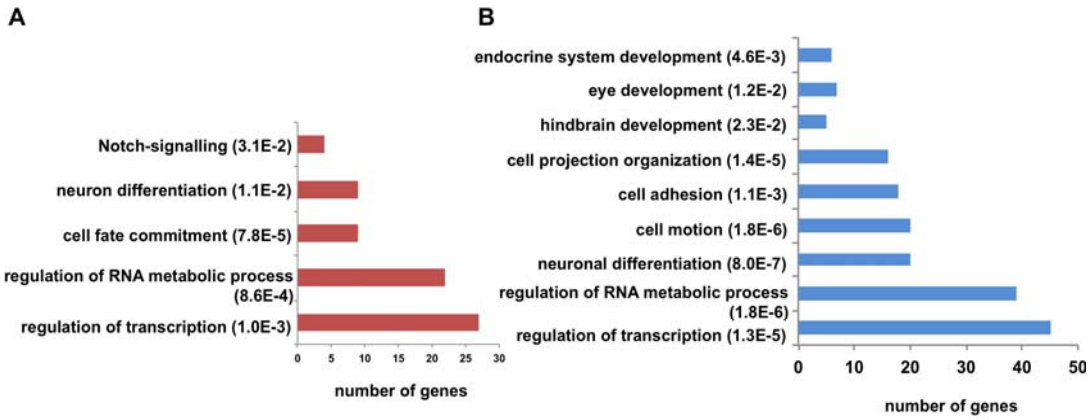

Figure 3.19 Enrichment of biological processes in Ptf1a/Su(H) direct target genes, which were also present in the time course analysis analysed by RNA-sequencing after 6 h (A) and 25 h (B).
The number of genes in each category is shown as well as the P value at false discovery rate.

3.17 Analysis of direct targets of Ptf1a and Ptf1a/Su(H)

The comparison of the two-independent RNA-sequencing experiments revealed that only a small number of the direct target genes were also present in the previous temporal expression analysis (Table 3.2). To analyse the total number of identified direct target genes, a minimal induction of two-fold was applied. Interestingly, Ptf1a-GR alone induced 64 genes (25% of total) that were not activated by Ptf1a-GR in combination with Su(H)-GR (Table 3.3). Gene ontology analysis revealed that translation (12 genes, P value = 3.1E-15) was the only biological process significantly enriched in this set of Ptf1a-GR unique target genes. In contrast, Ptf1a-GR together with Su(H)-GR induced 443 unique target genes (70% of total) (Table 3.3). The biological processes enriched in this data set were similar to the analysis of Ptf1a-GR/Su(H)-GR targets that were also present in the temporal expression analysis after 6 and 25 h (Fig. 3.19 B). One difference was that in the set of the total identified target genes, eye development was not significantly enriched anymore.

A more detailed analysis of the identified target genes revealed that also pancreas specific genes were induced in the presence of CHX, however, only when *Ptf1a-GR* was overexpressed in combination with *Su(H)-GR*. Among these were *Pdia2* and the digestive enzymes *Cpa1* and *Prss1*. This is consistent with the finding that Ptf1a directly activates acinar digestive enzymes in the exocrine pancreas (Cockell et al., 1989).

CHX			
Ptf1a	*Ptf1a+Su(H)*	*Su(H)*	shared and individual genes (2-fold CC)
0%	0%	50%	1
75%	30%		193
	0%	0%	0
0%		0%	0
25%			64
	70%		443
		50%	1
258	**638**	**2**	**Total**

Table 3.3 Whole transcriptome RNA-sequencing to identify direct target genes of Ptf1a-GR and Ptf1a-GR together with Su(H)-GR.
Summary of identified direct target genes of Ptf1a, Su(H) and both together represented in a table. Given is the number of shared and unique target genes of Ptf1a-GR and Su(H)-GR alone as well as in combination (right side) and the percentage of these compared to the total number of genes (yellow) identified with a two-fold or more increase compared to uninjected control caps (CC) for each transcription factor.

3.18 Identification and validation of direct trimeric-dependent Ptf1a target genes

Comparison of the two independent RNA-sequencing approaches allows identification of Su(H)-dependent direct Ptf1a target genes. Genes that are induced by Ptf1a-GR, but not by Ptf1a$^{W224A/W242A}$-GR and that are induced by Ptf1a-GR or Ptf1a-GR/Su(H)-GR in the presence of CHX are expected to be trimeric-dependent Ptf1a direct target genes. Using this comparative approach, 111 putative direct trimeric-dependent transcripts were identified. Of these, 13 genes (12%) were induced after 6 h, and 34 genes (31%) were induced without elevated Su(H)-GR expression levels. To verify selective candidate genes, eight (Table 3.4) of the 111 identified genes as well as the known direct target gene *Kirrel2* (Nishida et al., 2010) were analysed using the Nanostring nCounter RNA expression profiling system.

Table 3.4. Summary of the fold-activation compared to control caps of the selected Su(H)-dependent Ptf1a target genes.

Gene Symbol	*Ptf1a-GR* 6 h	*Ptf1a-GR* 25 h	*Ptf1a-GR* CHX	*Ptf1a-GR +SuH-GR* CHX
Prdm13	865.7	528.4	888.7	4650.1
Barhl2	-	26.9	-	108.5
Hmx3	-	2.4	53.4	84.8
Lhx2	-	-	58.1	63.7
Mecom	-	9.6	-	12.6
Sox9	-	37.2	-	5.3
ESR10	5.3	4.0	6.0	3.1
FoxD3	-	56.2	-	2.6

In a first approach, these genes were analysed for their temporal activation and their dependence on Su(H) interaction for gene induction in the animal cap assay (Fig. 3.20 and Appendix 6.1.3). Consistent with the results of the RNA-sequencing experiment, *Prdm13* (Fig. 3.20 B) and *Esr10* (Fig. 3.20 C) expression were activated by Ptf1a-GR after 6 h of dexamethasone induction, while the expression of the known direct target gene *Kirrel2* (Fig. 3.20 D) as well as of *Mecom* (Fig. 3.20 E), *Hmx3* (Fig. 3.20 F), *FoxD3* (Fig. 3.20 G), *Sox9* (Fig. 3.20 I) and *Barhl2* (Fig. 3.20 H) were only activated after 25 h. Microinjection of *Ptf1a*$^{W224A/W242A}$*-GR* mRNA compared to *Ptf1a-GR* wild-type did not considerably induce the expression of *Kirrel2* (Fig. 3.20 D)*, Prdm13* (Fig. 3.20 B), *Hmx3* (Fig. 3.20 F)*, Mecom* (Fig. 3.20 E), *Barhl2* (Fig. 3.20 H) and *FoxD3* (Fig. 3.20 G), demonstrating that their induction is strongly dependent on the interaction of Ptf1a with Su(H). Furthermore, *Ptf1a*$^{W224A/W242A}$*-GR* was not able to induce the early expression of *Esr10* (Fig. 3.20 C), while the late expression of this gene was not affected. Moreover, *Ptf1a*$^{W224A/W242A}$*-GR* mRNA overexpression was sufficient to induce the expression of *Sox9* (Fig. 3.20 I), albeit compared to *Ptf1a-GR* the induction was reduced about the half. In summary, the interaction with Su(H) is required for strong induction of the novel identified Su(H)-dependent direct Ptf1a target genes.

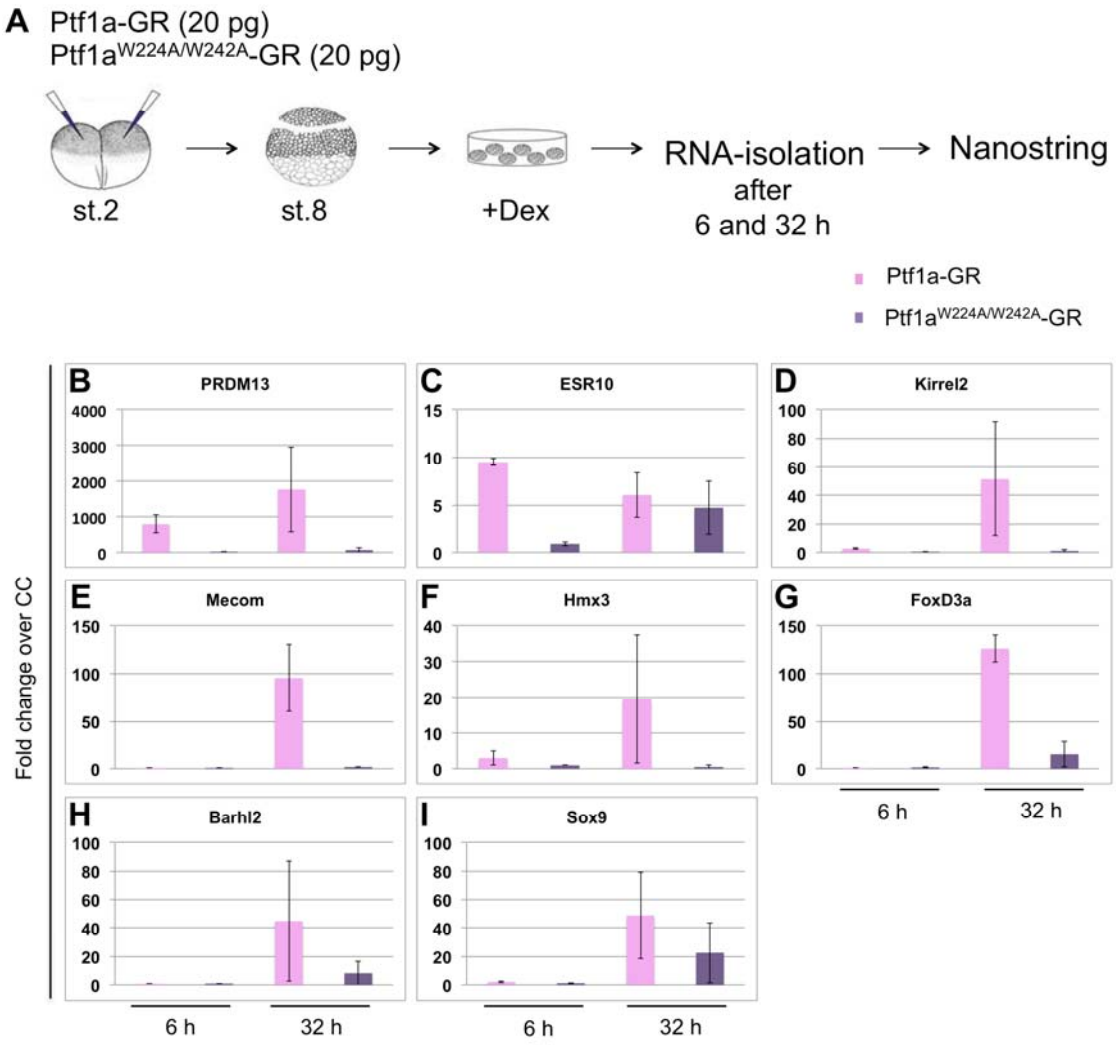

Figure 3.20 Verification of selected direct Ptf1a Su(H)-dependent target genes. Comparative temporal analysis of wild-type Ptf1a and a mutant Ptf1a (Ptf1a$^{W224A/W242A}$), containing two point mutations that disrupt the association with Su(H), to analyse, if the new identified Ptf1a target genes are dependent on Su(H) interaction. **(A)** The indicated mRNAs (20 pg each) were injected into both blastomeres of two-cell stage embryos, animal caps excised at the blastula stage and treated with dexamethasone (Dex) for 6 and 32 h. Total RNA was isolated and marker gene expression analysed by Nanostring. **(B-I)** Shown is the averaged fold change over uninjected control caps (CC) of two independent experiments. Error bars represent the standard error of the mean (+/-SEM). Note the different scales in each diagram. Shown are graphs of selected genes, for a full list see Appendix 6.1.3.

To further verify that these genes are trimeric Ptf1a target genes, their gene induction in the presence of elevated Su(H) expression levels were investigated in animal cap assays (Fig. 3.21 and Appendix 6.1.4). Corresponding with the RNA-sequencing analysis, overexpression of *Su(H)-GR* mRNA alone did not significantly increase the expression of any of the evaluated target genes. Ptf1a-GR activated after 3 and 6 h the expression of *Prdm13* (Fig. 3.21 B), consistent with the previous Nanostring analysis. Also

congruent to the previous experiment, Ptf1a-GR activated *Esr10* expression at the early time points (28-, 27-fold) (Fig. 3.21 C), however, the induction of *Esr10* after 25 h (Fig. 3.21 C) was so strong that the early induction is not apparent on the graph. The expression of *Kirrel2* (Fig. 3.21 D), *Mecom* (Fig. 3.21 J), *Hmx3* (Fig. 3.21 E), *FoxD3* (Fig. 3.21 F), *Sox9* (Fig. 3.21 G) and *Barhl2* (Fig. 3.21 H) was only activated by Ptf1a-GR after 25 h of dexamethasone induction, consistent with the previous analysis. Furthermore, *Lhx2* (Fig. 3.21 I), a gene that was identified as a direct target of Ptf1a-GR and Ptf1a-GR/Su(H)-GR, but was surprisingly not present in the temporal gene expression analysis, was also only activated at the 25 h time point. Similar to what was observed for *Ngn2* (Fig. 3.10 L), co-expression of *Su(H)-GR* with *Ptf1a-GR* mRNA led to an increase in gene induction of *Prdm13* (Fig. 3.21 B), *Esr10* (Fig. 3.21 C), *Kirrel2* (Fig. 3.21 D), *FoxD3* (Fig. 3.21 F) and *Sox9* (Fig. 3.21 G) as well as of *Barhl2* (Fig. 3.21 H), *Lhx2* (Fig. 3.21 I) and *Mecom* (Fig. 3.21 J). The effect on the latter group of genes was particularly strong. In contrast, the expression of *Hmx3* (Fig. 3.21 E) was highly reduced, if not even abolished by co-expression of *Ptf1a-GR* and *Su(H)-GR* mRNA. Thus, similar to the previous analysis of Su(H)-dependent target gene activation (Fig. 3.10), also the novel identified Ptf1a direct target genes respond differently to the co-expression of Su(H)-GR.

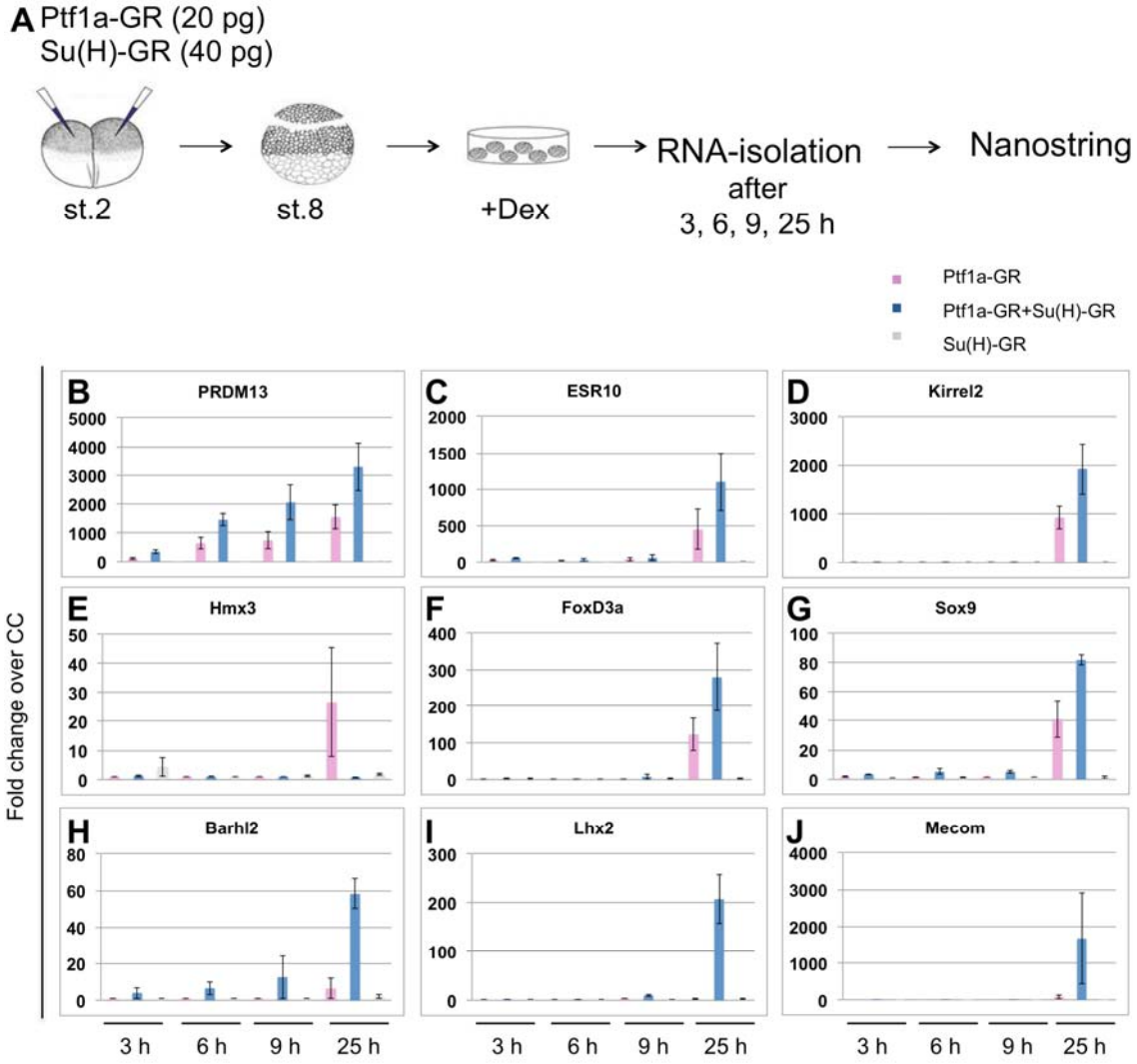

Figure 3.21 Co-expression of Ptf1a and Su(H) influences expression of new identified Su(H)-dependent direct Ptf1a target genes.
Comparative analysis of the activity of Ptf1a-GR alone and together with Su(H)-GR. **(A)** Ptf1a-GR (20 pg) and Su(H)-GR (40 pg) were injected into both blastomeres of two-cell stage embryos, animal caps excised at the blastula stage and treated with dexamethasone (Dex). Animal caps were cultured for 3, 6, 9 or 25 h, which corresponds to stage 9, 10, 10.5 and 23 of sibling embryos. RNA was isolated and gene expression analysed by Nanostring. **(B-J)** Shown is the averaged fold change over uninjected control caps (CC) of two independent experiments. Error bars represent the standard error of the mean (+/-SEM). Note the different scales in each diagram. Shown are graphs of selected genes, for a full list see Appendix 6.1.4.

4. Discussion

4.1 The proneural function of Ptf1a does not require interaction with Su(H)

The bHLH transcription factor Ptf1a was shown to act as a selector gene for GABAergic inhibitory neurons at the expense of glutamatergic excitatory neurons in the retina, the dorsal horn of the spinal cord and in the cerebellum (Glasgow et al., 2005; Hori et al., 2008; Hoshino et al., 2005; Fujitani et al., 2006; Nakhai et al., 2007; Pascual et al., 2007; Dullin et al., 2007; Lelievre et al., 2011). Consistent with this, Ptf1a overexpression in *X. laevis* embryos and animal caps promoted not only *Gad1* expression, but also induced the expression of *Pax2*, *Lbx1* and *Lhx1/5* at the expense of markers indicative of a glutamatergic excitatory neuronal identity (Fig. 3.1, Fig. 3.2 and Fig. 4.1). Furthermore, the use of a transcriptional activator Ptf1a (Ptf1a-VP16) provides evidence that the repression of the molecular markers indicative of glutamatergic neurons is indirect, probably due to the activation of a specific transcriptional repressor protein (Fig. 3.1).

Ptf1a was identified as a component of a heterotrimeric transcription factor complex, consisting of a commonly expressed class A bHLH transcription factor and Rbp-j/-l (Su(H)) (Beres et al., 2006). Detailed Nanostring analyses with a chimeric form of Ptf1a, which contained the bHLH domain of Ngn2, showed that the bHLH domain of Ptf1a is not essential for the determination of a GABAergic neuronal identity, even though the induction of genes involved in this process is reduced compared to wild-type Ptf1a (Fig. 3.7 and Fig. 4.1). Furthermore, the chimeric Ptf1a was still able to induce general neurogenesis and also marker genes indicative of glutamatergic excitatory neurons (Fig. 3.7 and Fig. 4.1). This suggests that the neuronal subtype inducing activity of Ngn2 is conferred through its bHLH domain and is consistent with experiments in *X. laevis* and *Drosophila* that implicated a role of the bHLH domain in target gene specificity (Talikka et al., 2002; Chien et al., 1996).

In *X. laevis* animal cap assays, a mutant version of Ptf1a ($Ptf1a^{W224A/W242A}$) that does not bind Su(H), is unable to promote the formation of GABAergic inhibitory neurons (Fig. 3.8 and Fig. 4.1); which is consistent with studies performed in the mouse and chick neural tube (Hori et al., 2008).

Surprisingly, it was found that the general neurogenesis-inducing activity of Ptf1a$^{W224A/W242A}$ was not impaired (Fig. 3.8), suggesting that the interaction with Su(H) is not required for the proneural function of Ptf1a. While Ptf1a was always considered to function in the context of a trimeric transcription factor complex, these findings suggest that Ptf1a forms a heterodimer with a general bHLH protein and only context-specifically additionally interacts with Su(H) as a co-factor. Through the formation of different transcription complexes, Ptf1a is able to promote distinct activities during the development of the nervous system: one complex drives general neurogenesis and another promotes neuronal subtype specification. This would be in line with the activity of other vertebrate proneural bHLH transcription factors that also play a role in neuronal subtype specification (Lee and Pfaff, 2003; Lo et al., 1998; Hatakeyama et al., 2001; Saba et al., 2005; Powell and Jarman, 2008; Guillemot, 2007; Brunet and Ghysen, 1999; Bertrand et al., 2002).

Through RNA-sequencing analysis, downstream target genes induced after 6 and 25 h by wild-type Ptf1a and Ptf1a$^{W224A/W242A}$ were identified. In line with the finding that Ptf1a forms two distinct transcription complexes during general neurogenesis and neuronal subtype specification, both shared and distinct genes were induced by the wild-type and mutant Ptf1a. As the proneural activity of Ptf1a was Su(H)-independent, it was anticipated that the genes shared by both would be involved in general neurogenesis. In contrast, those that were induced by the wild-type Ptf1a but not by the mutant would be expected to be involved in neuronal subtype specification. This, indeed, was what was observed in the RNA-sequencing analysis. Genes such as *Pax2*, *Lbx1* and *Lhx1/Lhx5*, indicative of GABAergic interneuronal subtype identity (Helms and Johnson, 2003), were only induced by wild-type Ptf1a after 25 h. Additionally, the Ptf1a-trimeric complex also induced after 25 h the direct target genes *Kirrel2* (Nishida et al., 2010) and *Ngn2* (Henke et al., 2009b) as well as *FoxD3* and *Olig3*, two genes with which Ptf1a promotes the formation of the glutamatergic climbing fiber neurons (Yamada et al., 2007; Storm et al. 2009). Moreover, among the genes shared between Ptf1a and the mutant Ptf1a were known genes involved in general neurogenesis. Correspondingly, the majority of the gene targets shared by the wild-type and mutant Ptf1a were also induced

by Ngn2. This further supports the notion that this group of genes represents the proneural function of these three bHLH transcription factors.

A defect in general neurogenesis in mice lacking *Ptf1a* in the CNS has not been reported. Furthermore, lineage tracing experiments in a viable Ptf1a mutant mice, in which Ptf1a expression is only absent in the cerebellum but not in the pancreas, indicated that the cerebellar ventricular zone can produce neurons even in the absence of Ptf1a expression (Hoshino et al., 2005). However, redundancy between Ptf1a and other proneural bHLH transcription factors as it has been shown for Ngn2 and Ascl1 (Mash1) (Fode et al., 2000) was not excluded (Hoshino, 2006). In order to investigate a putative redundancy between Ptf1a and other bHLH transcription factors, it should be analysed, if other proneural transcription factors are upregulated in the cerebellum and dorsal horn of the spinal cord in Ptf1a knockout and mutant mice. While no other member of the *Neurogenin* neuronal determination gene family is expressed in the inner ventricular zone of the hindbrain that will give rise to GABAergic inhibitory neurons (Fig. 3.5), the proneural bHLH transcription factor *Ascl1* is expressed in the mouse cerebellar ventricular zone similar to *Ptf1a* (Zordan et al., 2008) and might therefore compensate for the loss of Ptf1a proneural function. The strong proneural activity that Ptf1a exhibits in *X. laevis* embryos and explants, coupled with its expression in the progenitor cells suggests that Ptf1a may promote general neurogenesis also in other vertebrates.

4.2 Ptf1a$^{W224A/W242A}$ is a functional transcription factor

In animal cap assays evaluated by Nanostring analysis, Ptf1a$^{W224A/W242A}$ was not only able to drive general neurogenesis, but also to induce genes indicative of glutamatergic excitatory neurons (Fig. 3.8 and Fig. 4.1). That Ptf1a bearing these mutations still promoted general neurogenesis and activated markers indicative of an alternative neuronal subtype was also reflected by RNA-sequencing. A small number of genes, including *Hox11L2/Tlx3*, which is indicative of glutamatergic excitatory neurons, was both induced by Ptf1a$^{W224A/W242A}$ and Ngn2. Thus, glutamatergic excitatory neuronal subtype specification might be the 'default' activity of the heterodimeric Ptf1a, similar to Ngn2. A dramatic increase in glutamatergic excitatory neurons in the mouse

neural tube is observed upon depletion of Rbp-j (Su(H)) in the presence of Ptf1a, demonstrating that Rbp-j, similar to Ptf1a, is required to promote GABAergic neurons at the expense of glutamatergic neurons (Hori et al., 2008). The requirement of the Ptf1a-SuH trimeric complex for GABAergic neuronal specification was further demonstrated using a single mutation to disrupt the binding of Ptf1a with Su(H) (Ptf1a^{W298A}). Correspondingly, in homozygous Ptf1a^{W298A} mice, GABAergic inhibitory interneurons were lost, while the number of glutamatergic excitatory neurons was increased (Hori et al., 2008). As this phenotype is similar to that of *Ptf1a* knockout mice (Glasgow et al., 2005), it was concluded that the Ptf1a^{W298A} does not compensate for wild-type Ptf1a activity and is non-functional. However, it might be that the increase in glutamatergic neurons in Ptf1a^{W298A} mice was not only due to the loss of wild-type Ptf1a activity, but also that Ptf1a^{W298A} actively contributed to promote this neuronal subtype. To investigate this possibility, lineage tracing experiments in the Rbp-j deficient and Ptf1a^{W298A} mouse must be conducted to analyse the origin of these glutamatergic excitatory neurons. Moreover, RNA-sequencing identified genes induced by Ptf1a$^{W224A/W242A}$ after 6 and 25 h that were neither activated by Ptf1a nor by Ngn2, indicating that Ptf1a$^{W224A/W242A}$ activates a unique set of target genes. This group of genes might reflect an additional unknown function of the Ptf1a mutant, however, gene ontology analysis revealed no specific biological processes enriched in these candidates. Taken together, the experiments performed in *X. laevis* suggest that in absence of Su(H) binding, Ptf1a is still a functional proneural bHLH transcription factor, which specifies glutamatergic excitatory neurons in the nervous system.

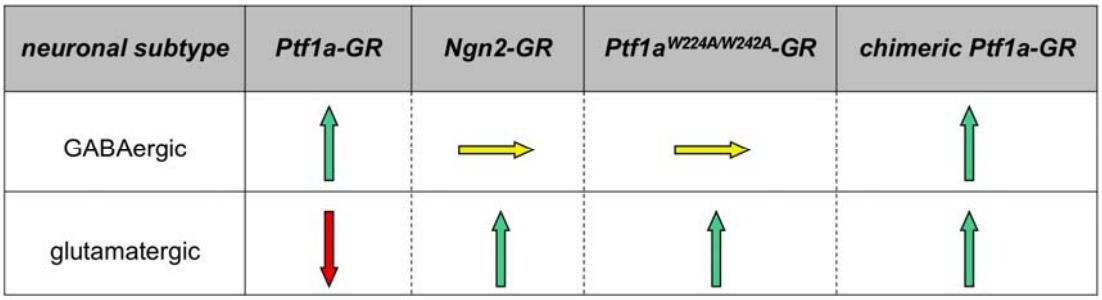

Figure 4.1 Distinct activities of Ptf1a, its mutated and chimeric version as well as of Ngn2 in regard to neuronal subtype specification. Shown are the different Ptf1a constructs as well as Ngn2 and their specificity in neuronal subtype specification. A green arrow represents specification of a neuronal subtype, while a yellow arrow represents no effect on the cell type. In contrast, a red arrow indicates inhibition of a specific neuronal subtype.

4.3 Regulation of gene induction of Su(H)-dependent and independent Ptf1a target genes

The context-specific cooperation with co-factors represents a common mechanism for how bHLH transcription factors are able to exert distinct activities (Bertrand et al., 2002; Powell and Jarman, 2008). However, the regulatory mechanism behind distinct transcriptional complex formation and activity often remains elusive.

The heterodimer of Ptf1a is sufficient to activate neurogenesis, while the heterotrimeric complex is essential for GABAergic inhibitory neuron formation. In contrast to the expectations based on the Nanostring experiments using a limited number of known genes, the RNA-sequencing analysis revealed that Ptf1a also induces Su(H)-dependent target genes after 6 h of protein induction. However, the number of Su(H)-dependent target genes is highly increased after 25 h. Furthermore, analysis of genes induced by Ptf1a in the presence of CHX through RNA-sequencing showed that, indeed, genes activated by Ptf1a after 25 h are direct target genes of Ptf1a. Consistent with observation in the mouse, the proneural bHLH transcription factor *Ngn2* was shown to be a direct target of the heterotrimeric Ptf1a transcription complex. *Ngn2* and *Ptf1a* are co-expressed in the region of the cerebellum that gives rise to the GABAergic inhibitory neurons (Fig. 3.5). In gain of function assays in *X. laevis* animal caps, the GABAergic neuronal subtype-inducing activity of Ptf1a was found to be dominant over the glutamatergic-inducing activity of Ngn2 (Fig. 3.6). This suggests that Ngn2 may act downstream of Ptf1a to participate in GABAergic interneuron formation. This hypothesis is supported by a slight increase in the number of GABAergic dI4 neurons in the chick neural tube after Ngn2 electroporation, as well as by the absence of this neuronal cell type in *Ascl1:Ngn2* double knockout mice, but not in the single *Ascl1* knockout mice (Helms et al., 2005).

The delayed activation of direct target genes raises the question, what regulates the timing of activation of Ptf1a direct target genes. In a first attempt to answer this question, it could be shown that neither the expression of *Su(H)* transcripts alters throughout development, nor that the interaction of Ptf1a and Su(H) is prevented *in vivo* (Fig. 3.9). As Su(H) protein levels may be limiting due to post-transcriptional mechanisms, expression levels of Su(H) in the embryo

were increased by microinjection of *Su(H)* mRNA together with *Ptf1a* mRNA (Fig. 3.10 and Fig. 3.21). The assays were analysed by the Nanostring nCounter system and revealed that while co-expression of *Ptf1a* mRNA and *Su(H)* mRNA did not result in an earlier onset of gene expression of the Su(H)-dependent target genes (Fig. 3.10 and Fig. 3.21), it did influence quantitatively the level of gene induction. This is important as it demonstrates that the injected Su(H) protein was functional and suggests that Su(H) protein availability is not the reason why direct target genes of the trimeric complex are delayed in their activation. As elevated Su(H) expression levels either increased or decreased the gene induction of Ptf1a Su(H)-dependent target genes (Fig. 3.10 and Fig. 3.21), they may have different threshold or kinetic responses to the heterotrimeric complex. Similarly, Ptf1a target genes in the context of pancreas development respond differently to Ptf1a expression (Fukuda et al., 2008; Dong et al., 2008). Low levels of Ptf1a promote endocrine, while high Ptf1a levels are required for exocrine cell differentiation. Therefore, such a dosage-dependent mechanism might generally apply for the regulation of Ptf1a target gene induction.

The early function of Ptf1a during neuronal differentiation and the late function during neuronal subtype specification are reminiscent of Ptf1a activity during pancreas development. Ptf1a first promotes the commitment of endodermal cells into pancreatic precursors of both, endocrine and exocrine cell lineages (Burlison et al., 2008; Kawaguchi et al., 2002) and later, Ptf1a is required for acinar exocrine cell differentiation (Zecchin et al., 2004; Lin et al., 2004; Kawaguchi et al., 2002). Notch-signalling also plays a key role during pancreas development. It is highly active in exocrine pancreatic precursor cells where it prevents their terminal differentiation (Hald et al., 2003; Murtaugh et al., 2003; Esni et al., 2004). In this regard, it could be shown that the Notch-pathway and its effectors of the Hes family inhibit Ptf1a activity (Esni et al., 2004; Ghosh and Leach, 2006). In the nervous system, Notch-signalling in the neural progenitor cells is high and also maintains an undifferentiated cell state. Repression of bHLH transcription factors by the Notch-signalling effectors is a common regulatory mechanism in general neurogenesis (Takke et al., 1999; Schneider et al., 2001) and thus it is possible that also Ptf1a function in the nervous system is regulated by this mechanism. Furthermore, binding of Su(H)

by Notch-ICD and Ptf1a was shown to be mutually exclusive (Beres et al., 2006) and therefore, a competition between Ptf1a and Notch-ICD for Su(H)-binding may also be involved in the regulation of the expression of the distinct Ptf1a target genes (Henke et al., 2009b). When the Notch-signalling activity declines, Su(H) might be released from Notch-ICD to form the heterotrimeric complex with Ptf1a. To analyse if a competition between Ptf1a and Notch-ICD controls complex formation and thus target genes, a dominant-negative *Dll1* ($Delta_{stu}$) was used to block Notch-signalling (data not shown), however, this did not lead to an alteration in the onset of gene expression of Su(H)-dependent Ptf1a target genes. However, more detailed experiments have to be conducted to analyse this possibility.

In the presence of cycloheximide (CHX), which blocks protein synthesis, activation of the Su(H)-dependent target gene *Ngn2* was observed within 8.5 h, but not in the absence of CHX (Fig. 3.16). This suggests that there is a mechanism which prevents early activation of Su(H)-dependent target genes that requires protein synthesis.

The formation of the two distinct Ptf1a transcription complexes might be regulated by posttranslational modification as has been shown for other bHLH proteins. For example, the distinct activities of the bHLH transcription factor Ngn2 were shown to be regulated through posttranslational phosphorylation (Hindley et al., 2012; Ma et al., 2008). In this context, it was also shown that the transcriptional activity of Ptf1a and its cooperation with Rbp-l is dependent on histone acetylation mediated by the acetyltransferase cofactor p/CAF (Rodolosse et al., 2009).

4.4 Identification of the genetic program regulated by Ptf1a during *X. laevis* neurogenesis

In contrast to the exocrine pancreas, the genetic regulatory network downstream of Ptf1a in the context of the nervous system is poorly understood. In the murine nervous system, only four direct target genes of Ptf1a have been identified so far, including *Ptf1a* itself, which undergoes positive autoregulation (Meredith et al., 2009), *Ngn2* (Henke et al., 2009b), *Kirrel2* and *Nephrin* (Nishida et al., 2010). Therefore, with the aim of identifying Ptf1a direct targets, genes induced in *X. laevis* animal caps by Ptf1a in the presence of CHX were

analysed by RNA-sequencing. The number of genes induced compared to uninjected control caps strongly increased when Ptf1a was co-expressed with Su(H). The identified direct target genes were compared to genes induced by Ptf1a after 6 or 25 h in the absence of CHX. Among the identified direct target genes (based on their presence in the CHX RNA-seq experiment) activated by Ptf1a after 25 h were *Kirrel2* (Nishida et al., 2010) and *Ngn2* (Henke et al., 2009b). However, none of the known transcription factors involved in GABAergic interneuron formation were identified, suggesting that their activation by Ptf1a is indirect. Gene ontology analysis of the direct target genes induced by Ptf1a in combination with Su(H) revealed that Ptf1a directly induces many transcription factors. Several of them are involved in general neurogenesis, including lateral inhibition and cell-cycle regulation, demonstrating that Ptf1a directly controls early steps of neurogenesis. Additionally, the Ptf1a target genes were compared to a previous Affymetrix microarray analysis screen, which identified 57 direct target genes of *X. laevis* Ngn2-GR in animal caps (Seo et al., 2007). Among the 258 direct genes of Ptf1a-GR alone, 19 genes were also shown by Seo et al. to be direct Ngn2 targets, while for Ptf1a-GR together with Su(H)-GR 24 out of the 638 direct genes were similarly identified (Appendix 6.4). The shared direct targets of Ptf1a-GR and Ngn2-GR included genes involved in neuronal differentiation (*MyT1, NeuroD4*) and cell migration (*Snail1, Twist1*).

Gene ontology analysis of the late target genes demonstrated that Ptf1a directly regulates a wide range of biological processes, including cell adhesion, cell motion and cell projection organisation. A similar wide program of biological processes was identified for the mammalian Ascl1 (Castro et al., 2011) and Atoh1 (Klisch et al., 2011), two proneural transcription factors with a distinct neuronal subtype specification in the vertebrate CNS.

Pancreas specific genes were also present in the group of genes induced by Ptf1a in the presence of CHX. Therefore, the direct target genes induced two-fold or more by Ptf1a-GR and Ptf1a/Su(H)-GR in the RNA-sequencing analysis were compared to published studies identifying Ptf1a targets by ChIP-sequencing. In the pancreatic cell line 266-6, which has an expression profile similar to pancreatic progenitor cells, Ptf1a was found to bind regulatory

elements near 936 genes (Thompson et al., 2012) and near 4632 genes in the adult mouse pancreas (Masui et al., 2010). Of these, in our set of direct target genes 38 genes were identified as Ptf1a-GR/Su(H)-GR and 15 genes as Ptf1a-GR direct targets (Appendix 6.4) (Thompson et al., 2012). In contrast, of the putative direct targets in the adult mouse pancreas, only seven were identified as Ptf1a-GR/Su(H)-GR and three as Ptf1a-GR direct target genes (Masui et al., 2010) (Appendix 6.4). In general, the number of overlapping genes was quite low. However, 19 direct candidates (Appendix 6.4) induced by Ptf1a-GR/Su(H)-GR were also found to be induced in endodermal explants of stage 32 and 36 *X. laevis* embryos (Bilogan and Horb, 2012), suggesting that genes functioning downstream of Ptf1a during pancreatic development are present in our list of candidate genes.

4.5 Identification of novel Su(H)-dependent Ptf1a direct target genes

To understand how Ptf1a induces neuronal subtype specification via the trimeric complex, genes were identified, which are present in both RNA-sequencing approaches, but are not activated by Ptf1a$^{W224A/W242A}$. This comparison identified 111 Su(H)-dependent Ptf1a target genes, among them *Ngn2* and *Kirrel2*. In a first step to verify selective candidates, eight of the new Su(H)-dependent direct target genes were analysed with the Nanostring nCounter RNA profiling system (Fig. 3.20 and Fig. 3.21, Appendix 6.1.3 and 6.1.4). The selected candidates represent different types of transcription factors and none of them, with the exception of *barhl2*, which is expressed in amacrine cells in the retina (Ding et al., 2009), were specifically described before as genes associated with GABAergic inhibitory neuronal subtype determination. Nanostring analyses demonstrated that all of the genes analysed were dependent on the interaction of Ptf1a and Su(H) as the induction by Ptf1a$^{W224A/W242A}$ was reduced at least to half or completely eliminated compared to wild-type Ptf1a. Similar to the known downstream targets of Ptf1a, the majority of the novel Su(H)-dependent genes were strongly increased when Ptf1a was co-expressed with Su(H). However, one gene was downregulated upon co-injection of Su(H). This differential gene induction by Ptf1a alone and in combination with Su(H) is similar to what we already observed for other Ptf1a

downstream targets such as *Gad1* and *Ngn2* (Fig. 3.10). This further supports the hypothesis that different Su(H)-dependent targets may have a different threshold response for the heterotrimeric Ptf1a complex, which regulates this activation. Analysis of additional Su(H)-dependent target genes will allow a classification of Ptf1a target genes into distinct groups and therefore may give insight into how Ptf1a promotes multiple developmental processes.

5. Conclusion

In summary, this study demonstrates that Ptf1a can function as proneural bHLH transcription factor in *X. laevis* and that for this activity, Ptf1a does not require the interaction with Su(H). Furthermore, through two independent RNA-sequencing approaches, the genetic network directly downstream of Ptf1a in the context of general neurogenesis as well as neuronal subtype specification could be defined. Analysis of the direct target genes will give new insight into the mechanism how Ptf1a activates general neurogenesis and neuronal subtype specification and may elucidate new mechanisms by which proneural transcription factors are able to confer distinct activities during the development of the nervous system.

Bibliography

Afelik, S., Chen, H. and Pieler, T. (2006). Combined ectopic expression of Pdx1 and Ptf1a/p48 results in the stable conversion of posterior endoderm into endocrine and exocrine pancreatic tissue. *Genes Dev* **20**, 1441-6.
Al-Shammari, M., Al-Husain, M., Al-Kharfy, T. and Alkuraya, F. S. (2011). A novel PTF1A mutation in a patient with severe pancreatic and cerebellar involvement. *Clin Genet* **80**, 196-8.
Alaynick, H. A., Jessell, T. M. and Pfaff, S. L. (2011). SnapShot: spinal cord development. *Cell* **146**, 178-178 e1.
Alvarez, I. S., Araujo, M. and Nieto, M. A. (1998). Neural induction in whole chick embryo cultures by FGF. *Dev Biol* **199**, 42-54.
Alvarez-Medina, R., Cayuso, J., Okubo, T., Takada, S., and Marti, E. (2008). Wnt canonical pathway restricts graded Shh/Gli patterning activity through the regulation of Gli3 expression. *Development* **135**, 237-47.
Amaya, E. (2005). Xenomics. *Genome Res* **15**, 1683-91.
Anders, S. and Huber, H. (2010). Differential expression analysis for sequence count data. *Genome Biol* **11**, R106.
Bachiller, D., Klingensmith, J., Kemp, C., Belo, J.A., Anderson, R.M., May, S.R., McMahon, J.A., McMahon, A.P., Harland, R.M., Rossant, J., et al. (2000). The organizer factors Chordin and Noggin are required for mouse forebrain development. *Nature* **403**, 658-61.
Bachiller, D., Klingensmith, J., Shneyder, N., Tran, U., Anderson, R., Rossant, J. and De Robertis, E. M. (2003). The role of chordin/Bmp signals in mammalian pharyngeal development and DiGeorge syndrome. *Development* **130**, 3567-78.
Barth, K. A., Kishimoto, H., Rohr, K. B., Seydler, C., Schulte-Merker, S. and Wilson, S. H. (1999). Bmp activity establishes a gradient of positional information throughout the entire neural plate. *Development* **126**, 4977-87.
Bellefroid, E. J., Bourguignon, C., Hollemann, T., Ma, Q., Anderson, D. J., Kintner, C. and Pieler, T. (1996). X-MyT1, a Xenopus C2HC-type zinc finger protein with a regulatory function in neuronal differentiation. *Cell* **87**, 1191-202.
Bellefroid, E. J., Kobbe, A., Gruss, P., Pieler, T., Gurdon, J. B. and Papalopulu, N. (1998). Xiro3 encodes a Xenopus homolog of the Drosophila Iroquois genes and functions in neural specification. *EMBO J* **17**, 191-203.
Beres, T. M., Masui, T., Swift, G. H., Shi, L., Henke, R. M. and MacDonald, R. J. (2006). PTF1 is an organ-specific and Notch-independent basic helix-loop-helix complex containing the mammalian Suppressor of Hairless (RBP-J) or its paralogue, RBP-L. *Mol Cell Biol* **26**, 117-30.
Bertrand, N., Castro, D. S. and Guillemot, F. (2002). Proneural genes and the specification of neural cell types. *Nat Rev Neurosci* **3**, 517-30.
Bilogan, C. K. and Horb, M. E. (2012). Microarray analysis of Xenopus endoderm expressing Ptf1a. *Genesis*.
Borchers A., Pieler T. (2010). Programming pluripotent precursor cells derived from *Xenopus* embryos to generate specific tissues. *Genes*, ***1*(3)**, 413-426.
Bouwmeester, T., Kim, S., Sasai, H., Lu, B. and De Robertis, E. M. (1996). Cerberus is a head-inducing secreted factor expressed in the anterior endoderm of Spemann's organizer. *Nature* **382**, 595-601.
Boy, S., Souopgui, J., Amato, M. A., Wegnez, M., Pieler, T. and Perron, M. (2004). XSEB4R, a novel RNA-binding protein involved in retinal cell

differentiation downstream of bHLH proneural genes. *Development* **131**, 851-62.
Bray, S. J. (2006). Notch signalling: a simple pathway becomes complex. *Nat Rev Mol Cell Biol* **7**, 678-89.
Brewster, R., Lee, J. and Ruiz i Altaba, A. (1998). Gli/Zic factors pattern the neural plate by defining domains of cell differentiation. *Nature* **393**, 579-83.
Briscoe, J., and Ericson, J. (2001). Specification of neuronal fates in the ventral neural tube. *Curr Opin Neurobiol* **11**, 43-49.
Briscoe, J., Pierani, A., Jessell, T. M. and Ericson, J. (2000). A homeodomain protein code specifies progenitor cell identity and neuronal fate in the ventral neural tube. *Cell* **101**, 435-45.
Brunet, J. F. und Ghysen, A. (1999). Deconstructing cell determination: proneural genes and neuronal identity. *Bioessays* **21**, 313-8.
Burlison, J. S., Long, Q., Fujitani, H., Wright, C. V. and Magnuson, M. A. (2008). Pdx-1 and Ptf1a concurrently determine fate specification of pancreatic multipotent progenitor cells. *Dev Biol* **316**, 74-86.
Castro, D. S. and Guillemot, F. (2011). Old and new functions of proneural factors revealed by the genome-wide characterization of their transcriptional targets. *Cell Cycle* **10**, 4026-31.
Castro, D. S., Martynoga, B., Parras, C., Ramesh, V., Pacary, E., Johnston, C., Drechsel, D., Lebel-Potter, M., Garcia, L. G., Hunt, C. et al. (2011). A novel function of the proneural factor Ascl1 in progenitor proliferation identified by genome-wide characterization of its targets. *Genes Dev* **25**, 930-45.
Cau, E., Gradwohl, G., Casarosa, S., Kageyama, R., and Guillemot, F. (2000). Hes genes regulate sequential stages of neurogenesis in the olfactory epithelium. *Development* **127**, 2323-32.
Chan, H. M. and Jan, H. N. (1999). Presenilins, processing of beta-amyloid precursor protein, and notch signaling. *Neuron* **23**, 201-4.
Chen, Y., Pan, F. C., Brandes, N., Afelik, S., Sölter, M., Pieler, T. (2004). Retinoic acid signaling is essential for pancreas development and promotes endocrine at the expense of exocrine cell differentiation in Xenopus. *Dev Biol* **271**, 144-60.
Cheng, L., Arata, A., Mizuguchi, R., Qian, H., Karunaratne, A., Gray, P. A., Arata, S., Shirasawa, S., Bouchard, M., Luo, P. et al. (2004). Tlx3 and Tlx1 are post-mitotic selector genes determining glutamatergic over GABAergic cell fates. *Nat Neurosci* **7**, 510-7.
Cheng, L., Samad, O. A., Xu, H., Mizuguchi, R., Luo, P., Shirasawa, S., Goulding, M. and Ma, Q. (2005). Lbx1 and Tlx3 are opposing switches in determining GABAergic versus glutamatergic transmitter phenotypes. *Nat Neurosci* **8**, 1510-5.
Chien, C. T., Hsiao, C. D., Jan, L. H. and Jan, H. N. (1996). Neuronal type information encoded in the basic-helix-loop-helix domain of proneural genes. *Proc Natl Acad Sci U S A* **93**, 13239-44.
Chitnis, A., Henrique, D., Lewis, J., Ish-Horowicz, D. and Kintner, C. (1995). Primary neurogenesis in Xenopus embryos regulated by a homologue of the Drosophila neurogenic gene Delta. *Nature* **375**, 761-6.
Chitnis, A. and Kintner, C. (1995). Neural induction and neurogenesis in amphibian embryos. *Perspect Dev Neurobiol* **3**, 3-15.
Chitnis, A. and Kintner, C. (1996). Sensitivity of proneural genes to lateral inhibition affects the pattern of primary neurons in Xenopus embryos. *Development* **122**, 2295-301.

Cockell, M., Stevenson, B. J., Strubin, M., Hagenbuchle, O. and Wellauer, P. K. (1989). Identification of a cell-specific DNA-binding activity that interacts with a transcriptional activator of genes expressed in the acinar pancreas. *Mol Cell Biol* **9**, 2464-76.

Coffman, C., Harris, H. and Kintner, C. (1990). Xotch, the Xenopus homolog of Drosophila notch. *Science* **249**, 1438-41.

Damianitsch, K. (2008). Doctoral Thesis: Die Funktion des Wnt Antagonisten XsFRP5 während der frühembryonalen Musterbildung des Entoderms in Xenopus laevis. University of Goettingen, Goettingen

Davis, R. L. and Turner, D. L. (2001). Vertebrate hairy and Enhancer of split related proteins: transcriptional repressors regulating cellular differentiation and embryonic patterning. *Oncogene* **20**, 8342-57.

de la Calle-Mustienes, E., Glavic, A., Modolell, J., and Gomez-Skarmeta, J.L. (2002). Xiro homeoproteins coordinate cell cycle exit and primary neuron formation by upregulating neuronal-fate repressors and downregulating the cell-cycle inhibitor XGadd45-gamma. *Mech Dev* **119**, 69-80.

Delaune, E., Lemaire, P. and Kodjabachian, L. (2005). Neural induction in Xenopus requires early FGF signalling in addition to BMP inhibition. *Development* **132**, 299-310.

Ding, Q., Chen, H., Xie, X., Libby, R.T., Tian, N., and Gan, L. (2009). BARHL2 differentially regulates the development of retinal amacrine and ganglion neurons. *J Neurosci* **29**, 3992-4003

Dong, P. D., Provost, E., Leach, S. D. and Stainier, D. H. (2008). Graded levels of Ptf1a differentially regulate endocrine and exocrine fates in the developing pancreas. *Genes Dev* **22**, 1445-50.

Dreau, G. L. and Marti, E. (2012). Dorsal-ventral patterning of the neural tube: A tale of three signals. *Dev Neurobiol*.

Dubois, L., Bally-Cuif, L., Crozatier, M., Moreau, J., Paquereau, L. and Vincent, A. (1998). XCoe2, a transcription factor of the Col/Olf-1/EBF family involved in the specification of primary neurons in Xenopus. *Curr Biol* **8**, 199-209.

Dullin, J. P., Locker, M., Robach, M., Henningfeld, K. A., Parain, K., Afelik, S., Pieler, T. and Perron, M. (2007). Ptf1a triggers GABAergic neuronal cell fates in the retina. *BMC Dev Biol* **7**, 110.

Echelard, Y., Epstein, D.J., St-Jacques, B., Shen, L., Mohler, J., McMahon, J.A., and McMahon, A.P. (1993). Sonic hedgehog, a member of a family of putative signaling molecules, is implicated in the regulation of CNS polarity. *Cell* **75**, 1417-30.

Ellis, P., Fagan, B. M., Magness, S. T., Hutton, S., Taranova, O., Hayashi, S., McMahon, A., Rao, M. and Pevny, L. (2004). SOX2, a persistent marker for multipotential neural stem cells derived from embryonic stem cells, the embryo or the adult. *Dev Neurosci* **26**, 148-65.

Ericson, J., Rashbass, P., Schedl, A., Brenner-Morton, S., Kawakami, A., van Heyningen, V., Jessell, T.M., and Briscoe, J. (1997). Pax6 controls progenitor cell identity and neuronal fate in response to graded Shh signaling. *Cell* **90**, 169-80.

Ericson, J., Briscoe, J., Rashbass, P., van Heyningen, V. and Jessell, T. M. (1997). Graded sonic hedgehog signaling and the specification of cell fate in the ventral neural tube. *Cold Spring Harb Symp Quant Biol* **62**, 451-66.

Ericson, J., Morton, S., Kawakami, A., Roelink, H. and Jessell, T. M. (1996). Two critical periods of Sonic Hedgehog signaling required for the specification of motor neuron identity. *Cell* **87**, 661-73.

Esni, F., Ghosh, B., Biankin, A. V., Lin, J. H., Albert, M. A., Yu, X., MacDonald, R. J., Civin, C. I., Real, F. X., Pack, M. A. et al. (2004a). Notch inhibits Ptf1 function and acinar cell differentiation in developing mouse and zebrafish pancreas. *Development* **131**, 4213-24.

Ferreiro, B., Skoglund, P., Bailey, A., Dorsky, R. and Harris, H. A. (1993). XASH1, a Xenopus homolog of achaete-scute: a proneural gene in anterior regions of the vertebrate CNS. *Mech Dev* **40**, 25-36.

Fode, C., Ma, Q., Casarosa, S., Ang, S. L., Anderson, D. J. and Guillemot, F. (2000). A role for neural determination genes in specifying the dorsoventral identity of telencephalic neurons. *Genes Dev* **14**, 67-80.

Fog, C. K., Galli, G. G. and Lund, A. H. (2012). PRDM proteins: important players in differentiation and disease. *Bioessays* **34**, 50-60.

Fujitani, H., Fujitani, S., Luo, H., Qiu, F., Burlison, J., Long, Q., Kawaguchi, H., Edlund, H., MacDonald, R. J., Furukawa, T. et al. (2006). Ptf1a determines horizontal and amacrine cell fates during mouse retinal development. *Development* **133**, 4439-50.

Fukuda, A., Kawaguchi, H., Furuyama, K., Kodama, S., Horiguchi, M., Kuhara, T., Kawaguchi, M., Terao, M., Doi, R., Wright, C. V. et al. (2008). Reduction of Ptf1a gene dosage causes pancreatic hypoplasia and diabetes in mice. *Diabetes* **57**, 2421-31.

Furthauer, M., Thisse, C. and Thisse, B. (1997). A role for FGF-8 in the dorsoventral patterning of the zebrafish gastrula. *Development* **124**, 4253-64.

Gammill, L. S. and Sive, H. (1997). Identification of otx2 target genes and restrictions in ectodermal competence during Xenopus cement gland formation. *Development* **124**, 471-81.

Ge, H., He, F., Kim, K. J., Blanchi, B., Coskun, V., Nguyen, L., Wu, X., Zhao, J., Heng, J. I., Martinowich, K. et al. (2006). Coupling of cell migration with neurogenesis by proneural bHLH factors. *Proc Natl Acad Sci U S A* **103**, 1319-24.

Geiss G.K. , Bumgarner R.E., Birditt B., Dahl T., Dowidar N., Dunaway D.L., Fell H.P., Ferree S., George R.D., Grogan T., James J.J., Maysuria M., Mitton J.D., Oliveri P., Osborn J.L., Peng T., Ratcliffe A.L., Webster P.J., Davidson E.H., Hood L., Dimitrov K. (2008). Direct multiplexed measurement of gene expression with color-coded probe pairs. *Nat. Biotechnol*. **26(3)**, 317-25.

Ghosh, B. and Leach, S. D. (2006). Interactions between hairy/enhancer of split-related proteins and the pancreatic transcription factor Ptf1-p48 modulate function of the PTF1 transcriptional complex. *Biochem J* **393**, 679-85.

Ghysen, A. and Dambly-Chaudiere, C. (1989). Genesis of the Drosophila peripheral nervous system. *Trends Genet* **5**, 251-5.

Glasgow, S. M., Henke, R. M., Macdonald, R. J., Wright, C. V. and Johnson, J. E. (2005). Ptf1a determines GABAergic over glutamatergic neuronal cell fate in the spinal cord dorsal horn. *Development* **132**, 5461-9.

Godsave, S. F. and Slack, J. M. (1989). Clonal analysis of mesoderm induction in Xenopus laevis. *Dev Biol* **134**, 486-90.

Gomez-Skarmeta, J. L., Glavic, A., de la Calle-Mustienes, E., Modolell, J. and Mayor, R. (1998). Xiro, a Xenopus homolog of the Drosophila Iroquois complex genes, controls development at the neural plate. *EMBO J* **17**, 181-90.

Graham, V., Khudyakov, J., Ellis, P. and Pevny, L. (2003). SOX2 functions to maintain neural progenitor identity. *Neuron* **39**, 749-65.
Grunz, H. and Tacke, L. (1989). Neural differentiation of Xenopus laevis ectoderm takes place after disaggregation and delayed reaggregation without inducer. *Cell Differ Dev* **28**, 211-7.
Guillemot, F. (1999). Vertebrate bHLH genes and the determination of neuronal fates. *Exp Cell Res* **253**, 357-64.
Guillemot, F. (2007). Spatial and temporal specification of neural fates by transcription factor codes. *Development* **134**, 3771-80.
Hald, J., Hjorth, J. P., German, M. S., Madsen, O. D., Serup, P. and Jensen, J. (2003). Activated Notch1 prevents differentiation of pancreatic acinar cells and attenuate endocrine development. *Dev Biol* **260**, 426-37.
Haldin, C. E., Nijjar, S., Masse, K., Barnett, M. H. and Jones, E. A. (2003) 'Isolation and growth factor inducibility of the Xenopus laevis Lmx1b gene'. *Int J Dev Biol* **47(4)**, 253-62.
Hamburger, V. (1969). Hans Spemann and the organizer concept. *Experientia* **25**, 1121-5.
Hardcastle, Z., Chalmers, A.D., and Papalopulu, N. (2000). FGF-8 stimulates neuronal differentiation through FGFR-4a and interferes with mesoderm induction in Xenopus embryos. *Curr Biol* **10**, 1511-14.
Hardcastle, Z. and Papalopulu, N. (2000). Distinct effects of XBF-1 in regulating the cell cycle inhibitor p27(XIC1) and imparting a neural fate. *Development* **127**, 1303-14.
Harland, R.M. (1991). In situ hybridization: an improved whole-mount method for Xenopus embryos. *Methods Cell Biol* **36**, 685-95.
Harland, R. M. and Grainger, R. M. (2011). Xenopus research: metamorphosed by genetics and genomics. *Trends Genet* **27**, 507-15.
Hartenstein, V. (1989). Early neurogenesis in Xenopus: the spatio-temporal pattern of proliferation and cell lineages in the embryonic spinal cord. *Neuron* **3**, 399-411.
Hartenstein, V. (1993). Early pattern of neuronal differentiation in the Xenopus embryonic brainstem and spinal cord. *J Comp Neurol* **328**, 213-31.
Hatakeyama, J., Tomita, K., Inoue, T., and Kageyama, R. (2001). Roles of homeobox and bHLH genes in specification of a retinal cell type. *Development* **128**, 1313-22.
Hedderich, M. (2008). Diploma Thesis: Charakterisierung der proneuralen Aktivität von Ptf1a/p48 in Xenopus (Characterisation of the proneural activity of Ptf1a/p48 in Xenopus). University of Goettingen, Goettingen
Hellsten, U., Harland, R. M., Gilchrist, M. J., Hendrix, D., Jurka, J., Kapitonov, V., Ovcharenko, I., Putnam, N. H., Shu, S., Taher, L. et al. (2010). The genome of the Western clawed frog Xenopus tropicalis. *Science* **328**, 633-6.
Helms, A. H., Battiste, J., Henke, R. M., Nakada, H., Simplicio, N., Guillemot, F. and Johnson, J. E. (2005). Sequential roles for Mash1 and Ngn2 in the generation of dorsal spinal cord interneurons. *Development* **132**, 2709-19.
Helms, A. H. and Johnson, J. E. (2003). Specification of dorsal spinal cord interneurons. *Curr Opin Neurobiol* **13**, 42-9.
Hemmati-Brivanlou, A. and Melton, D. A. (1994). Inhibition of activin receptor signaling promotes neuralization in Xenopus. *Cell* **77**, 273-81.

Henke, R. M., Meredith, D. M., Borromeo, M. D., Savage, T. K. and Johnson, J. E. (2009a). Ascl1 and Neurog2 form novel complexes and regulate Delta-like3 (Dll3) expression in the neural tube. *Dev Biol* **328**, 529-40.
Henke, R. M., Savage, T. K., Meredith, D. M., Glasgow, S. M., Hori, K., Dumas, J., MacDonald, R. J. and Johnson, J. E. (2009b). Neurog2 is a direct downstream target of the Ptf1a-Rbpj transcription complex in dorsal spinal cord. *Development* **136**, 2945-54.
Hindley, C., Ali, F., McDowell, G., Cheng, K., Jones, A., Guillemot, F. and Philpott, A. (2012). Post-translational modification of Ngn2 differentially affects transcription of distinct targets to regulate the balance between progenitor maintenance and differentiation. *Development* **139**, 1718-23.
Hollemann, T. and Pieler, T. (1999). Xpitx-1: a homeobox gene expressed during pituitary and cement gland formation of Xenopus embryos. *Mech Dev* **88**, 249-52.
Hollyday, M., McMahon, J. A. and McMahon, A. P. (1995). Wnt expression patterns in chick embryo nervous system. *Mech Dev* **52**, 9-25.
Hongo, I., Kengaku, M. and Okamoto, H. (1999). FGF signaling and the anterior neural induction in Xenopus. *Dev Biol* **216**, 561-81.
Honjo, T. (1996). The shortest path from the surface to the nucleus: RBP-J kappa/Su(H) transcription factor. *Genes Cells* **1**, 1-9.
Hori, K., Cholewa-Waclaw, J., Nakada, H., Glasgow, S. M., Masui, T., Henke, R. M., Wildner, H., Martarelli, B., Beres, T. M., Epstein, J. A. et al. (2008). A nonclassical bHLH Rbpj transcription factor complex is required for specification of GABAergic neurons independent of Notch signaling. *Genes Dev* **22**, 166-78.
Hori, K. and Hoshino, M. (2012). GABAergic neuron specification in the spinal cord, the cerebellum, and the cochlear nucleus. *Neural Plast* **2012**, 921732.
Hoshino, M. (2006). Molecular machinery governing GABAergic neuron specification in the cerebellum. *Cerebellum* **5**, 193-98.
Hoshino, M., Nakamura, S., Mori, K., Kawauchi, T., Terao, M., Nishimura, H. V., Fukuda, A., Fuse, T., Matsuo, N., Sone, M. et al. (2005). Ptf1a, a bHLH transcriptional gene, defines GABAergic neuronal fates in cerebellum. *Neuron* **47**, 201-13.
Hoveyda, N., Shield, J. P., Garrett, C., Chong, H. K., Beardsall, K., Bentsi-Enchill, E., Mallya, H. and Thompson, M. H. (1999). Neonatal diabetes mellitus and cerebellar hypoplasia/agenesis: report of a new recessive syndrome. *J Med Genet* **36**, 700-4.
Imayoshi, I. and Kageyama, R. (2011). The role of Notch signaling in adult neurogenesis. *Mol Neurobiol* **44**, 7-12.
Ishibashi, M., Ang, S. L., Shiota, K., Nakanishi, S., Kageyama, R. and Guillemot, F. (1995). Targeted disruption of mammalian hairy and Enhancer of split homolog-1 (HES-1) leads to up-regulation of neural helix-loop-helix factors, premature neurogenesis, and severe neural tube defects. *Genes Dev* **9**, 3136-48.
Iype, T., Taylor, D. G., Ziesmann, S. M., Garmey, J. C., Watada, H. and Mirmira, R. G. (2004). The transcriptional repressor Nkx6.1 also functions as a deoxyribonucleic acid context-dependent transcriptional activator during pancreatic beta-cell differentiation: evidence for feedback activation of the nkx6.1 gene by Nkx6.1. *Mol Endocrinol* **18**, 1363-75.
Jan, H. N. and Jan, L. H. (1994). Neuronal cell fate specification in Drosophila. *Curr Opin Neurobiol* **4**, 8-13.

Jarman, A. P., Grau, H., Jan, L. H. and Jan, H. N. (1993). atonal is a proneural gene that directs chordotonal organ formation in the Drosophila peripheral nervous system. *Cell* **73**, 1307-21.
Jessell, T. M. (2000). Neuronal specification in the spinal cord: inductive signals and transcriptional codes. *Nat Rev Genet* **1**, 20-9.
Kanekar, S., Perron, M., Dorsky, R., Harris, H. A., Jan, L. H., Jan, H. N. and Vetter, M. L. (1997). Xath5 participates in a network of bHLH genes in the developing Xenopus retina. *Neuron* **19**, 981-94.
Kawaguchi, H., Cooper, B., Gannon, M., Ray, M., MacDonald, R. J. and Wright, C. V. (2002). The role of the transcriptional regulator Ptf1a in converting intestinal to pancreatic progenitors. *Nat Genet* **32**, 128-34.
Kengaku, M. and Okamoto, H. (1995). bFGF as a possible morphogen for the anteroposterior axis of the central nervous system in Xenopus. *Development* **121**, 3121-30.
Kim, P., Helms, A. H., Johnson, J. E. and Zimmerman, K. (1997). XATH-1, a vertebrate homolog of Drosophila atonal, induces a neuronal differentiation within ectodermal progenitors. *Dev Biol* **187**, 1-12.
Klisch, T. J., Xi, H., Flora, A., Wang, L., Li, H. and Zoghbi, H. H. (2011). In vivo Atoh1 targetome reveals how a proneural transcription factor regulates cerebellar development. *Proc Natl Acad Sci U S A* **108**, 3288-93.
Krapp, A., Knofler, M., Frutiger, S., Hughes, G. J., Hagenbuchle, O. and Wellauer, P. K. (1996). The p48 DNA-binding subunit of transcription factor PTF1 is a new exocrine pancreas-specific basic helix-loop-helix protein. *EMBO J* **15**, 4317-29.
Krapp, A., Knofler, M., Ledermann, B., Burki, K., Berney, C., Zoerkler, N., Hagenbuchle, O. and Wellauer, P. K. (1998). The bHLH protein PTF1-p48 is essential for the formation of the exocrine and the correct spatial organization of the endocrine pancreas. *Genes Dev* **12**, 3752-63.
Kroll, K. L. (2007). Geminin in embryonic development: coordinating transcription and the cell cycle during differentiation. *Front Biosci* **12**, 1395-409.
Kroll, K. L., Salic, A. N., Evans, L. M. and Kirschner, M. H. (1998). Geminin, a neuralizing molecule that demarcates the future neural plate at the onset of gastrulation. *Development* **125**, 3247-58.
Kulkarni M.M. (2011). Digital multiplexed gene expression analysis using the NanoString nCounter system. Curr Protoc Mol Biol. **25**,Unit25B.10.
Laemmli, U. K. (1970). Cleavage of structural proteins during the assembly of the head of bacteriophage T4. *Nature* **227(5259)**, 680-85.
Lamb, T. M. and Harland, R. M. (1995). Fibroblast growth factor is a direct neural inducer, which combined with noggin generates anterior-posterior neural pattern. *Development* **121**, 3627-36.
Lamb, T.M., Knecht, A.K., Smith, W.C., Stachel, S.E., Economides, A.N., Stahl, N., Yancopolous, G.D., and Harland, R.M. (1993). Neural induction by the secreted polypeptide noggin. *Science* **262**, 713-18.
Langmead, B. and Salzberg, S. L. (2012). Fast gapped-read alignment with Bowtie 2. *Nat Methods* **9**, 357-9.
Launay, C., Fromentoux, V., Shi, D. L. and Boucaut, J. C. (1996). A truncated FGF receptor blocks neural induction by endogenous Xenopus inducers. *Development* **122**, 869-80.
Le Dreau, G., Garcia-Campmany, L., Rabadan, M. A., Ferronha, T., Tozer, S., Briscoe, J. and Marti, E. (2012). Canonical BMP7 activity is required for the

generation of discrete neuronal populations in the dorsal spinal cord. *Development* **139**, 259-68.
Leclerc, C., Daguzan, C., Nicolas, M. T., Chabret, C., Duprat, A. M. and Moreau, M. (1997). L-type calcium channel activation controls the in vivo transduction of the neuralizing signal in the amphibian embryos. *Mech Dev* **64**, 105-10.
Leclerc, C., Webb, S. E., Daguzan, C., Moreau, M, Miller, A. L. (2000). Imaging patterns of calcium transients during neural induction in Xenopus laevis emrbyos. *J Cell Sci* **113**, 3519-29.
Leclerc, C., Lee, M., Webb, S. E., Moreau, M. and Miller, A. L. (2003). Calcium transients triggered by planar signals induce the expression of ZIC3 gene during neural induction in Xenopus. *Dev Biol* **261**, 381-90.
Leclerc, C., Neant, I. and Moreau, M. (2012). The calcium: an early signal that initiates the formation of the nervous system during embryogenesis. *Front Mol Neurosci* **5**, 3.
Lee, S. K. and Pfaff, S.L. (2003). Synchronization of neurogenesis and motor neuron specification by direct coupling of bHLH and homeodomain transcription factors. *Neuron* **38**, 731-45.
Lee, J. E. (1997). Basic helix-loop-helix genes in neural development. *Curr Opin Neurobiol* **7**, 13-20.
Lee, J. E., Hollenberg, S. M., Snider, L., Turner, D. L., Lipnick, N. and Weintraub, H. (1995). Conversion of Xenopus ectoderm into neurons by NeuroD, a basic helix-loop-helix protein. *Science* **268**, 836-44.
Lelievre, E. C., Lek, M., Boije, H., Houille-Vernes, L., Brajeul, V., Slembrouck, A., Roger, J. E., Sahel, J. A., Matter, J. M., Sennlaub, F. et al. (2011). Ptf1a/Rbpj complex inhibits ganglion cell fate and drives the specification of all horizontal cell subtypes in the chick retina. *Dev Biol* **358**, 296-308.
Levin, M. (1998). The roles of activin and follistatin signaling in chick gastrulation. *Int J Dev Biol* **42**, 553-9.
Lewis, J. (1996). Neurogenic genes and vertebrate neurogenesis. *Curr Opin Neurobiol* **6**, 3-10.
Li, M., Sipe, C. H., Hoke, K., August, L. L., Wright, M. A. and Saha, M. S. (2006). The role of early lineage in GABAergic and glutamatergic cell fate determination in Xenopus laevis. *J Comp Neurol* **495**, 645-57.
Liem, K. F., Jr., Tremml, G. and Jessell, T. M. (1997). A role for the roof plate and its resident TGFbeta-related proteins in neuronal patterning in the dorsal spinal cord. *Cell* **91**, 127-38.
Liem, K. F., Jr., Tremml, G., Roelink, H. and Jessell, T. M. (1995). Dorsal differentiation of neural plate cells induced by BMP-mediated signals from epidermal ectoderm. *Cell* **82**, 969-79.
Lin, J. H., Biankin, A. V., Horb, M. E., Ghosh, B., Prasad, N. B., Yee, N. S., Pack, M. A. and Leach, S. D. (2004). Differential requirement for ptf1a in endocrine and exocrine lineages of developing zebrafish pancreas. *Dev Biol* **274**, 491-503.
Lindsell, C. E., Boulter, J., diSibio, G., Gossler, A. and Weinmaster, G. (1996). Expression patterns of Jagged, Delta1, Notch1, Notch2, and Notch3 genes identify ligand-receptor pairs that may function in neural development. *Mol Cell Neurosci* **8**, 14-27.

Linker, C. and Stern, C. D. (2004). Neural induction requires BMP inhibition only as a late step, and involves signals other than FGF and Wnt antagonists. *Development* **131**, 5671-81.
Litingtung, H. and Chiang, C. (2000). Specification of ventral neuron types is mediated by an antagonistic interaction between Shh and Gli3. *Nat Neurosci* **3**, 979-85.
Lo, L., Tiveron, M.C., and Anderson, D.J. (1998). MASH1 activates expression of the paired homeodomain transcription factor Phox2a, and couples pan-neuronal and subtype-specific components of autonomic neuronal identity. *Development* **125**, 609-20.
Louvi, A. and Artavanis-Tsakonas, S. (2006). Notch signalling in vertebrate neural development. *Nat Rev Neurosci* **7**, 93-102.
Ma, Q., Kintner, C. and Anderson, D. J. (1996). Identification of neurogenin, a vertebrate neuronal determination gene. *Cell* **87**, 43-52.
Ma, H. C., Song, M. R., Park, J. P., Henry Ho, H. H., Hu, L., Kurtev, M. V., Zieg, J., Ma, Q., Pfaff, S. L. and Greenberg, M. E. (2008). Regulation of motor neuron specification by phosphorylation of neurogenin 2. *Neuron* **58**, 65-77.
Mandel, M., and Higa, A. (1970). Calcium-dependent bacteriophage DNA infection. *J Mol Biol* **53**, 159-62.
Marchal, L., Luxardi, G., Thome, V. and Kodjabachian, L. (2009). BMP inhibition initiates neural induction via FGF signaling and Zic genes. *Proc Natl Acad Sci U S A* **106**, 17437-42.
Marti, E., Bumcrot, D. A., Takada, R. and McMahon, A. P. (1995a). Requirement of 19K form of Sonic hedgehog for induction of distinct ventral cell types in CNS explants. *Nature* **375**, 322-5.
Marti, E., Takada, R., Bumcrot, D. A., Sasaki, H. and McMahon, A. P. (1995b). Distribution of Sonic hedgehog peptides in the developing chick and mouse embryo. *Development* **121**, 2537-47.
Martin, B. L. and Harland, R. M. (2006) 'A novel role for lbx1 in Xenopus hypaxial myogenesis'. *Development* **133(2)**, 195-208.
Masui, T., Long, Q., Beres, T. M., Magnuson, M. A. and MacDonald, R. J. (2007). Early pancreatic development requires the vertebrate Suppressor of Hairless (RBPJ) in the PTF1 bHLH complex. *Genes Dev* **21**, 2629-43.
Masui, T., Swift, G. H., Deering, T., Shen, C., Coats, H. S., Long, Q., Elsasser, H. P., Magnuson, M. A. and MacDonald, R. J. (2010). Replacement of Rbpj with Rbpjl in the PTF1 complex controls the final maturation of pancreatic acinar cells. *Gastroenterology* **139**, 270-80.
Masui, T., Swift, G. H., Hale, M. A., Meredith, D. M., Johnson, J. E. and Macdonald, R. J. (2008). Transcriptional autoregulation controls pancreatic Ptf1a expression during development and adulthood. *Mol Cell Biol* **28**, 5458-68.
Matzuk, M. M., Lu, N., Vogel, H., Sellheyer, K., Roop, D. R. and Bradley, A. (1995). Multiple defects and perinatal death in mice deficient in follistatin. *Nature* **374**, 360-3.
McCormick, D. A. and Contreras, D. (2001). On the cellular and network bases of epileptic seizures. *Annu Rev Physiol* **63**, 815-46.
McMahon, J. A., Takada, S., Zimmerman, L. B., Fan, C. M., Harland, R. M. and McMahon, A. P. (1998). Noggin-mediated antagonism of BMP signaling is required for growth and patterning of the neural tube and somite. *Genes Dev* **12**, 1438-52.
Megason, S. G. and McMahon, A. P. (2002). A mitogen gradient of dorsal midline Wnts organizes growth in the CNS. *Development* **129**, 2087-98.

Meredith, D. M., Masui, T., Swift, G. H., MacDonald, R. J. and Johnson, J. E. (2009). Multiple transcriptional mechanisms control Ptf1a levels during neural development including autoregulation by the PTF1-J complex. *J Neurosci* **29**, 11139-48.

Miyatsuka, T., Matsuoka, T. A., Shiraiwa, T., Yamamoto, T., Kojima, I. and Kaneto, H. (2007). Ptf1a and RBP-J cooperate in activating Pdx1 gene expression through binding to Area III. *Biochem Biophys Res Commun* **362**, 905-9.

Mizuhara, E., Minaki, H., Nakatani, T., Kumai, M., Inoue, T., Muguruma, K., Sasai, H. and Ono, H. (2010). Purkinje cells originate from cerebellar ventricular zone progenitors positive for Neph3 and E-cadherin. *Dev Biol* **338**, 202-14.

Mizuseki, K., Kishi, M., Matsui, M., Nakanishi, S. and Sasai, H. (1998a). Xenopus Zic-related-1 and Sox-2, two factors induced by chordin, have distinct activities in the initiation of neural induction. *Development* **125**, 579-87.

Mizuseki, K., Kishi, M., Shiota, K., Nakanishi, S. and Sasai, H. (1998b). SoxD: an essential mediator of induction of anterior neural tissues in Xenopus embryos. *Neuron* **21**, 77-85.

Moreau, M., Leclerc, C., Gualandris-Parisot, L. and Duprat, A. M. (1994). Increased internal Ca2+ mediates neural induction in the amphibian embryo. *Proc Natl Acad Sci U S A* **91**, 12639-43.

Mullis, K., Faloona, F., Scharf, S., Saiki, R., Horn, G., and Erlich, H. (1986). Specific enzymatic amplification of DNA in vitro: the polymerase chain reaction. *Cold Spring Harb Symp Quant Biol 51 Pt* **1**, 263-73.

Munoz-Sanjuan, I. and Brivanlou, A.H. (2002). Neural induction, the default model and embryonic stem cells. *Nat Rev Neurosci* **3**, 271-80.

Muroyama, H., Fujihara, M., Ikeya, M., Kondoh, H. and Takada, S. (2002). Wnt signaling plays an essential role in neuronal specification of the dorsal spinal cord. *Genes Dev* **16**, 548-53.

Murre, C., McCaw, P. S. & Baltimore, D. (1989). A new DNA binding and dimerization motif in immunoglobulin enhancer binding, daughterless, MyoD, and myc proteins. Cell 56, 777-83.

Murre, C., McCaw, P. S., Vaessin, H., Caudy, M., Jan, L. H., Jan, H. N., Cabrera, C. V., Buskin, J. N., Hauschka, S. D., Lassar, A. B. et al. (1989). Interactions between heterologous helix-loop-helix proteins generate complexes that bind specifically to a common DNA sequence. *Cell* **58**, 537-44.

Murtaugh, L. C., Stanger, B. Z., Kwan, K. M. and Melton, D. A. (2003). Notch signaling controls multiple steps of pancreatic differentiation. *Proc Natl Acad Sci U S A* **100**, 14920-5.

Nakata, K., Nagai, T., Aruga, J. and Mikoshiba, K. (1997). Xenopus Zic3, a primary regulator both in neural and neural crest development. *Proc Natl Acad Sci U S A* **94**, 11980-5.

Nakhai, H., Sel, S., Favor, J., Mendoza-Torres, L., Paulsen, F., Duncker, G. I. and Schmid, R. M. (2007). Ptf1a is essential for the differentiation of GABAergic and glycinergic amacrine cells and horizontal cells in the mouse retina. *Development* **134**, 1151-60.

Nguyen, V. H., Trout, J., Connors, S. A., Andermann, P., Weinberg, E. and Mullins, M. C. (2000). Dorsal and intermediate neuronal cell types of the spinal cord are established by a BMP signaling pathway. *Development* **127**, 1209-20.

Nieber, F., Pieler, T. and Henningfeld, K. A. (2009). Comparative expression analysis of the neurogenins in Xenopus tropicalis and Xenopus laevis. *Dev Dyn* **238**, 451-8.
Niehrs, C. and Pollet, N. (1999). Synexpression groups in eukaryotes. *Nature* **402**, 483-7.
Nieuwkoop, P.D., Faber, J. (Eds.) (1967). Normal table of *Xenopus laevis* (Daudin). Second Edition. North Holland Publ. Co. Amsterdam.
Nishida, K., Hoshino, M., Kawaguchi, H. and Murakami, F. (2010). Ptf1a directly controls expression of immunoglobulin superfamily molecules Nephrin and Neph3 in the developing central nervous system. *J Biol Chem* **285**, 373-80.
Ohtsuka, T., Ishibashi, M., Gradwohl, G., Nakanishi, S., Guillemot, F. and Kageyama, R. (1999). Hes1 and Hes5 as notch effectors in mammalian neuronal differentiation. *EMBO J* **18**, 2196-207.
Oschwald, R., Richter, K. and Grunz, H. (1991). Localization of a nervous system-specific class II beta-tubulin gene in Xenopus laevis embryos by whole-mount in situ hybridization. *Int J Dev Biol* **35**, 399-405.
Papalopulu, N. and Kintner, C. (1996). A posteriorising factor, retinoic acid, reveals that anteroposterior patterning controls the timing of neuronal differentiation in Xenopus neuroectoderm. *Development* **122**, 3409-18.
Parr, B. A., Shea, M. J., Vassileva, G. and McMahon, A. P. (1993). Mouse Wnt genes exhibit discrete domains of expression in the early embryonic CNS and limb buds. *Development* **119**, 247-61.
Pascual, M., Abasolo, I., Mingorance-Le Meur, A., Martinez, A., Del Rio, J. A., Wright, C. V., Real, F. X. and Soriano, E. (2007). Cerebellar GABAergic progenitors adopt an external granule cell-like phenotype in the absence of Ptf1a transcription factor expression. *Proc Natl Acad Sci U S A* **104**, 5193-8.
Patterson, K. D. and Krieg, P. A. (1999). Hox11-family genes XHox11 and XHox11L2 in xenopus: XHox11L2 expression is restricted to a subset of the primary sensory neurons. *Dev Dyn* **214**, 34-43.
Pera, E. M., Ikeda, A., Eivers, E. and De Robertis, E. M. (2003). Integration of IGF, FGF, and anti-BMP signals via Smad1 phosphorylation in neural induction. *Genes Dev* **17**, 3023-8.
Perron, M., Opdecamp, K., Butler, K., Harris, H. A. and Bellefroid, E. J. (1999). X-ngnr-1 and Xath3 promote ectopic expression of sensory neuron markers in the neurula ectoderm and have distinct inducing properties in the retina. *Proc Natl Acad Sci U S A* **96**, 14996-5001.
Pevny, L. and Placzek, M. (2005). SOX genes and neural progenitor identity. *Curr Opin Neurobiol* **15**, 7-13.
Piccolo, S., Agius, E., Leyns, L., Bhattacharyya, S., Grunz, H., Bouwmeester, T., and De Robertis, E.M. (1999). The head inducer Cerberus is a multifunctional antagonist of Nodal, BMP and Wnt signals. *Nature* **397**, 707-10.
Piccolo, S., Sasai, H., Lu, B. and De Robertis, E. M. (1996). Dorsoventral patterning in Xenopus: inhibition of ventral signals by direct binding of chordin to BMP-4. *Cell* **86**, 589-98.
Pillai, A., Mansouri, A., Behringer, R., Westphal, H., and Goulding, M. (2007). Lhx1 and Lhx5 maintain the inhibitory-neurotransmitter status of interneurons in the dorsal spinal cord. *Development* **134**, 357-66.
Pitulescu, M., Kessel, M. and Luo, L. (2005). The regulation of embryonic patterning and DNA replication by geminin. *Cell Mol Life Sci* **62**, 1425-33.

Placzek, M., Yamada, T., Tessier-Lavigne, M., Jessell, T. and Dodd, J. (1991). Control of dorsoventral pattern in vertebrate neural development: induction and polarizing properties of the floor plate. *Development* **Suppl 2**, 105-22.

Powell, L. M. and Jarman, A. P. (2008). Context dependence of proneural bHLH proteins. *Curr Opin Genet Dev* **18**, 411-7.

Pozzoli, O., Bosetti, A., Croci, L., Consalez, G. G. and Vetter, M. L. (2001). Xebf3 is a regulator of neuronal differentiation during primary neurogenesis in Xenopus. *Dev Biol* **233**, 495-512.

Roberts, A., Li, H. C. and Soffe, S. R. (2012). A functional scaffold of CNS neurons for the vertebrates: The developing Xenopus laevis spinal cord. *Dev Neurobiol* **72**, 575-84.

Roberts, A. (2000). Early functional organization of spinal neurons in developing lower vertebrates. *Brain Res Bull* **53**, 585-93.

Rodolosse, A., Campos, M. L., Rooman, I., Lichtenstein, M. and Real, F. X. (2009). p/CAF modulates the activity of the transcription factor p48/Ptf1a involved in pancreatic acinar differentiation. *Biochem J* **418**, 463-73.

Roelink, H., Porter, J. A., Chiang, C., Tanabe, H., Chang, D. T., Beachy, P. A. and Jessell, T. M. (1995). Floor plate and motor neuron induction by different concentrations of the amino-terminal cleavage product of sonic hedgehog autoproteolysis. *Cell* **81**, 445-55.

Rogers, C. D., Harafuji, N., Archer, T., Cunningham, D. D. and Casey, E. S. (2009a). Xenopus Sox3 activates sox2 and geminin and indirectly represses Xvent2 expression to induce neural progenitor formation at the expense of non-neural ectodermal derivatives. *Mech Dev* **126**, 42-55.

Rogers, C. D., Moody, S. A. and Casey, E. S. (2009b). Neural induction and factors that stabilize a neural fate. *Birth Defects Res C Embryo Today* **87**, 249-62.

Rossi, C. C., Hernandez-Lagunas, L., Zhang, C., Choi, I. F., Kwok, L., Klymkowsky, M. and Artinger, K. B. (2008). Rohon-Beard sensory neurons are induced by BMP4 expressing non-neural ectoderm in Xenopus laevis. *Dev Biol* **314**, 351-61.

Rossignol, E. (2011). Genetics and function of neocortical GABAergic interneurons in neurodevelopmental disorders. *Neural Plast* **2011**, 649325.

Roux, E., Strubin, M., Hagenbuchle, O., and Wellauer, P.K. (1989). The cell-specific transcription factor PTF1 contains two different subunits that interact with the DNA. *Genes Dev* **3**, 1613-24.

Saba, R., Johnson, J.E., and Saito, T. (2005). Commissural neuron identity is specified by a homeodomain protein, Mbh1, that is directly downstream of Math1. *Development* **132**, 2147-55.

Sadowski, I., Ma, J., Triezenberg, S. and Ptashne, M. (1988). GAL4-VP16 is an unusually potent transcriptional activator. *Nature* **335**, 563-4.

Sakabe, N. J., Aneas, I., Shen, T., Shokri, L., Park, S. H., Bulyk, M. L., Evans, S. M. and Nobrega, M. A. (2012). Dual transcriptional activator and repressor roles of TBX20 regulate adult cardiac structure and function. *Hum Mol Genet* **21**, 2194-204.

Sambrook, J. and Russel, D.W. (Eds.) (2001). Molecular Cloning: a laboratory manual. Third Edition. *Cold Spring Harbour Laboratory Press*, Cold Spring Harbour, New York.

Sanes, D.H., Reh, T.A., Harris, H.A. (Eds.) (2006). Development of the nervous system. Second Edition. Amsterdam.

Sanger, F., Nicklen, S., and Coulson, A.R. (1977). DNA sequencing with chain-terminating inhibitors. *Proc Natl Acad Sci U S A* **74**, 5463-67.

Sasai, H., Kageyama, R., Tagawa, H., Shigemoto, R. and Nakanishi, S. (1992). Two mammalian helix-loop-helix factors structurally related to Drosophila hairy and Enhancer of split. *Genes Dev* **6**, 2620-34.

Sasai, H., Lu, B., Piccolo, S. and De Robertis, E. M. (1996). Endoderm induction by the organizer-secreted factors chordin and noggin in Xenopus animal caps. *EMBO J* **15**, 4547-55.

Sasai, H., Lu, B., Steinbeisser, H., Geissert, D., Gont, L. K. and De Robertis, E. M. (1994). Xenopus chordin: a novel dorsalizing factor activated by organizer-specific homeobox genes. *Cell* **79**, 779-90.

Sato, S. M. and Sargent, T. D. (1989). Development of neural inducing capacity in dissociated Xenopus embryos. *Dev Biol* **134**, 263-6.

Schlosser, G., Koyano-Nakagawa, N. and Kintner, C. (2002). Thyroid hormone promotes neurogenesis in the Xenopus spinal cord. *Dev Dyn* **225**, 485-98.

Schneider, M. L., Turner, D. L. and Vetter, M. L. (2001). Notch signaling can inhibit Xath5 function in the neural plate and developing retina. *Mol Cell Neurosci* **18**, 458-72.

Schroeter, E. H., Kisslinger, J. A. and Kopan, R. (1998). Notch-1 signalling requires ligand-induced proteolytic release of intracellular domain. *Nature* **393**, 382-6.

Selkoe, D. and Kopan, R. (2003). Notch and Presenilin: regulated intramembrane proteolysis links development and degeneration. *Annu Rev Neurosci* **26**, 565-97.

Sellick, G. S., Barker, K. T., Stolte-Dijkstra, I., Fleischmann, C., Coleman, R. J., Garrett, C., Gloyn, A. L., Edghill, E. L., Hattersley, A. T., Wellauer, P. K. et al. (2004). Mutations in PTF1A cause pancreatic and cerebellar agenesis. *Nat Genet* **36**, 1301-5.

Seo, S. and Kroll, K. L. (2006). Geminin's double life: chromatin connections that regulate transcription at the transition from proliferation to differentiation. *Cell Cycle* **5**, 374-9.

Seo, S., Lim, J. H., Yellajoshyula, D., Chang, L. H. and Kroll, K. L. (2007). Neurogenin and NeuroD direct transcriptional targets and their regulatory enhancers. *EMBO J* **26**, 5093-108.

Sharp, P.A., Sugden, B., and Sambrook, J. (1973). Detection of two restriction endonuclease activities in Haemophilus parainfluenzae using analytical agarose--ethidium bromide electrophoresis. *Biochemistry* **12**, 3055-63.

Sommer, L., Ma, Q. and Anderson, D. J. (1996). neurogenins, a novel family of atonal-related bHLH transcription factors, are putative mammalian neuronal determination genes that reveal progenitor cell heterogeneity in the developing CNS and PNS. *Mol Cell Neurosci* **8**, 221-41.

Souopgui, J., Solter, M. and Pieler, T. (2002). XPak3 promotes cell cycle withdrawal during primary neurogenesis in Xenopus laevis. *EMBO J* **21**, 6429-39.

Storey, K. G., Crossley, J. M., De Robertis, E. M., Norris, H. E. and Stern, C. D. (1992). Neural induction and regionalisation in the chick embryo. *Development* **114**, 729-41.

Storey, K. G., Goriely, A., Sargent, C. M., Brown, J. M., Burns, H. D., Abud, H. M. and Heath, J. K. (1998). Early posterior neural tissue is induced by FGF in the chick embryo. *Development* **125**, 473-84.
Storm, R., Cholewa-Waclaw, J., Reuter, K., Brohl, D., Sieber, M., Treier, M., Muller, T. and Birchmeier, C. (2009). The bHLH transcription factor Olig3 marks the dorsal neuroepithelium of the hindbrain and is essential for the development of brainstem nuclei. *Development* **136**, 295-305.
Streit, A., Berliner, A. J., Papanayotou, C., Sirulnik, A. and Stern, C. D. (2000). Initiation of neural induction by FGF signalling before gastrulation. *Nature* **406**, 74-8.
Streit, A., Lee, K. J., Woo, I., Roberts, C., Jessell, T. M. and Stern, C. D. (1998). Chordin regulates primitive streak development and the stability of induced neural cells, but is not sufficient for neural induction in the chick embryo. *Development* **125**, 507-19.
Sullivan, S.A., Akers, L., and Moody, S.A. (2001). foxD5a, a Xenopus winged helix gene, maintains an immature neural ectoderm via transcriptional repression that is dependent on the C-terminal domain. *Dev Biol* **232**, 439-57.
Taelman, V., Opdecamp, K., Avalosse, B., Ryan, K., Bellefroid, E. J. (2001). Xath2, a bHLH gene expressed during late transition stage of neurogenesis in the forebrain of Xenopus embryos. *Mech Dev* **101**, 199-202.
Taira, M., Otani, H., Saint-Jeannet, J. P. and Dawid, I. B. (1994) 'Role of the LIM class homeodomain protein Xlim-1 in neural and muscle induction by the Spemann organizer in Xenopus'. *Nature* **372** (6507), 677-9.
Takke, C., Dornseifer, P., v Weizsacker, E. and Campos-Ortega, J. A. (1999). her4, a zebrafish homologue of the Drosophila neurogenic gene E(spl), is a target of NOTCH signalling. *Development* **126**, 1811-21.
Talikka, M., Perez, S. E. and Zimmerman, K. (2002). Distinct patterns of downstream target activation are specified by the helix-loop-helix domain of proneural basic helix-loop-helix transcription factors. *Dev Biol* **247**, 137-48.
Thompson, N., Gesina, E., Scheinert, P., Bucher, P. and Grapin-Botton, A. (2012). RNA profiling and chromatin immunoprecipitation-sequencing reveal that PTF1a stabilizes pancreas progenitor identity via the control of MNX1/HLXB9 and a network of other transcription factors. *Mol Cell Biol* **32**, 1189-99.
Timmer, J. R., Wang, C. and Niswander, L. (2002). BMP signaling patterns the dorsal and intermediate neural tube via regulation of homeobox and helix-loop-helix transcription factors. *Development* **129**, 2459-72.
Towbin, H., Staehelin, T. and Gordon, J. (1979). Electrophoretic transfer of proteins from polyacrylamide gels to nitrocellulose sheets: procedure and some applications. *Proc Natl Acad Sci U S A* **76**, 4350-4.
Turner, D. L. and Weintraub, H. (1994). Expression of achaete-scute homolog 3 in Xenopus embryos converts ectodermal cells to a neural fate. *Genes Dev* **8**, 1434-47.
Tutak, E., Satar, M., Yapicioglu, H., Altintas, A., Narli, N., Herguner, O. and Bayram, H. (2009). A Turkish newborn infant with cerebellar agenesis/neonatal diabetes mellitus and PTF1A mutation. *Genet Couns* **20**, 147-52.
Vallstedt, A., Muhr, J., Pattyn, A., Pierani, A., Mendelsohn, M., Sander, M., Jessell, T. M. and Ericson, J. (2001). Different levels of repressor activity assign redundant and specific roles to Nkx6 genes in motor neuron and interneuron specification. *Neuron* **31**, 743-55.

Vernon, A. E., Devine, C. and Philpott, A. (2003). The cdk inhibitor p27Xic1 is required for differentiation of primary neurones in Xenopus. *Development* **130**, 85-92.
Wallingford, J. B. and Harland, R. M. (2001). Xenopus Dishevelled signaling regulates both neural and mesodermal convergent extension: parallel forces elongating the body axis. Development **128**, 2581-92.
Wang, S. and Barres, B. A. (2000). Up a notch: instructing gliogenesis. *Neuron* **27**, 197-200.
Wawersik, S., Evola, C. and Whitman, M. (2005). Conditional BMP inhibition in Xenopus reveals stage-specific roles for BMPs in neural and neural crest induction. *Dev Biol* **277**, 425-42.
Wettstein, D. A., Turner, D. L. and Kintner, C. (1997). The Xenopus homolog of Drosophila Suppressor of Hairless mediates Notch signaling during primary neurogenesis. *Development* **124**, 693-702.
Wiebe, P. O., Kormish, J. D., Roper, V. T., Fujitani, H., Alston, N. I., Zaret, K. S., Wright, C. V., Stein, R. H. and Gannon, M. (2007). Ptf1a binds to and activates area III, a highly conserved region of the Pdx1 promoter that mediates early pancreas-wide Pdx1 expression. *Mol Cell Biol* **27**, 4093-104.
Wilson, P. A. and Hemmati-Brivanlou, A. (1995). Induction of epidermis and inhibition of neural fate by Bmp-4. *Nature* **376**, 331-3.
Wilson, S. I. and Edlund, T. (2001). Neural induction: toward a unifying mechanism. *Nat Neurosci* **4 Suppl**, 1161-8.
Wilson, S. I., Graziano, E., Harland, R., Jessell, T. M. and Edlund, T. (2000). An early requirement for FGF signalling in the acquisition of neural cell fate in the chick embryo. *Curr Biol* **10**, 421-9.
Wullimann, M. F., Rink, E., Vernier, P. and Schlosser, G. (2005). Secondary neurogenesis in the brain of the African clawed frog, Xenopus laevis, as revealed by PCNA, Delta-1, Neurogenin-related-1, and NeuroD expression. *J Comp Neurol* **489**, 387-402.
Yamada, M., Terao, M., Terashima, T., Fujiyama, T., Kawaguchi, H., Nabeshima, H. and Hoshino, M. (2007). Origin of climbing fiber neurons and their developmental dependence on Ptf1a. *J Neurosci* **27**, 10924-34.
Yamada, T., Placzek, M., Tanaka, H., Dodd, J. and Jessell, T. M. (1991). Control of cell pattern in the developing nervous system: polarizing activity of the floor plate and notochord. *Cell* **64**, 635-47.
Yu, H., McDonnell, K., Taketo, M. M. and Bai, C. B. (2008). Wnt signaling determines ventral spinal cord cell fates in a time-dependent manner. *Development* **135**, 3687-96.
Yu, Z., Syu, L. J. and Mellerick, D. M. (2005). Contextual interactions determine whether the Drosophila homeodomain protein, Vnd, acts as a repressor or activator. *Nucleic Acids Res* **33**, 1-12.
Zecchin, E., Mavropoulos, A., Devos, N., Filippi, A., Tiso, N., Meyer, D., Peers, B., Bortolussi, M. and Argenton, F. (2004). Evolutionary conserved role of ptf1a in the specification of exocrine pancreatic fates. *Dev Biol* **268**, 174-84.
Zimmerman, L. B., De Jesus-Escobar, J. M. and Harland, R. M. (1996). The Spemann organizer signal noggin binds and inactivates bone morphogenetic protein 4. *Cell* **86**, 599-606.
Zordan, P., Croci, L., Hawkes, R. & Consalez, G. G. (2008). Comparative analysis of proneural gene expression in the embryonic cerebellum. *Dev Dyn* **237**, 1726-35.

6. Appendix

6.1 Summary of processed Nanostring data. Given is the averaged fold change over CC of two independent experiments for each sample and gene, respectively. In a second table, the calculated standard error of the mean (SEM) is given for each sample and gene, respectively. Data were processed as described in Methods and Materials.

6.1.1 Experiment 3.2

Table 6.1 Summary of the averaged fold change over CC of two independent Nanostring experiments for each sample and gene

	3 h		6 h		25 h		25 h	
Genes	Ptf1a	Ngn2	Ptf1a	Ngn2	Ptf1a	Ngn2	Ptf1a -Dex	Ngn2 -Dex
Ascl1/Xash1 new	0,7	1,1	0,8	0,8	0,6	0,6	1,0	7,6
Cdknx (p27Xic1)	5,8	2,5	4,7	2,6	1,3	1,8	1,0	1,0
Dll1 (Delta1)	35,0	16,0	16,7	20,2	10,4	14,0	1,1	1,7
Ebf2-a/b	59,4	10,1	162,4	73,8	2857,7	2361,0	1,0	5,2
Ebf3 (Coe3)	1,0	1,0	1,0	1,0	85,5	184,2	1,1	5,4
Gad1	1,0	1,0	1,0	1,0	1069,2	10,2	1,0	1,0
H4 new	1,1	1,3	1,2	1,2	0,7	0,7	1,1	0,9
Hb9/mnx1	0,4	0,3	2,5	1,9	1,0	1,0	1,0	1,0
Hox11L2/Tlx3	1,5	1,0	0,7	0,5	1,0	1182,6	3,5	4,9
Hpx6 (Lbx1)	1,0	1,0	1,0	1,0	11,2	1,0	1,0	1,0
Islet1 (isl1)	0,8	3,0	0,4	0,7	0,2	1,9	1,1	1,1
Lhx1 (Lim1)	0,2	0,1	0,4	0,4	62,3	1,0	1,0	1,0
Lhx2	1,0	1,0	4,9	1,0	2,8	1,0	1,0	1,0
Lhx5	1,1	0,8	0,9	0,8	372,2	0,7	1,0	1,0
Lmx1b	0,4	0,6	0,5	0,8	40,8	1,0	1,0	1,0
Mxi1	4,3	3,3	4,5	4,2	0,5	1,9	0,8	1,2
MyT1	31,4	16,1	12,3	12,0	3,5	8,2	1,1	2,0
NCAMa/b	3,4	3,1	0,4	0,8	14,0	44,6	1,4	3,1
NeuroD1a/b	1,0	1,0	1,0	1,0	569,0	2342,8	1,0	1,0
NeuroD4 (Xath3)	1,0	1,0	1,0	14,5	945,9	5388,3	1,0	22,5
Ngn1	1,0	1,0	1,0	1,0	174,7	1313,4	1,0	1,0
Ngn3	0,8	0,5	0,6	0,6	1,0	8,1	1,0	1,0
Nrgn-1b (Ngn2-b)	0,7	1,1	0,7	0,7	71,4	7,8	1,0	1,0
Numbl	0,9	1,0	0,8	0,9	0,5	0,7	1,1	0,9
ODC	1,0	1,0	1,0	1,0	1,0	1,0	1,0	1,0
PRDM13	67,1	3,5	41,8	1,6	1719,9	32,0	4,7	1,0
PRDM14	1,9	2,4	1,1	4,5	73,2	2256,9	1,0	1,0
Pak3	1,2	0,9	0,9	0,8	216,4	972,7	0,3	0,8
Pax2-a	1,0	1,0	1,0	1,0	183,3	0,5	1,0	1,0
Ptf1a-a/b 5'UTR	0,8	1,0	1,1	1,1	3,8	1,9	1,5	1,0
RBM38/Seb4R	1,2	1,2	1,1	1,2	0,7	1,2	0,9	1,1
RBPJ 3'UTR	1,0	1,0	0,9	0,9	0,7	0,7	1,1	1,0
Sox3	1,1	1,0	0,9	0,9	2,0	0,7	1,1	1,0
Xbra-a/b	1,4	1,0	3,8	1,1	0,1	0,9	1,3	1,2
actc1	1,4	1,0	3,5	4,2	0,3	2,2	1,5	1,0
g6pd	1,0	1,0	0,9	1,0	0,6	0,9	1,0	0,9
tubb2b (N-tubulin)	0,9	1,8	1,7	3,5	73,5	133,4	1,4	1,2
vGlut1	0,8	1,0	1,2	1,1	39,5	1670,3	1,0	1,0

Table 6.2 Summary of the calculated standard error of the mean (SEM) of the fold change shown in table 6.1 for each sample and gene

	3 h		6 h		25 h		25 h	
Genes	**Ptf1a**	**Ngn2**	**Ptf1a**	**Ngn2**	**Ptf1a**	**Ngn2**	**Ptf1a –Dex**	**Ngn2 -Dex**
Ascl1/Xash1 new	0,0	0,3	0,3	0,2	0,4	0,4	0,0	6,6
Cdknx (p27Xic1)	2,5	1,3	0,5	0,3	0,1	0,5	0,0	0,1
Dll1 (Delta1)	21,2	5,0	1,4	2,9	2,7	8,3	0,3	0,7
Ebf2-a/b	20,8	4,8	110,1	40,2	318,3	574,5	0,0	4,2
Ebf3 (Coe3)	0,0	0,0	0,0	0,0	33,5	137,5	0,8	5,2
Gad1	0,0	0,0	0,0	0,0	272,6	3,0	0,0	0,0
H4 new	0,1	0,1	0,4	0,4	0,2	0,1	0,0	0,0
Hb9/mnx1	0,4	0,2	2,1	1,4	0,0	0,0	0,0	0,0
Hox11L2/Tlx3	0,5	0,0	0,5	0,4	0,0	418,9	3,0	3,9
Hpx6 (Lbx1)	0,0	0,0	0,0	0,0	2,1	0,0	0,0	0,0
Islet1 (isl1)	0,2	1,1	0,1	0,5	0,0	0,6	0,1	0,2
Lhx1 (Lim1)	0,1	0,0	0,1	0,1	0,5	0,0	0,0	0,0
Lhx2	0,0	0,0	1,9	0,0	1,8	0,0	0,0	0,0
Lhx5	0,1	0,0	0,1	0,2	190,0	0,3	0,0	0,0
Lmx1b	0,3	0,2	0,4	0,6	17,0	0,0	0,0	0,0
Mxi1	0,9	0,1	0,0	0,5	0,1	0,5	0,0	0,1
MyT1	2,9	6,3	0,2	0,8	0,0	1,7	0,0	0,3
NCAMa/b	0,5	2,4	0,2	0,6	0,3	11,5	0,6	0,2
NeuroD1a/b	0,0	0,0	0,0	0,0	10,1	1228,8	0,0	0,0
NeuroD4 (Xath3)	0,0	0,0	0,0	5,8	116,6	1307,2	0,0	21,5
Ngn1	0,0	0,0	0,0	0,0	31,5	440,6	0,0	0,0
Ngn3	0,2	0,5	0,4	0,4	0,0	2,3	0,0	0,0
Nrgn-1b (Ngn2-b)	0,0	0,4	0,1	0,0	23,4	7,2	0,0	0,0
Numbl	0,1	0,2	0,0	0,0	0,0	0,0	0,1	0,1
ODC	0,0	0,0	0,0	0,0	0,0	0,0	0,0	0,0
PRDM13	58,1	2,3	9,1	0,1	364,9	29,2	3,7	0,0
PRDM14	0,3	0,5	0,0	0,5	19,0	915,3	0,0	0,0
Pak3	0,3	0,3	0,1	0,0	189,5	937,6	0,2	0,5
Pax2-a	0,0	0,0	0,0	0,0	118,1	0,5	0,0	0,0
Ptf1a-a/b 5'UTR	0,1	0,2	0,2	0,2	0,2	0,5	0,3	0,0
RBM38/Seb4R	0,3	0,4	0,1	0,0	0,0	0,1	0,1	0,0
RBPJ 3'UTR	0,0	0,1	0,1	0,1	0,0	0,0	0,1	0,1
Sox3	0,0	0,1	0,1	0,1	0,5	0,1	0,2	0,0
Xbra-a/b	0,7	0,4	3,3	0,4	0,1	0,6	0,5	0,4
actc1	0,4	0,0	2,5	3,2	0,1	0,2	0,5	0,4
g6pd	0,0	0,1	0,0	0,0	0,1	0,0	0,0	0,0
tubb2b (N-tubulin)	0,0	0,6	0,3	0,4	10,1	41,3	0,3	0,2
vGlut1	0,2	0,0	0,2	0,1	34,3	1111,7	0,0	0,0

6.1.2 Experiment 3.7

Table 6.3 Summary of the averaged fold change over CC of two independent Nanostring experiments for each sample and gene

Genes	Ptf1a	Ngn2	chimeric Ptf1a
Arx-a	0,5	0,5	0,9
Ascl1/Xash1	0,6	0,6	0,6
Cdknx (p27Xic1)	1,8	1,6	1,8
Dll1 (Delta1)	7,4	4,4	5,0
Delta2	41,4	19,9	37,3
ESR10	91,6	88,5	50,3
ESR6e (Hes3.1)	0,9	1,6	1,2
ESR9.1a	85,1	33,3	26,1
Ebf2-a/b	902,6	385,0	634,5
Ebf3 (Coe3)	159,9	149,9	131,2
Eng1-a/b	1,0	1,0	1,0
FGF8	12,1	3,6	4,7
FoxD3a (XfD6)	2,4	1,0	2,3
Gad1	685,5	1,0	273,5
H4	3,0	1,0	5,0
Hb9/mnx1	1,9	4,8	4,8
Hes1a(Hairy1)	0,8	1,3	1,7
Hes2	3,5	1,0	1,0
Hes5.1 (ESR1)	6,5	2,3	2,6
Hes6.1	1,0	0,8	1,0
Hes7 (XHR1)	0,3	0,5	0,6
Hox11L2/Tlx3	0,6	433,1	56,0
Hpx6 (Lbx1)	20,1	2,7	4,3
Insm1	14,3	17,0	10,9
Islet1 (isl1)	0,3	1,9	1,0
Jagged1 (Serrate-1)	1,9	1,7	2,0
Krox20/egr2	1,0	1,0	1,0
Lhx1 (Lim1)	95,2	2,0	10,6
Lhx2	1,0	1,0	1,0
Lhx5	83,0	1,0	19,4
Lmx1b	96,0	8,7	12,1
Mxi1	1,1	1,9	1,3
MyT1	7,4	7,5	7,9
NCAMa/b	27,4	55,4	38,9
NeuroD1a/b	21,3	30,1	30,8
NeuroD4 (Xath3)	606,1	1332,2	1125,2
NeuroD6 (Xath2)	1,0	1,0	1,0
Ngn1	178,0	317,3	289,1
Ngn3	0,3	2,9	0,6
Ngnr-1a (ngn2a)	1,7	1,0	1,0
Nkx6.1	31,4	1,0	19,1
Nkx6.2	0,7	1,0	1,3
Notch1	1,5	1,0	1,4
Nrgn-1b (Ngn2-b)	55,9	5,1	2,6
Nrp1	2,8	3,1	3,7
Numb	1,0	1,0	1,0
Numbl	0,3	0,6	0,8
ODC	1,0	1,0	1,0
Olig3	0,3	0,3	0,3
Pak3	13,2	27,3	14,8
Pax2-a	103,4	1,0	3,9
Pax3	139,1	18,4	33,0
Pax6-a	2,1	0,7	1,2
Pax6-b	23,3	0,6	0,8
PRDM14	2,4	54,2	9,5
Ptf1a-a/b	48,8	1,0	75,7
RBM38/Seb4R	0,5	1,5	1,0
RBPJ	0,6	0,8	1,0
Slug	18,9	1,0	4,5
Sox1	0,8	0,7	1,2
Sox2	18,3	3,8	6,4
Sox3	4,2	1,1	2,0
Sox9-a/b	26,0	1,4	4,4
SoxD	0,7	0,7	0,9
Twist1-a	47,8	17,3	33,7
Xbra-a/b	0,5	2,1	1,0
actb	0,6	0,8	1,1
actc1	2,1	3,4	4,8
c-myc	0,3	0,7	0,7
g6pd	1,0	1,1	1,4
gapdh	0,9	2,2	1,3

runx1 (Xaml)	0,2	0,6	0,5
tubb2b (N-tubulin)	101,9	110,5	77,7
vGlut1	2,6	80,9	22,3

Table 6.4 Summary of the calculated standard error of the mean (SEM) of the fold change shown in table 6.3 for each sample and gene

Genes	Ptf1a	Ngn2	chimeric Ptf1a
Arx-a	0,5	0,5	0,1
Ascl1/Xash1	0,4	0,4	0,4
Cdknx (p27Xic1)	0,0	0,3	0,2
Dll1 (Delta1)	3,1	1,5	0,8
Delta2	24,7	14,6	20,0
ESR10	38,2	2,8	23,7
ESR6e (Hes3.1)	0,1	0,3	0,0
ESR9.1a	54,8	13,9	10,3
Ebf2-a/b	56,8	81,9	44,0
Ebf3 (Coe3)	22,6	70,7	40,3
Eng1-a/b	0,0	0,0	0,0
FGF8	0,3	0,6	1,4
FoxD3a (XfD6)	0,2	0,2	0,5
Gad1	101,5	0,0	9,2
H4	2,0	0,0	4,0
Hb9/mnx1	0,7	4,5	3,1
Hes1a(Hairy1)	0,1	0,2	0,0
Hes2	2,5	0,0	0,0
Hes5.1 (ESR1)	2,7	0,0	0,4
Hes6.1	0,1	0,2	0,1
Hes7 (XHR1)	0,2	0,0	0,3
Hox11L2/Tlx3	0,4	355,0	23,3
Hpx6 (Lbx1)	18,5	1,7	3,7
Insm1	2,1	6,5	0,1
Islet1 (isl1)	0,2	0,5	0,0
Jagged1 (Serrate-1)	0,3	0,2	0,1
Krox20/egr2	0,0	0,0	0,0
Lhx1 (Lim1)	39,6	1,0	9,6
Lhx2	0,0	0,0	0,0
Lhx5	43,8	0,0	5,3
Lmx1b	33,0	7,7	6,4
Mxi1	0,1	0,2	0,3
MyT1	1,2	1,6	0,2
NCAMa/b	1,2	4,7	4,4
NeuroD1a/b	5,7	16,1	9,2
NeuroD4 (Xath3)	146,5	379,5	109,1
NeuroD6 (Xath2)	0,0	0,0	0,0
Ngn1	47,9	72,6	72,7
Ngn3	0,2	1,9	0,1
Ngnr-1a (ngn2a)	0,7	0,0	0,0
Nkx6.1	13,1	0,0	18,1
Nkx6.2	0,1	0,0	0,2
Notch1	0,4	0,2	0,2
Nrgn-1b (Ngn2-b)	40,5	4,1	1,6
Nrp1	0,2	1,1	1,4
Numb	0,0	0,0	0,0
Numbl	0,2	0,1	0,1
ODC	0,0	0,0	0,0
Olig3	0,1	0,1	0,1
Pak3	2,7	13,5	5,2
Pax2-a	7,6	0,0	2,9
Pax3	44,8	17,4	24,0
Pax6-a	1,1	0,4	0,7
Pax6-b	17,4	0,4	0,6
PRDM14	1,3	16,9	1,2
Ptf1a-a/b	1,3	0,0	13,4
RBM38/Seb4R	0,1	0,3	0,0
RBPJ	0,1	0,1	0,0
Slug	11,7	0,0	1,2
Sox1	0,1	0,2	0,1
Sox2	3,0	1,3	3,6
Sox3	1,9	0,3	1,3
Sox9-a/b	13,4	0,3	2,8
SoxD	0,1	0,1	0,1
Twist1-a	9,3	12,4	30,5
Xbra-a/b	0,3	1,1	0,0
actb	0,2	0,0	0,2
actc1	1,4	0,2	1,4
c-myc	0,1	0,2	0,0
g6pd	0,4	0,1	0,4

gapdh	0,4	0,4	0,2
runx1 (Xaml)	0,0	0,0	0,0
tubb2b (N-tubulin)	9,6	28,4	4,6
vGlut1	1,2	58,7	8,0

6.1.3 Experiment 3.8 and 3.20

Table 6.5 Summary of the averaged fold change over CC of two independent Nanostring experiments for each sample and gene

	6 h		32 h	
Genes	**Ptf1a**	**Ptf1a$^{W224A/W242A}$**	**Ptf1a**	**Ptf1a$^{W224A/W242A}$**
Ascl1/Xash1 new	9,8	3,9	0,6	0,4
Barhl2	1,0	1,0	45,0	8,3
Cdknx (p27Xic1)	7,1	5,7	2,2	1,8
Cpa1	1,0	1,0	2,2	0,7
Dll1 (Delta1)	20,0	22,2	6,0	3,0
ESR10	9,5	0,9	6,1	4,7
Ebf2-a/b	234,1	51,2	2195,2	1290,9
Ebf3 (Coe3)	1,0	1,0	34,0	45,5
FoxD3a (XfD6)	0,8	1,5	126,2	15,5
Gad1	1,0	1,0	928,7	24,4
H4 new	1,0	0,9	0,6	0,4
HNF6 gene2	16,1	6,1	2261,6	1177,2
Hb9/mnx1	3,2	3,3	1,0	9,5
Hes5.1 (ESR1)	34,8	6,4	214,3	136,6
Hmx3	3,0	1,0	19,5	0,5
Hox11L2/Tlx3	5,0	12,7	17,3	219,3
Hpx6 (Lbx1)	1,0	1,0	205,8	79,2
Islet1 (isl1)	1,0	1,0	0,5	0,7
Kirrel2	3,0	0,4	51,8	1,2
Lhx1 (Lim1)	10,5	9,4	171,0	36,5
Lhx2	0,7	0,7	34,2	23,8
Lhx5	0,7	0,7	274,4	2,5
Lmx1b	4,1	0,7	66,7	51,2
Mecom	1,0	1,0	95,5	1,9
Mxi1	4,7	3,4	0,7	0,6
MyT1	27,1	14,1	4,9	4,5
NCAMa/b	1,5	1,2	16,5	19,5
NeuroD1a/b	1,0	1,0	528,4	463,3
NeuroD4 (Xath3)	4,0	1,0	776,2	1210,6
Ngn1	1,0	1,0	217,9	315,1
Ngn3	7,8	4,1	1,0	1,0
Nrgn-1b (Ngn2-b)	1,8	1,5	111,8	5,2
ODC	1,0	1,0	1,0	1,0
PRDM13	804,2	26,7	1768,6	71,7
PRDM14	1,5	2,3	135,3	761,7
Pak3	1,8	1,3	223,6	252,9
Pax2-a	6,8	0,6	20,8	1,1
Ptf1a-a/b 5'UTR	13,6	6,6	4,6	0,7
RBM38/Seb4R	1,6	1,8	0,8	0,6
RBPJ 3'UTR	1,3	1,0	0,9	0,6
Sox3	0,9	1,1	2,9	1,4
Sox9-a/b	2,3	1,3	48,8	22,6
Pdia2 (XPDip)	1,0	1,0	5,3	1,0
Xbra-a/b	2,3	2,9	0,8	0,7
actc1	6,9	1,1	3,2	1,9
g6pd	1,0	1,0	0,8	0,8
tubb2b (N-tubulin)	3,6	1,1	161,2	259,6
vGlut1	1,0	1,0	23,2	523,7

Table 6.6 Summary of the calculated standard error of the mean (SEM) of the fold change shown in table 6.5 for each sample and gene

	6 h		32 h	
Genes	**Ptf1a**	**Ptf1a$^{W224A/W242A}$**	**Ptf1a**	**Ptf1a$^{W224A/W242A}$**
Ascl1/Xash1 new	9,7	3,5	0,0	0,4
Barhl2	0,0	0,0	42,4	8,2
Cdknx (p27Xic1)	1,5	0,9	0,9	1,3
Cpa1	0,0	0,0	2,1	0,3
Dll1 (Delta1)	2,9	1,8	1,3	1,0
ESR10	0,3	0,2	2,4	2,8
Ebf2-a/b	94,1	26,0	457,0	673,6
Ebf3 (Coe3)	0,0	0,0	3,2	1,7
FoxD3a (XfD6)	0,3	0,5	13,9	13,6
Gad1	0,0	0,0	43,1	0,1
H4 new	0,0	0,1	0,0	0,2
HNF6 gene2	13,0	5,5	2074,7	1133,0
Hb9/mnx1	3,0	1,2	0,0	9,4
Hes5.1 (ESR1)	22,5	1,4	28,9	70,1
Hmx3	2,0	0,0	17,9	0,5
Hox11L2/Tlx3	3,2	8,4	15,8	102,4
Hpx6 (Lbx1)	0,0	0,0	7,4	72,5
Islet1 (isl1)	0,0	0,0	0,2	0,1
Kirrel2	0,6	0,1	40,0	1,1
Lhx1 (Lim1)	5,7	0,9	8,3	33,4
Lhx2	0,3	0,3	14,5	10,2
Lhx5	0,2	0,2	179,7	1,5
Lmx1b	0,7	0,3	20,6	36,0
Mecom	0,0	0,0	34,8	0,1
Mxi1	1,3	1,3	0,1	0,4
MyT1	8,4	7,5	2,9	3,0
NCAMa/b	0,4	0,3	10,2	13,5
NeuroD1a/b	0,0	0,0	504,9	445,1
NeuroD4 (Xath3)	3,0	0,0	263,4	556,6
Ngn1	0,0	0,0	180,9	283,7
Ngn3	6,8	3,1	0,0	0,0
Nrgn-1b (Ngn2-b)	1,3	0,7	23,7	4,2
ODC	0,0	0,0	0,0	0,0
PRDM13	253,0	16,1	1194,2	67,4
PRDM14	0,7	1,1	117,1	726,6
Pak3	0,4	0,0	191,9	227,5
Pax2-a	6,2	0,4	15,7	0,5
Ptf1a-a/b 5'UTR	12,3	5,0	3,2	0,5
RBM38/Seb4R	0,0	0,1	0,2	0,2
RBPJ 3'UTR	0,3	0,1	0,1	0,1
Sox3	0,2	0,0	1,3	1,2
Sox9-a/b	0,6	0,2	30,4	21,1
Pdia2 (XPDip)	0,0	0,0	4,3	0,0
Xbra-a/b	1,1	2,5	0,4	0,6
actc1	6,1	0,1	0,4	0,8
g6pd	0,0	0,0	0,0	0,2
tubb2b (N-tubulin)	1,4	0,1	106,0	172,7
vGlut1	0,0	0,0	0,1	61,7

6.1.4 Experiment 3.10 and 3.21

Table 6.7 Summary of the averaged fold change over CC of two independent Nanostring experiments for each sample and gene

	3 h			6 h			9 h			25 h		
Genes	**Ptf1a**	**Ptf1a+Su(H)**	**Su(H)**	**Ptf1a**	**Ptf1a+Su(H)**	**Su(H)**	**Ptf1a**	**Ptf1a+Su(H)**	**Su(H)**	**Ptf1a**	**Ptf1a+Su(H)**	**Su(H)**
Ascl1/Xash1 new	1,6	2,6	1,8	0,3	0,9	0,3	0,6	1,9	8,3	1,0	1,0	7,3
Barhl2	1,0	4,0	1,0	1,0	6,5	1,0	1,0	12,5	1,0	6,4	58,2	2,1
Cdknx (p27Xic1)	6,3	5,3	1,4	3,8	3,9	1,0	3,0	3,6	1,3	1,8	1,8	1,4
Cpa1	1,0	1,0	1,0	1,0	1,0	1,0	1,0	1,0	1,0	0,4	2,9	1,2
Dll1 (Delta1)	38,7	19,2	2,8	10,9	3,8	1,4	3,9	2,8	1,1	13,9	22,1	1,2
ESR10	28,1	58,7	1,4	16,4	26,6	2,1	40,4	58,1	3,8	446,7	1099,4	5,0
Ebf2-a/b	26,4	8,4	2,5	189,1	132,2	1,0	213,3	305,4	3,0	1071,4	947,6	2,1
Ebf3 (Coe3)	1,0	1,0	1,0	1,0	1,0	1,0	1,0	1,0	1,0	247,5	126,7	1,9
FoxD3a (XfD6)	1,0	2,4	2,9	0,3	0,7	0,9	0,9	7,7	2,7	123,0	279,9	2,1
Gad1	1,0	1,0	1,0	1,0	9,7	1,0	1,0	24,4	1,0	330,0	126,3	2,1
H4 new	0,7	1,1	1,5	0,9	1,2	1,0	1,1	1,3	1,2	0,8	1,1	1,6
HNF6 gene2	1,2	2,2	1,9	10,7	20,5	4,5	6,5	5,5	2,5	1090,4	1172,9	6,7
Hb9/mnx1	4,3	8,3	3,0	1,0	17,5	1,0	1,0	6,1	1,0	1,0	1,0	2,1
Hes5.1 (ESR1)	95,7	123,8	2,2	52,7	73,7	3,8	42,6	69,2	2,2	249,9	367,9	10,4
Hmx3	1,0	1,3	4,4	1,0	1,0	1,0	1,0	1,0	1,3	26,7	0,8	1,8
Hox11L2/Tlx3	1,0	1,0	1,0	1,0	1,0	1,0	1,0	1,0	1,0	1,0	1,0	2,1
Hpx6 (Lbx1)	1,0	1,0	1,0	1,0	1,0	1,0	1,0	1,0	1,0	1,8	14,0	6,8
Islet1 (isl1)	1,0	1,0	1,0	1,0	1,0	1,0	1,0	1,0	1,0	0,2	0,1	1,2
Kirrel2	0,8	0,8	1,1	1,3	1,5	1,3	1,2	1,6	1,0	927,1	1926,2	2,1
Lhx1 (Lim1)	1,0	1,0	1,5	1,0	2,7	1,0	1,0	1,0	1,0	20,8	124,4	2,1
Lhx2	1,0	1,2	1,0	1,0	1,0	1,0	3,7	9,8	1,0	2,0	207,4	2,1
Lhx5	1,3	1,4	0,8	1,2	1,1	0,9	1,1	1,2	0,6	99,2	101,6	2,1
Lmx1b	2,3	7,4	2,2	2,7	3,5	4,2	0,8	1,1	0,9	19,9	25,7	2,1
Mecom	1,0	1,0	1,0	1,0	1,0	1,0	1,0	3,5	1,0	82,8	1675,8	3,9
Mxi1	3,5	2,5	1,5	3,4	2,4	1,4	2,8	2,1	1,4	1,0	1,5	1,4
MyT1	12,8	12,8	1,2	13,9	16,0	0,9	11,1	19,7	0,9	3,5	5,8	0,7
NCAMa/b	1,3	0,8	1,4	0,9	1,1	1,4	1,8	0,9	2,0	33,5	15,6	1,8
NeuroD1a/b	1,0	1,0	1,0	1,0	1,0	1,0	1,0	1,1	1,0	290,3	73,1	2,1
NeuroD4 (Xath3)	1,0	1,0	1,0	9,9	11,5	1,0	8,8	14,7	1,0	585,2	266,9	2,1
Ngn1	1,1	1,0	1,0	0,7	0,7	0,7	1,0	1,0	1,0	177,4	375,1	2,1
Ngn3	1,1	1,9	3,7	1,0	2,8	1,0	1,0	1,5	1,0	1,0	1,0	2,1
Nrgn-1b (Ngn2-b)	0,6	1,2	0,6	0,5	0,9	0,4	1,8	3,9	1,0	58,5	264,4	2,1
ODC	1,0	1,0	1,0	1,0	1,0	1,0	1,0	1,0	1,0	1,0	1,0	1,0
PRDM13	118,0	352,3	1,0	645,2	1456,8	1,0	745,7	2056,8	1,0	1549,8	3285,7	2,1
PRDM14	1,9	2,1	1,5	1,0	1,1	2,0	0,8	0,8	2,0	29,9	7,6	7,3
Pak3	1,1	0,7	0,8	1,0	1,4	0,8	1,6	1,9	1,0	49,9	108,0	1,0
Pax2-a	0,7	0,7	0,7	1,0	1,3	1,0	1,0	1,0	1,0	267,5	101,2	24,4
Ptf1a-a/b 5'UTR	2,4	16,9	3,3	1,5	6,8	0,2	10,9	115,0	7,2	1,6	11,3	3,9
RBM38/Seb4R	1,2	1,1	0,8	1,3	1,2	0,6	2,0	1,9	1,0	0,6	1,0	0,7
RBPJ 3'UTR	0,9	1,0	0,9	0,8	0,9	0,8	1,0	1,1	1,0	0,8	0,6	1,7
Sox3	0,9	1,0	1,0	0,8	0,9	0,8	1,0	1,0	0,9	2,3	39,7	1,6
Sox9-a/b	1,9	3,5	1,0	1,6	5,3	1,4	1,7	5,2	1,6	41,2	81,9	1,5
Pdia2 (XPDip)	1,0	1,3	1,0	1,0	20,1	1,0	6,4	88,5	1,0	2,4	743,6	2,1
Xbra-a/b	29,0	5,8	0,8	1,0	1,8	1,0	1,5	5,2	1,0	0,1	0,1	0,3
actc1	0,7	6,7	9,6	1,6	1,7	0,4	6,0	1,6	1,8	0,6	0,2	1,6
g6pd	0,9	1,0	0,9	0,9	1,0	0,9	0,9	1,0	1,0	0,8	0,5	0,9
tubb2b (N-tubulin)	3,4	6,6	2,4	2,2	3,0	0,2	1,3	1,6	0,8	132,3	38,0	1,0
vGlut1	1,0	1,0	1,0	1,0	1,0	1,0	1,0	1,0	1,0	1,6	1,0	2,1

Table 6.8 Summary of the calculated standard error of the mean (SEM) of the fold change shown in table 6.7 for each sample and gene

	3 h			6 h			9 h			25 h		
Genes	**Ptf1a**	**Ptf1a+Su(H)**	**Su(H)**	**Ptf1a**	**Ptf1a+Su(H)**	**Su(H)**	**Ptf1a**	**Ptf1a+Su(H)**	**Su(H)**	**Ptf1a**	**Ptf1a+Su(H)**	**Su(H)**
Ascl1/Xash1 new	1,3	0,2	0,4	0,3	0,2	0,3	0,4	0,4	6,9	0,0	0,0	4,1
Barhl2	0,0	3,0	0,0	0,0	3,5	0,0	0,0	11,5	0,0	5,4	8,1	1,1
Cdknx (p27Xic1)	0,4	0,1	0,2	0,3	0,0	0,1	0,6	0,6	0,3	0,2	0,5	0,2
Cpa1	0,0	0,0	0,0	0,0	0,0	0,0	0,0	0,0	0,0	0,3	1,0	0,4
Dll1 (Delta1)	1,7	6,5	0,6	3,8	1,0	0,3	0,8	0,8	0,1	0,8	1,8	0,2
ESR10	11,9	9,0	0,0	10,9	20,8	0,4	23,8	38,8	0,4	275,6	395,4	1,8
Ebf2-a/b	1,5	1,4	1,5	15,7	25,2	0,0	34,8	43,5	2,0	262,1	188,2	1,1
Ebf3 (Coe3)	0,0	0,0	0,0	0,0	0,0	0,0	0,0	0,0	0,0	70,2	39,9	1,2
FoxD3a (XfD6)	1,0	2,2	2,3	0,0	0,3	0,9	0,1	6,2	1,4	44,4	92,0	1,1
Gad1	0,0	0,0	0,0	0,0	8,7	0,0	0,0	21,5	0,0	40,3	41,5	1,1
H4 new	0,3	0,2	0,2	0,3	0,2	0,2	0,5	0,1	0,3	0,1	0,0	0,6
HNF6 gene2	0,2	0,5	1,8	5,8	1,5	3,9	1,9	1,4	1,5	720,8	800,8	6,0
Hb9/mnx1	3,3	7,3	2,0	0,0	15,0	0,0	0,0	5,1	0,0	0,0	0,0	1,1
Hes5.1 (ESR1)	58,3	58,2	0,6	17,6	14,2	1,3	0,6	9,3	0,3	70,6	58,6	7,2
Hmx3	0,0	0,3	3,2	0,0	0,0	0,0	0,0	0,0	0,3	18,8	0,2	0,4
Hox11L2/Tlx3	0,0	0,0	0,0	0,0	0,0	0,0	0,0	0,0	0,0	0,0	0,0	1,1
Hpx6 (Lbx1)	0,0	0,0	0,0	0,0	0,0	0,0	0,0	0,0	0,0	0,8	9,9	5,8
Islet1 (isl1)	0,0	0,0	0,0	0,0	0,0	0,0	0,0	0,0	0,0	0,0	0,0	0,2
Kirrel2	0,2	0,1	0,3	0,2	0,2	0,1	0,1	0,2	0,2	236,4	524,6	1,1
Lhx1 (Lim1)	0,0	0,0	0,5	0,0	1,7	0,0	0,0	0,0	0,0	7,8	19,4	1,1
Lhx2	0,0	0,2	0,0	0,0	0,0	0,0	0,0	1,9	0,0	1,0	49,9	1,1
Lhx5	0,0	0,1	0,1	0,4	0,2	0,3	0,1	0,0	0,1	11,2	30,2	1,1
Lmx1b	1,9	4,1	0,1	1,7	1,0	3,2	0,2	0,1	0,7	9,0	1,9	1,1
Mecom	0,0	0,0	0,0	0,0	0,0	0,0	0,0	2,3	0,0	58,9	1238,8	2,9
Mxi1	0,9	0,1	0,1	1,2	0,6	0,4	0,3	0,2	0,2	0,1	0,2	0,3
MyT1	4,5	6,3	0,6	0,8	0,2	0,2	0,1	0,9	0,0	0,9	0,8	0,2
NCAMa/b	1,1	0,2	0,6	0,8	0,6	1,1	1,6	0,7	1,7	6,4	0,7	1,0
NeuroD1a/b	0,0	0,0	0,0	0,0	0,0	0,0	0,0	0,1	0,0	125,7	15,0	1,1
NeuroD4 (Xath3)	0,0	0,0	0,0	8,9	10,5	0,0	7,8	6,0	0,0	251,1	40,6	1,1
Ngn1	0,1	0,0	0,0	0,3	0,3	0,3	0,0	0,0	0,0	79,0	84,1	1,1
Ngn3	0,1	0,9	2,7	0,0	1,2	0,0	0,0	0,5	0,0	0,0	0,0	1,1
Nrgn-1b (Ngn2-b)	0,3	0,4	0,2	0,1	0,3	0,3	0,8	1,1	0,1	19,8	38,7	1,1
ODC	0,0	0,0	0,0	0,0	0,0	0,0	0,0	0,0	0,0	0,0	0,0	0,0
PRDM13	34,5	66,1	0,0	199,8	204,6	0,0	290,9	600,5	0,0	417,3	822,8	1,1
PRDM14	0,5	0,3	0,3	0,1	0,1	0,8	0,2	0,0	0,5	7,6	6,3	4,1
Pak3	0,0	0,0	0,1	0,3	0,2	0,1	0,2	0,3	0,1	22,6	42,3	0,8
Pax2-a	0,3	0,3	0,4	0,0	0,3	0,0	0,0	0,0	0,0	46,6	8,7	2,3
Ptf1a-a/b 5'UTR	2,2	14,8	2,7	1,0	4,2	0,1	8,2	93,0	6,3	0,0	1,8	3,2
RBM38/Seb4R	0,5	0,3	0,2	0,2	0,2	0,1	0,3	0,2	0,1	0,1	0,1	0,1
RBPJ 3'UTR	0,3	0,2	0,1	0,1	0,2	0,2	0,1	0,0	0,0	0,0	0,1	0,7
Sox3	0,2	0,1	0,1	0,0	0,0	0,1	0,1	0,1	0,0	0,2	3,8	0,8
Sox9-a/b	0,5	0,3	0,1	0,3	2,0	0,3	0,1	1,2	0,1	12,7	3,3	0,8
Pdia2 (XPDip)	0,0	0,3	0,0	0,0	2,6	0,0	5,4	48,2	0,0	1,4	215,4	1,1
Xbra-a/b	28,7	5,5	0,2	0,0	0,8	0,0	0,5	4,2	0,0	0,0	0,0	0,1
actc1	0,3	4,6	5,7	0,3	1,3	0,2	5,0	0,6	1,6	0,2	0,0	0,2
g6pd	0,2	0,0	0,1	0,1	0,0	0,1	0,1	0,0	0,0	0,2	0,1	0,1
tubb2b (N-tubulin)	0,0	1,0	0,9	1,3	1,5	0,0	0,7	0,1	0,3	79,2	16,7	0,1
vGlut1	0,0	0,0	0,0	0,0	0,0	0,0	0,0	0,0	0,0	0,6	0,0	1,1

6.2 Summary of the primary Nanostring data. Given are the primary data for each individual Nanostring experiment for each sample and gene.

6.2.1 Experiment 3.2

Table 6.9 Primary data of the first Nanostring experiment

	3 h			6 h			25 h			25 h -Dex		
Genes	**Ptf1a**	**Ngn2**	**CC**	**Ptf1a**	**Ngn2**	**CC**	**Ptf1a**	**Ngn2**	**CC**	**Ptf1a**	**Ngn2**	**CC**
Ascl1/Xash1 new	21	27	28	28	21	18	8	1	8	6	4	4
Cdknx (p27Xic1)	1.125	415	160	1.168	799	230	1.821	951	544	476	591	589
Dll1 (Delta1)	4.216	1.280	96	2.364	3.473	132	5.894	2.177	283	246	343	338
Ebf2-a/b	102	16	13	345	221	15	4.732	1.351	5	2	9	3
Ebf3 (Coe3)	2	4	5	6	16	2	2.282	1.040	21	16	15	26
Gad1	1	3	1	2	2	1	2.012	15	2	7	4	4
H4 new	234.325	238.913	268.862	258.756	281.627	264.463	99.148	60.339	69.450	64.557	67.722	71.375
Hb9/mnx1	8	18	32	17	17	13	5	1	1	3	1	1
Hox11L2/Tlx3	10	7	10	11	12	15	9	583	3	16	6	2
Hpx6 (Lbx1)	3	2	1	4	3	2	42	1	2	3	1	1
Islet1 (isl1)	12	13	14	15	21	14	298	774	428	508	587	617
Lhx1 (Lim1)	15	6	24	11	8	12	114	1	1	1	1	1
Lhx2	8	3	1	25	7	3	29	1	1	1	1	1
Lhx5	1.513	1.088	1.781	1.450	1.088	1.505	856	5	5	3	2	3
Lmx1b	10	14	23	12	17	17	108	1	3	1	3	1
Mxi1	1.523	781	337	1.890	1.930	343	829	1.414	730	461	819	686
MyT1	1.679	396	67	2.051	2.101	143	3.285	3.001	341	382	776	432
NCAMa/b	17	9	15	18	15	15	2.665	3.117	73	65	123	41
NeuroD1a/b	3	3	3	2	5	2	851	846	2	1	1	1
NeuroD4 (Xath3)	6	1	1	18	39	1	1.252	3.074	1	2	6	1
Ngn1	1	5	3	1	1	2	328	665	1	1	1	1
Ngn3	10	3	6	2	15	7	3	14	1	1	1	1
Nrgn-1b (Ngn2-b)	127	200	182	137	164	179	270	10	6	3	3	3
Numbl	781	743	847	847	909	833	706	511	567	740	752	881
ODC	23.923	19.286	26.463	25.529	24.940	20.340	31.638	16.020	11.606	14.529	17.972	17.380
PRDM13	674	36	19	1.548	67	34	7.258	17	7	11	10	8
PRDM14	570	610	291	368	1.304	276	159	1.017	4	5	2	3
Pak3	249	164	189	258	252	237	826	541	16	14	19	14
Pax2-a	2	3	8	11	4	7	1.081	8	11	3	4	4
Ptf1a-a/b 5'UTR	23	22	26	35	32	26	143	31	16	27	22	19
RBM38/Seb4R	1.670	1.490	1.249	1.726	2.034	1.327	337	267	173	214	329	302
RBPJ 3'UTR	1.957	1.789	2.242	1.978	2.049	1.907	1.416	692	722	846	1.060	1.054
Sox3	10.671	9.240	11.328	11.248	9.970	10.602	766	115	111	96	128	130
Xbra-a/b	29	25	42	27	28	27	16	53	91	37	47	50
actc1	14	8	7	15	10	8	84	306	114	247	204	304
g6pd	1.633	1.401	1.764	1.652	1.702	1.457	651	407	330	427	523	508
tubb2b (N-tubulin)	26	40	30	46	97	27	12.092	6.745	58	190	133	134
vGlut1	9	12	11	8	15	8	30	429	2	8	6	4
NEG_A	7	2	4	6	3	3	6	4	2	6	8	4
NEG_B	3	4	4	9	2	9	4	3	3	3	3	2
NEG_C	3	2	6	5	6	1	4	2	4	3	5	5
NEG_D	2	4	1	7	7	6	7	9	5	10	6	5
NEG_E	3	4	6	6	6	5	6	3	3	9	3	3
NEG_F	9	11	10	11	12	5	16	13	8	17	14	11
NEG_G	8	10	7	13	10	8	6	3	8	5	1	1
NEG_H	7	7	5	3	4	6	9	4	2	1	1	1
POS_A	10.882	12.610	11.204	12.750	11.576	12.511	14.805	13.681	14.149	15.447	14.521	12.036
POS_B	5.928	6.360	5.864	6.497	5.732	6.389	7.356	6.590	6.838	7.745	8.548	6.456
POS_C	1.653	1.790	1.611	1.807	1.630	1.721	2.058	1.870	1.894	2.181	2.356	1.780
POS_D	412	402	347	434	366	381	478	429	420	470	494	380
POS_E	68	79	61	95	65	86	78	84	91	89	101	81
POS_F	48	45	36	26	33	30	62	43	52	51	52	46

Table 6.10 Primary data of the second Nanostring experiment

	3 h			6 h			25 h			25 h -Dex		
Genes	**Ptf1a**	**Ngn2**	**CC**	**Ptf1a**	**Ngn2**	**CC**	**Ptf1a**	**Ngn2**	**CC**	**Ptf1a**	**Ngn2**	**CC**
Ascl1/Xash1 new	36	40	62	33	32	24	1	2	5	4	22	4
Cdknx (p27Xic1)	690	243	253	1.733	519	184	1.188	1.767	606	512	562	489
Dll1 (Delta1)	1.768	1.282	162	2.740	1.701	86	2.682	3.850	148	206	393	153
Ebf2-a/b	41	22	11	372	107	4	3.273	3.190	4	3	18	6
Ebf3 (Coe3)	1	3	2	2	6	5	1.418	3.211	18	9	19	4
Gad1	3	1	1	2	3	3	1.038	29	5	6	4	3
H4 new	241.378	244.122	227.724	376.957	256.086	131.144	86.171	68.804	66.216	73.555	64.327	64.809
Hb9/mnx1	34	15	52	49	26	10	6	8	2	1	1	3
Hox11L2/Tlx3	11	7	15	18	12	8	6	1.747	4	6	24	7
Hpx6 (Lbx1)	2	3	1	1	1	3	28	3	1	1	1	1
Islet1 (isl1)	8	16	17	16	6	9	205	1.960	636	519	574	437
Lhx1 (Lim1)	16	17	72	28	20	35	97	3	1	1	1	1
Lhx2	9	3	4	17	4	2	4	1	3	1	2	1
Lhx5	1.074	682	1.017	1.398	872	711	546	13	12	5	9	3
Lmx1b	25	26	40	29	26	16	47	8	2	1	1	1
Mxi1	841	757	292	2.390	1.293	289	418	1.330	444	379	607	424
MyT1	419	304	32	1.490	866	69	2.214	5.273	436	373	847	346
NCAMa/b	18	22	18	24	25	15	2.172	7.437	116	43	163	54
NeuroD1a/b	1	2	1	7	8	3	759	3.878	1	1	2	1
NeuroD4 (Xath3)	1	3	1	11	17	1	1.379	7.257	3	3	47	1
Ngn1	2	3	2	1	1	1	200	1.912	1	1	1	1
Ngn3	14	11	26	11	7	10	1	26	1	1	1	1
Nrgn-1b (Ngn2-b)	146	135	232	144	93	99	78	31	2	1	1	1
Numbl	720	618	977	1.019	667	635	750	964	1.061	873	816	713
ODC	15.778	14.327	18.146	25.357	16.449	13.544	24.683	20.819	16.692	14.987	16.066	15.075
PRDM13	116	24	29	942	38	21	2.690	81	7	14	5	4
PRDM14	183	197	140	166	456	80	86	3.446	1	3	7	1
Pak3	69	56	99	105	62	57	537	2.081	5	9	13	14
Pax2-a	6	4	7	5	7	6	403	3	4	2	10	2
Ptf1a-a/b 5'UTR	43	45	69	63	40	25	80	50	22	22	23	18
RBM38/Seb4R	1.033	970	1.439	1.579	1.028	710	201	297	191	139	176	147
RBPJ 3'UTR	1.490	1.301	1.779	1.833	1.217	1.018	1.111	1.054	1.138	875	888	763
Sox3	9.577	7.820	10.190	14.031	9.105	7.517	235	87	108	105	90	80
Xbra-a/b	68	47	48	82	19	11	36	139	76	95	91	55
actc1	4	6	7	21	16	4	112	546	189	137	101	69
g6pd	1.106	950	1.356	1.453	977	818	373	563	485	333	323	330
tubb2b (N-tubulin)	49	55	63	90	91	27	14.184	32.903	161	117	157	105
vGlut1	33	42	56	63	41	26	111	3.024	2	3	1	2
NEG_A	2	1	7	4	2	1	12	8	5	4	4	2
NEG_B	6	6	7	7	1	2	6	6	5	5	3	4
NEG_C	3	3	2	1	4	1	6	4	2	1	6	3
NEG_D	3	6	9	6	2	1	8	11	9	3	5	6
NEG_E	5	4	1	5	6	1	6	7	5	4	5	3
NEG_F	6	15	15	6	8	4	11	13	11	10	13	6
NEG_G	12	7	11	8	10	9	5	5	5	5	2	2
NEG_H	4	8	4	7	6	3	5	7	3	2	1	1
POS_A	11.995	10.430	11.453	11.338	10.769	4.119	14.514	14.988	15.429	15.767	12.424	8.790
POS_B	5.902	5.418	5.365	5.745	5.295	2.138	6.762	7.119	7.493	7.493	6.351	4.420
POS_C	1.631	1.518	1.529	1.566	1.476	587	1.882	2.000	2.120	1.997	1.796	1.176
POS_D	395	326	377	340	346	144	437	411	471	482	431	277
POS_E	64	56	66	48	68	25	92	73	97	93	69	48
POS_F	40	29	34	32	36	10	52	64	50	48	44	31

6.2.2 Experiment 3.7

Table 6.11 Primary data of the first Nanostring experiment

Genes	Ptf1a	Ngn2	chimeric Ptf1a	CC
Arx-a	17	5	29	12
Ascl1/Xash1	17	7	16	6
Cdknx (p27Xic1)	1.201	482	950	320
Dll1 (Delta1)	623	242	548	74
Delta2	591	111	547	22
ESR10	92	74	50	3
ESR6e (Hes3.1)	208	201	208	91
ESR9.1a	61	24	37	1
Ebf2-a/b	1.157	238	726	1
Ebf3 (Coe3)	1.890	615	1.123	12
Eng1-a/b	2	2	1	4
FGF8	61	17	36	7
FoxD3a (XfD6)	313	58	199	60
Gad1	1.078	7	335	3
H4	27	9	29	3
Hb9/mnx1	34	9	26	8
Hes1a(Hairy1)	668	453	1.160	361
Hes2	1	6	6	4
Hes5.1 (ESR1)	149	53	87	22
Hes6.1	155	59	140	77
Hes7 (XHR1)	39	21	53	26
Hox11L2/Tlx3	22	334	234	9
Hpx6 (Lbx1)	79	29	38	23
Insm1	390	186	307	20
Islet1 (isl1)	301	498	537	302
Jagged1 (Serrate-1)	491	193	402	107
Krox20/egr2	5	6	4	3
Lhx1 (Lim1)	95	3	9	1
Lhx2	11	4	6	2
Lhx5	73	4	35	3
Lmx1b	105	8	25	4
Mxi1	351	346	416	141
MyT1	881	467	970	72
NCAMa/b	1.001	988	1.344	22
NeuroD1a/b	621	312	759	24
NeuroD4 (Xath3)	638	728	1.498	3
NeuroD6 (Xath2)	3	3	3	1
Ngn1	195	194	452	5
Ngn3	21	17	27	12
Ngnr-1a (ngn2a)	6	2	2	2
Nkx6.1	80	5	15	1
Nkx6.2	54	33	63	26
Notch1	1.033	429	910	433
Nrgn-1b (Ngn2-b)	41	8	18	2
Nrp1	106	40	75	19
Numb	3	5	5	3
Numbl	600	389	938	575
ODC	14.005	7.860	12.492	6.763
Olig3	7	5	8	7
Pak3	404	291	331	23
Pax2-a	149	10	9	4
Pax3	147	8	29	1
Pax6-a	63	16	37	26
Pax6-b	64	6	5	9
PRDM14	78	338	168	13
Ptf1a-a/b	84	3	125	5
RBM38/Seb4R	76	79	110	53
RBPJ	404	217	531	289
Slug	30	8	25	3
Sox1	78	26	76	35
Sox2	1.023	103	182	37
Sox3	350	72	107	75
Sox9-a/b	192	23	37	12
SoxD	2.093	999	2.055	1.299
Twist1-a	97	13	22	5
Xbra-a/b	45	63	101	50
actb	309.705	177.958	419.321	178.041
actc1	1.984	1.015	3.163	280
c-myc	159	105	229	153
g6pd	470	229	507	159
gapdh	398	312	315	149
runx1 (Xaml)	52	60	92	81
tubb2b (N-tubulin)	6.434	3.213	4.552	39

vGlut1	72	179	192	12
NEG_A	3	2	2	2
NEG_B	3	5	5	5
NEG_C	3	3	1	2
NEG_D	3	1	5	3
NEG_E	6	2	3	5
NEG_F	6	7	7	6
NEG_G	12	4	7	6
NEG_H	14	13	16	7
POS_A	13.666	12.441	11.328	13.077
POS_B	7.112	6.564	6.221	6.748
POS_C	2.392	2.164	2.052	2.172
POS_D	428	368	368	394
POS_E	96	86	74	80
POS_F	30	38	20	39

Table 6.12 Primary data of the second Nanostring experiment

Genes	Ptf1a	Ngn2	chimeric Ptf1a	CC
Arx-a	7	13	13	4
Ascl1/Xash1	8	8	13	7
Cdknx (p27Xic1)	1.200	885	1.084	262
Dll1 (Delta1)	1.264	516	583	52
Delta2	689	263	489	9
ESR10	194	104	100	3
ESR6e (Hes3.1)	135	160	162	65
ESR9.1a	208	61	58	3
Ebf2-a/b	1.341	470	775	1
Ebf3 (Coe3)	1.414	1.207	1.079	8
Eng1-a/b	2	2	3	1
FGF8	31	18	21	2
FoxD3a (XfD6)	243	106	249	46
Gad1	822	10	333	4
H4	2	3	2	2
Hb9/mnx1	18	32	34	6
Hes1a(Hairy1)	457	718	948	277
Hes2	23	1	6	2
Hes5.1 (ESR1)	484	99	141	25
Hes6.1	192	140	160	73
Hes7 (XHR1)	17	24	26	17
Hox11L2/Tlx3	12	783	106	2
Hpx6 (Lbx1)	115	23	34	6
Insm1	431	436	243	15
Islet1 (isl1)	69	786	400	186
Jagged1 (Serrate-1)	372	315	360	94
Krox20/egr2	6	3	9	4
Lhx1 (Lim1)	201	18	40	1
Lhx2	13	5	4	2
Lhx5	190	10	45	1
Lmx1b	193	31	38	5
Mxi1	191	233	157	76
MyT1	949	709	730	48
NCAMa/b	1.212	1.950	1.288	23
NeuroD1a/b	835	1.009	1.003	17
NeuroD4 (Xath3)	1.055	1.683	1.152	4
NeuroD6 (Xath2)	8	3	3	3
Ngn1	327	395	259	2
Ngn3	14	24	16	6
Ngnr-1a (ngn2a)	18	7	4	1
Nkx6.1	40	8	59	3
Nkx6.2	48	58	92	29
Notch1	1.179	555	820	252
Nrgn-1b (Ngn2-b)	148	24	22	1
Nrp1	113	128	173	20
Numb	9	5	5	3
Numbl	214	600	636	466
ODC	14.140	9.967	11.421	5.580
Olig3	3	2	1	7
Pak3	339	600	346	13
Pax2-a	168	5	25	3
Pax3	269	50	81	1
Pax6-a	70	29	45	12
Pax6-b	71	14	19	5
PRDM14	35	907	138	12
Ptf1a-a/b	84	6	87	4
RBM38/Seb4R	44	100	73	32
RBPJ	271	342	419	215
Slug	57	7	21	1
Sox1	45	42	66	23
Sox2	1.098	197	426	25
Sox3	603	114	280	43
Sox9-a/b	317	21	62	8
SoxD	1.367	1.288	1.832	929
Twist1-a	68	44	89	1
Xbra-a/b	50	118	51	23
actb	119.965	181.584	237.167	127.128
actc1	276	1.051	1.147	164
c-myc	76	205	187	126
g6pd	252	254	306	147
gapdh	177	607	392	132
runx1 (Xaml)	38	54	50	41
tubb2b (N-tubulin)	7.652	6.724	4.566	32
vGlut1	22	520	143	7
NEG_A	3	6	1	3
NEG_B	5	5	3	1

NEG_C	2	4	1	2
NEG_D	3	1	1	1
NEG_E	4	1	1	3
NEG_F	6	8	4	4
NEG_G	8	11	3	1
NEG_H	10	14	18	10
POS_A	9.701	11.659	13.983	9.955
POS_B	5.454	5.933	6.721	4.774
POS_C	1.740	1.871	2.214	1.520
POS_D	295	327	342	261
POS_E	81	64	92	64
POS_F	23	26	27	24

6.2.3 Experiment 3.8 and 3.20

Table 6.13 Primary data of the first Nanostring experiment

	6 h			32 h		
Genes	**Ptf1a**	**Ptf1a$^{W224A/W242A}$**	**CC**	**Ptf1a**	**Ptf1a$^{W224A/W242A}$**	**CC**
Ascl1/Xash1 new	10	20	26	23	34	25
Barhl2	5	3	1	106	30	3
Cdknx (p27Xic1)	784	701	93	1.192	1.368	304
Cpa1	2	1	1	13	5	5
Dll1 (Delta1)	3.115	4.298	181	5.389	3.345	571
ESR10	624	64	66	823	828	80
Ebf2-a/b	296	90	3	2.980	2.509	1
Ebf3 (Coe3)	5	5	1	982	1.700	30
FoxD3a (XfD6)	18	59	25	134	46	1
Gad1	3	2	1	1.097	40	2
H4 new	133.016	143.976	123.942	36.571	45.747	47.895
HNF6 gene2	25	16	11	4.867	2.949	5
Hb9/mnx1	8	28	12	7	33	2
Hes5.1 (ESR1)	982	166	22	755	730	8
Hmx3	6	8	3	50	7	5
Hox11L2/Tlx3	15	33	1	17	760	10
Hpx6 (Lbx1)	3	1	4	247	202	2
Islet1 (isl1)	2	2	1	97	289	241
Kirrel2	229	67	94	1.122	41	15
Lhx1 (Lim1)	12	22	1	209	98	2
Lhx2	3	3	8	41	35	6
Lhx5	305	613	577	517	14	2
Lmx1b	20	5	8	106	120	2
Mecom	3	4	1	116	13	7
Mxi1	1.094	998	181	625	847	578
MyT1	2.229	1.574	66	2.718	2.948	274
NCAMa/b	25	28	21	2.335	3.279	73
NeuroD1a/b	3	6	2	1.166	1.165	1
NeuroD4 (Xath3)	14	11	1	1.173	2.258	2
Ngn1	1	2	4	455	771	3
Ngn3	2	19	5	1	4	1
Nrgn-1b (Ngn2-b)	26	47	43	160	21	1
ODC	11.580	13.401	11.191	14.778	16.784	11.418
PRDM13	936	55	1	3.328	186	1
PRDM14	85	398	102	291	1.903	6
Pak3	98	103	65	746	978	7
Pax2-a	10	8	9	1.065	59	28
Ptf1a-a/b 5'UTR	22	33	17	42	15	9
RBM38/Seb4R	893	1.141	542	222	203	175
RBPJ 3'UTR	728	781	731	566	512	468
Sox3	4.238	7.499	5.825	812	554	152
Sox9-a/b	108	116	63	456	290	10
XPDip	3	2	2	19	2	1
Xbra-a/b	32	21	25	103	20	166
actc1	13	21	12	734	810	205
g6pd	503	596	488	184	180	193
tubb2b (N-tubulin)	51	41	25	18.125	33.288	58
vGlut1	1	1	1	34	597	1
NEG_A	2	7	5	3	3	1
NEG_B	2	1	1	1	1	6
NEG_C	3	1	1	1	2	1
NEG_D	6	6	6	6	7	3
NEG_E	9	8	3	4	2	5
NEG_F	1	9	3	6	5	2
NEG_G	1	1	2	1	2	1
NEG_H	2	1	1	2	1	1
POS_A	5.392	6.917	6.116	6.147	7.891	7.303
POS_B	2.813	3.382	3.010	3.226	3.900	3.563
POS_C	864	1.047	892	1.010	1.192	1.069
POS_D	175	226	198	206	242	203
POS_E	24	30	30	38	45	34
POS_F	33	32	29	20	30	28

Table 6.14 Primary data of the second Nanostring experiment

	6 h			32 h		
Genes	**Ptf1a**	**Ptf1a$^{W224A/W242A}$**	**CC**	**Ptf1a**	**Ptf1a$^{W224A/W242A}$**	**CC**
Ascl1/Xash1 new	16	16	21	12	36	7
Barhl2	1	1	3	16	14	3
Cdknx (p27Xic1)	277	377	146	459	1.502	141
Cpa1	1	1	3	2	51	3
Dll1 (Delta1)	688	1.113	96	615	2.060	51
ESR10	241	53	86	61	283	7
Ebf2-a/b	91	33	6	538	1.564	1
Ebf3 (Coe3)	1	1	3	206	1.962	3
FoxD3a (XfD6)	64	93	162	45	40	1
Gad1	1	1	1	275	96	1
H4 new	98.113	124.321	239.505	24.893	63.752	16.260
HNF6 gene2	22	20	11	1.028	1.981	3
Hb9/mnx1	19	26	26	7	18	3
Hes5.1 (ESR1)	174	115	55	59	200	1
Hmx3	7	3	6	15	12	4
Hox11L2/Tlx3	5	13	5	12	832	1
Hpx6 (Lbx1)	4	2	5	63	52	1
Islet1 (isl1)	1	2	2	130	897	75
Kirrel2	145	27	118	97	31	4
Lhx1 (Lim1)	14	17	17	52	43	1
Lhx2	3	4	5	7	23	10
Lhx5	290	223	826	31	10	1
Lmx1b	6	8	11	16	73	1
Mecom	2	2	4	42	40	1
Mxi1	945	871	718	207	813	145
MyT1	952	523	150	589	3.503	113
NCAMa/b	19	27	40	855	6.549	52
NeuroD1a/b	2	4	7	193	1.218	4
NeuroD4 (Xath3)	4	1	2	160	1.655	1
Ngn1	1	5	6	108	761	2
Ngn3	13	4	11	1	4	1
Nrgn-1b (Ngn2-b)	60	72	67	29	25	1
ODC	6.931	10.663	17.736	3.435	27.572	1.312
PRDM13	347	19	1	179	46	1
PRDM14	218	182	266	149	2.322	4
Pak3	49	52	72	176	1.157	3
Pax2-a	12	8	8	97	127	8
Ptf1a-a/b 5'UTR	20	20	19	21	56	6
RBM38/Seb4R	567	995	871	66	311	40
RBPJ 3'UTR	452	460	757	344	1.661	166
Sox3	5.523	7.875	11.863	242	255	58
Sox9-a/b	112	68	116	151	134	4
Pdia2 (XPDip)	4	2	3	1	4	1
Xbra-a/b	12	29	26	31	288	10
actc1	12	9	14	254	670	28
g6pd	310	479	854	65	670	31
tubb2b (N-tubulin)	7	4	14	2.905	36.739	21
vGlut1	1	1	1	9	1.485	1
NEG_A	3	6	11	2	5	6
NEG_B	4	2	7	2	3	3
NEG_C	4	3	1	2	2	1
NEG_D	3	5	6	5	16	1
NEG_E	2	7	9	3	5	6
NEG_F	6	8	6	5	5	5
NEG_G	1	2	3	1	3	1
NEG_H	2	2	3	1	2	1
POS_A	9.006	9.492	7.183	9.700	7.705	6.893
POS_B	4.727	4.675	3.742	4.913	4.638	3.554
POS_C	1.321	1.372	1.123	1.477	1.439	1.005
POS_D	291	306	242	340	325	222
POS_E	61	64	37	47	49	32
POS_F	38	40	44	37	39	23

6.2.4 Experiment 3.10 and 3.21

Table 6.15 Primary data of the first Nanostring experiment

	Ptf1a				Ptf1a+Su(H)				Su(H)				CC			
Genes	**3 h**	**6 h**	**9 h**	**25 h**	**3 h**	**6 h**	**9 h**	**25 h**	**3 h**	**6 h**	**9 h**	**25 h**	**3 h**	**6 h**	**9 h**	**25 h**
Ascl1/Xash1 new	17	11	14	2	18	18	19	7	10	8	12	1	7	13	14	4
Barhl2	5	1	6	22	2	11	11	94	1	1	1	1	1	1	1	1
Cdknx (p27Xic1)	625	631	584	573	199	353	464	588	56	145	110	27	31	51	139	171
Cpa1	1	2	1	34	1	1	4	61	1	1	1	2	1	1	1	14
Dll1 (Delta1)	2.458	1.819	1.889	2.509	545	369	952	4.082	66	232	192	12	19	74	232	119
ESR10	1.108	603	1.003	337	1.175	521	1.003	1.166	33	55	35	1	21	9	18	1
Ebf2-a/b	56	282	329	1.504	10	109	319	1.257	5	2	7	1	1	3	3	1
Ebf3 (Coe3)	1	2	3	605	1	1	2	285	1	1	1	1	1	1	1	5
FoxD3a (XfD6)	13	21	14	168	10	10	27	320	16	8	10	1	21	12	7	1
Gad1	1	1	1	554	1	3	14	151	1	1	1	1	1	1	1	5
H4 new	102.500	111.754	127.584	38.854	71.736	96.562	151.963	46.345	86.761	119.900	75.116	5.829	62.650	53.195	106.944	26.719
HNF6 gene2	31	33	66	3.336	12	17	40	3.248	3	18	18	2	6	1	13	5
Hb9/mnx1	3	6	7	7	2	6	10	1	3	4	2	1	1	1	4	1
Hes5.1 (ESR1)	1.043	1.028	1.613	352	632	643	1.484	519	17	72	37	1	10	7	30	3
Hmx3	2	6	3	58	2	5	10	14	7	7	4	1	1	1	2	8
Hox11L2/Tlx3	5	5	8	3	1	5	1	2	1	2	1	1	1	1	1	1
Hpx6 (Lbx1)	3	1	3	29	1	2	6	51	1	2	2	2	1	2	5	1
Islet1 (isl1)	1	1	2	78	3	1	3	17	1	1	2	32	2	1	1	238
Kirrel2	243	189	333	1.287	82	141	272	2.310	107	182	112	1	66	48	168	1
Lhx1 (Lim1)	10	5	2	48	4	2	7	184	4	4	1	1	2	2	2	1
Lhx2	3	7	19	8	5	4	20	270	2	4	2	1	1	2	2	1
Lhx5	460	293	336	185	158	122	265	129	83	183	81	1	99	51	183	1
Lmx1b	20	17	20	77	11	6	20	57	4	17	3	1	2	3	16	2
Mecom	3	5	8	166	1	4	12	2.344	1	1	1	1	1	1	1	9
Mxi1	1.041	1.204	1.674	267	359	496	892	335	164	433	357	22	111	154	384	136
MyT1	867	1.475	1.220	1.415	333	893	1.474	1.892	31	78	50	11	16	34	69	196
NCAMa/b	15	10	6	1.864	8	10	9	918	7	14	7	4	7	9	13	46
NeuroD1a/b	7	3	11	325	3	2	12	107	2	1	2	1	1	2	2	1
NeuroD4 (Xath3)	4	36	42	635	3	19	35	383	1	1	1	1	1	1	2	1
Ngn1	1	1	1	204	1	1	3	489	2	2	1	1	1	1	5	1
Ngn3	2	9	1	1	3	7	13	1	3	8	2	1	1	2	3	1
Nrgn-1b (Ngn2-b)	31	42	35	95	24	29	55	382	11	13	16	1	21	25	23	2
ODC	12.073	9.175	12.309	12.691	4.193	4.615	8.175	11.380	3.733	7.757	5.371	731	3.293	2.540	6.828	7.585
PRDM13	158	600	819	2.095	177	837	1.726	4.050	1	1	1	1	1	1	1	1
PRDM14	315	178	214	65	136	88	172	14	79	174	225	1	58	48	189	2
Pak3	78	57	72	370	18	34	61	757	18	31	23	2	18	13	28	13
Pax2-a	9	6	1	428	3	2	5	192	1	7	4	3	4	2	4	3
Ptf1a-a/b 5'UTR	18	29	34	77	33	51	130	397	10	11	10	14	13	13	14	25
RBM38/Seb4R	702	846	849	144	299	383	556	209	186	294	206	12	279	208	278	148
RBPJ 3'UTR	766	627	659	737	347	349	536	475	321	507	311	122	332	251	423	544
Sox3	7.473	5.484	6.041	235	3.140	2.854	4.181	3.311	2.925	4.034	2.765	12	2.749	1.862	3.984	56
Sox9-a/b	190	139	183	525	153	165	293	667	48	101	78	1	39	30	68	11
Pdia2 (XPDip)	2	9	14	18	4	16	58	878	2	4	1	1	1	1	3	2
Xbra-a/b	4	9	10	13	4	6	10	4	4	2	4	1	4	1	4	25
actc1	16	25	21	223	11	15	23	106	14	6	3	64	5	5	14	379
g6pd	514	458	496	214	222	227	424	105	165	339	251	15	183	131	345	186
tubb2b (N-tubulin)	44	37	61	8.515	22	26	39	3.058	7	13	12	9	5	11	23	101
vGlut1	9	8	5	19	1	3	3	4	1	4	1	1	1	1	4	1
NEG_A	1	4	3	6	2	2	3	1	5	7	5	1	2	1	6	1
NEG_B	1	3	1	10	1	3	2	3	3	1	1	2	2	6	7	2
NEG_C	2	1	1	1	1	1	1	3	1	3	1	1	1	1	2	3
NEG_D	5	6	6	7	3	1	7	7	2	2	7	3	4	5	6	4
NEG_E	5	8	5	3	7	7	8	2	4	6	7	1	5	3	7	3
NEG_F	6	4	3	11	4	3	5	5	1	4	4	7	2	7	5	4
NEG_G	1	1	2	1	1	1	2	1	2	1	1	1	1	1	1	1
NEG_H	4	2	5	1	1	1	4	1	1	3	1	1	1	1	1	1
POS_A	6.133	6.816	5.679	7.231	5.288	5.724	6.930	7.843	7.713	7.231	6.749	5.695	6.402	5.512	9.721	7.005
POS_B	3.066	3.436	2.752	3.688	2.446	2.867	3.274	3.615	3.536	3.379	3.149	2.612	3.308	2.870	5.089	3.714
POS_C	927	1.026	797	1.143	765	842	936	1.083	1.017	1.066	901	802	1.029	850	1.502	1.150
POS_D	188	238	199	220	166	198	180	257	236	214	198	164	233	189	344	243
POS_E	35	44	28	43	33	26	39	38	38	29	47	29	40	33	66	54
POS_F	35	36	37	35	27	34	42	28	24	33	27	10	30	26	39	27

Table 6.16 Primary data of the second Nanostring experiment

	Ptf1a				Ptf1a+Su(H)				Su(H)				CC			
Genes	**3 h**	**6 h**	**9 h**	**25 h**	**3 h**	**6 h**	**9 h**	**25 h**	**3 h**	**6 h**	**9 h**	**25 h**	**3 h**	**6 h**	**9 h**	**25 h**
Ascl1/Xash1 new	28	24	12	5	25	20	25	2	19	14	13	11	18	28	15	3
Barhl2	1	2	1	25	13	8	62	70	1	1	1	1	1	3	3	2
Cdknx (p27Xic1)	605	845	624	923	462	541	1.112	575	97	153	153	363	118	214	262	388
Cpa1	1	1	5	8	1	2	7	21	1	1	1	7	1	1	1	10
Dll1 (Delta1)	2.410	1.843	1.649	3.065	825	406	1.630	3.120	126	140	327	157	89	135	774	144
ESR10	1.558	630	887	911	2.621	452	1.577	1.379	51	134	98	8	57	124	92	3
Ebf2-a/b	35	195	286	1.673	13	82	613	1.050	5	3	7	1	6	5	5	1
Ebf3 (Coe3)	6	3	7	690	1	2	5	254	1	1	1	5	1	1	1	7
FoxD3a (XfD6)	22	22	31	219	37	31	73	350	36	51	20	1	18	48	47	1
Gad1	1	1	2	472	3	19	99	163	1	1	1	4	1	3	2	1
H4 new	124.506	210.768	195.625	57.345	155.480	158.466	254.992	62.736	168.362	129.976	99.010	38.717	147.306	176.711	177.596	50.263
HNF6 gene2	8	21	60	3.640	9	31	87	2.695	10	7	10	7	6	11	31	11
Hb9/mnx1	16	9	8	1	21	29	40	1	11	3	3	1	9	9	13	3
Hes5.1 (ESR1)	1.548	1.148	1.470	410	1.821	1.310	4.196	400	30	59	51	15	22	42	66	3
Hmx3	4	4	8	67	8	6	12	8	8	3	5	5	9	3	7	4
Hox11L2/Tlx3	5	8	11	2	4	2	6	5	2	1	1	3	5	4	6	2
Hpx6 (Lbx1)	5	5	4	9	4	6	6	13	3	1	3	2	1	4	9	1
Islet1 (isl1)	1	5	4	70	2	1	4	31	2	1	1	167	1	2	3	226
Kirrel2	106	177	307	1.461	128	112	647	2.255	116	108	138	1	218	126	331	3
Lhx1 (Lim1)	8	7	6	46	6	9	14	141	6	3	3	2	3	2	3	1
Lhx2	4	7	16	14	5	5	41	245	1	6	3	1	5	2	3	2
Lhx5	353	304	350	148	398	238	507	130	208	169	101	1	321	387	404	1
Lmx1b	10	12	5	24	15	9	15	31	12	8	5	3	13	8	15	1
Mecom	5	4	3	187	2	6	31	2.680	2	3	1	8	3	1	1	5
Mxi1	734	1.506	1.887	314	408	637	2.158	338	223	376	508	204	209	333	897	230
MyT1	459	1.418	1.398	1.131	358	1.059	3.655	1.562	35	74	67	210	76	106	198	289
NCAMa/b	27	27	38	1.953	14	16	40	593	20	21	19	75	19	18	27	37
NeuroD1a/b	1	1	9	529	6	2	17	90	1	2	2	1	1	5	1	1
NeuroD4 (Xath3)	1	9	8	1.053	1	4	36	291	1	1	1	1	1	1	1	1
Ngn1	10	3	1	330	5	3	3	430	4	5	2	1	3	12	2	1
Ngn3	10	11	6	2	9	7	10	1	12	2	2	1	2	8	5	1
Nrgn-1b (Ngn2-b)	59	51	57	108	99	67	154	287	48	42	14	1	82	82	41	1
ODC	8.015	8.980	9.436	10.650	7.993	6.083	14.490	7.827	6.634	5.686	5.023	5.584	9.766	9.077	13.658	7.115
PRDM13	152	901	1.157	2.463	398	1.189	4.529	3.774	1	1	1	1	2	1	1	1
PRDM14	385	300	448	57	376	247	589	22	251	556	598	11	200	325	668	2
Pak3	82	72	89	397	57	66	155	598	46	50	31	4	92	88	96	8
Pax2-a	5	7	11	402	7	7	5	94	8	5	2	21	5	4	7	5
Ptf1a-a/b 5'UTR	17	44	33	117	63	99	374	477	16	10	12	28	12	22	13	49
RBM38/Seb4R	603	771	645	152	479	464	928	203	278	223	164	77	436	509	424	156
RBPJ 3'UTR	962	878	770	631	1.059	728	1.250	382	707	626	368	392	1.040	980	1.018	500
Sox3	6.726	6.927	5.455	289	7.008	5.108	8.027	3.583	5.502	5.078	2.291	62	7.427	8.248	7.028	95
Sox9-a/b	110	110	127	376	164	255	644	812	39	60	60	19	61	60	107	13
Pdia2 (XPDip)	5	10	25	15	8	22	253	888	1	1	1	1	2	1	4	3
Xbra-a/b	63	4	14	10	17	5	37	2	4	1	2	8	9	3	8	20
actc1	9	23	24	88	17	8	22	20	19	10	6	76	9	17	9	69
g6pd	525	489	478	233	509	373	804	115	425	366	265	128	599	566	724	158
tubb2b (N-tubulin)	15	29	24	9.367	20	20	70	1.787	12	7	17	30	12	14	46	34
vGlut1	1	1	1	13	1	1	1	3	1	2	1	1	1	1	3	1
NEG_A	4	8	5	2	2	6	5	5	6	9	3	1	5	7	9	2
NEG_B	5	7	6	1	5	3	2	1	3	2	1	2	3	5	2	5
NEG_C	1	1	1	1	1	1	4	2	3	1	1	1	5	1	4	2
NEG_D	9	7	5	3	6	5	7	6	3	4	5	5	6	3	4	4
NEG_E	6	10	5	4	4	1	13	8	5	9	6	3	5	4	6	3
NEG_F	4	6	11	9	2	7	6	8	9	6	4	4	7	7	7	2
NEG_G	3	1	3	1	1	1	2	3	1	1	1	1	1	1	2	1
NEG_H	1	3	3	2	4	1	4	1	4	1	1	1	1	1	1	1
POS_A	6.711	9.436	8.775	8.486	6.152	5.987	7.380	8.693	8.133	5.911	6.992	6.544	6.507	7.327	7.343	8.616
POS_B	3.569	4.606	4.440	4.494	3.352	3.048	3.757	4.104	4.199	3.001	3.329	3.295	3.355	3.465	3.676	4.352
POS_C	1.089	1.503	1.277	1.334	1.031	933	1.165	1.237	1.321	935	970	998	999	1.028	1.156	1.304
POS_D	221	292	272	312	222	194	245	280	293	201	226	206	221	237	252	251
POS_E	33	61	51	41	32	34	43	42	44	36	35	43	41	46	32	51
POS_F	28	43	60	38	46	43	59	41	50	29	32	18	26	43	29	33

6.3 Summary of the genes analysed with the Nanostring

Table 6.17 Summary of the genes analysed with the Nanostring. Given is the symbol of the gene and its accession number as well as the target region and the target sequence of the reporter probe. (Grey marks a non-functional H4 probe).

Gene	Accession	Target Region	Target Sequence
Sox1	NM_001095674.1	1663-1763	CTGTGCTCATCCTTTTAGAGACAATGCGTCCAGCCTGCTCATCAAGGATCGGGCAGCACACTTGCCTCCACTTTGCCACAACTGCCCTCTCTTTTTCTTT
Sox2	NM_001088222.1	901-1001	CCGGGCATGTCTCTGGGATCCATGGGCTCGGTAGTCAAGTCGGAATCCAGCTCCAGTCCACCTGTAGTCACCTCTTCTTCCCATTCGCGGGCTCCGTGCC
Sox3	NM_001090679.1	998-1098	GCTCACTCACATATAACACTTTGTGCCCTTTGCTAAAGACGCTTTACTTGCCTGCTGGCAACTATCAGACTGCCGCATAAAACATTTAAAAAAAAAAATC
SoxD	NM_001087732.1	684-784	CCCTGGAAGTGGAGGGAACCTCTTTCACGGACCTCTGACCCCTGTGACTGAATGGGACATTCCGAGGGTCTCCGCTCTACTGACTTGAGAATCTAGGGGA
NCAMa/b	NM_001087827.1	44-144	CATCTGGACTTTATATTTCATAGGAACTGCAGTGGCGTTGGAAGTGAACATTGTTCCAGATCAAGGAGAAATAAGCCTTGGGGAGTCCAAATTCTTCCTG
Ngn1	DC113851.1	121-221	CCGACTATGACACCTGCAGCCAGATGTCCTATTCCTCTTCAGATGATGAGGACTCCTTCAGCATGCAGTCTTCTTCTCCCTTCTCCTCTGGACACATGAC
Ngnr-1a (Ngn2a)	NM_001088333.1	274-374	TGGGTTATTATAGTAAGTGGATGTGAAGTTGTCAGTGCAACATTGGGGCTAACCATTGGCTGTGTGTTTGCGCTTGTCTAGGATGGTGCTGCTCAAGTGC
Nrgn-1b (Ngn2-b)	NM_001088335.1	1172-1272	CATCGTTAGCTATGTGTATTAGGAAACTGTCTATCCCTCATCTGCACCTGTTAGACTACAGCTACCAACTTCCTGTTACCAGGGGGCTACTGGGTAATGT
Ngn3	NM_001134785.1	216-316	AAAGAAGCAAAGGGTCAAGCGAATGAGATCAAAAGTAAAGAGCGACGGCGTCGTCGTAAAACAGAGGAGAAATCGCAGGGTGAAAGCCAATGACAGAGAG
Ascl1/Xash1	NM_001085778.1	142-242	CTCCTCCTGCCCAGCAGCCTGTCAGCATGGACAACTGCGTCGCTGCCAAGATCATGGACAGCAACTTATCCAGCCAGCAGCAGCATTTCCTACAGCCCCA
Mxi1	NM_001095701.1	2418-2518	GCTGCTGCAGGTCATTATCATTCTGCAATCTGTGTTTGGGTGGACTTCCCCTTTAATCTGTTACAAACCAGAAATGACACATCCCAGAATCCTCAGCTCC
NeuroD1a/b	NM_001085794.1	370-470	GCCCTGGACAGTCTGCGCAAAGTTGTGCCCTGCTACTCCAAAACACAAAAGTTGTCTAAGATTGAAACTCTGCGCCTGGCTAAGAACTACATCTGGGCTC
NeuroD4 (Xath3)	NM_001087744.1	665-765	AGTAATGGATCCTTCTGTGGTAACCCATACACTTAACTGTACCACTCCACCATATGAAGGAGCTCTAACACCTCCACTCAGCATCGGTGGTAATTTTTCT
NeuroD6 (Xath2)	NM_001085749.1	732-832	TACAAGATCCCCATATACTTCTGTTTACCCACCTTATCACAGTCCTGAGCTTAGTACCCCTCCAAGTCACGGGACCCTTGATAATTCCAAAACCATGAAA
MyT1	NM_001088192.1	684-784	GAGCTAAACAATGAAAAGCCAACTTCAGTAAAGTCGGGTCAAGCGGAAATAGAACAACTTATGGTAGAAGAGGCGTGTGAGAAAGAAATCATCATCCAGA
Ebf2-a/b	NM_001085677.1	1085-1185	CATACAAATCCAAACAGTTCTGCAAAGGAGCCCCAGGGAGGTTTATTTACACAGCTTTAAATGAGCCTACAATTGATTATGGATTCCAGAGGCTGCAAAA
Ebf3 (Coe3)	NM_001090332.1	1998-2098	ATGGGAGTAAACTCTTTCAGCAGCCAGCTAGCAGTTAATGTTTCAGAGACCTCTCAAGCTAATGACCAAGTAGGTTACAGTCGCAACACAAGCAGTGTTT
RBM38/Seb4R	NM_001089144.1	1053-1153	GTAAGAAAATGCTGCAGTCAAGTTCTGTGGATCCCAGCTTTCAGTTCTGTTTCAGGCAATATCAAGGTCATGGATTTCTTTGGCGGATTCCAGGCAAGAG
Pak3	NM_001085763.1	2397-2497	GCATTTGAGTGGAAAGAGGCCCATTTGTTGCTGAACGATCCTGGCACCTTGTGCTTTGCTTTCCTGGCAGTGAAGAGGTTAGCAGCCTGAATCTATGGCA
Cdknx (p27Xic1)	NM_001114803.1	1076-1176	TTAACCGTGAAACAGCTTGAATCTATTGCTCAGGGATGAACTACCTATGGCTCTCCAGATGTCGTTGAATTACAGCTCCCAACGGAGTCGTGGCTCAGCA
Nrp1	NM_001087911.1	1655-1755	GGAATACTGACGCAACTGATGTAGTCTACCGGCCATTCTCTAAACCTGTTATCACTCGCTTTGTTAGACTCCGTCCGGTTACATGGGAAAATGGAATATC
tubb2b (N-tubulin)	NM_001086064.1	900-1000	TGCACTTTTTTATGCCAGGCTTTGCCCCATTAACAAGTCGTGGCAGCCAACAATACCGAGCCCTGACAGTGCCAGAACTAACACAGCAAATGTTTGATTC
Pax2-a	NM_001086361.1	1494-1594	GAGTGGCCTACTCTGCTTTCCCTACTGACGTTTCTCAGCTGTAATAAGCTGCTCTTACCTCTGCTGCAAGCCTCTTTGTTGTTATTGTGCACGGTAGCTA
Twist	NM_001085883.1	619-719	AGGGAGCCTGGTCCATGTCTGCATCTCACTAACAGCAATGCCACTACAGCTCAGGCCACACACAAAGATTATACTTATACCAATGAATGGGAAAAAAAAAC
Hb9/mnx1	NM_001096823.1	1727-1827	GTTACACAGGCTACTGGGAGTCCCCTACTTTTGTGTTGACACCATCATAAGAAAACCCGCTGGGCACCTGAAGGCTACACTATAGGCTGTCTTTATTTTT
Hox11L2/Tlx3	NM_001085746.1	186-286	TCGTGTCTCTCCGCTAATTTCCCCGCCGGCATCGGGGCCACGTTTGATGAGTCGGGATGTTACAGTGTCAATGTGAGTCTGGCTCCTGCCGGAGTGATTA
Hpx6 (Lbx1)	NM_001095723.1	30-130	GCGTCCTCGGTGGAGGAAAGAAGAAGGAATGCCTTGGACCTTTTACCACCTCCTGCTAATTCTAACAAGCCCCTGACTCCTTTCAGCATTGAGGATATCC
Lhx1 (Lim1)	NM_001090659.1	21-121	TCTATTCTCCTAATCCGCCCATTCCTCTAAAATCCCAAATAACCAAAGGCAATGGTTCACTGTGCTGGATGCGAAAGGCCCATTCTGGACCGTTTCTTGT
Lhx2	AJ311712.1	264-364	GTATACTGCCGGCTCCACTTTGAGACTTTGATACAGGGAGAATACCAAGTTCATTTCGGTCACTCGGATGTAGCATCAAGGAAGGGCTCAGGGGCTACCT
Lhx5	NM_001090569.1	440-540	CCAGGGACATTTGCGTACAAGGCCCGCTGGGACTCAAGTTATATTTGGGTCTTTGGTTGGGGAGTCTATGAGGATTTCACTGGACTTGGCTTCTGCTGCA
Lmx1b	NM_001090433.1	688-788	AGGACAATCCTCACAACCCAACAAAGAAGGGCGTTCAAAGCATCTTTTGAGGTTTCATCGAAACCCTGTAGGAAGGTCAGAGAGACATTAGCTGCTGAAA
runx1 (Xaml)	NM_001086497.1	1150-1250	CTGACAGCGTTCAGTGATCCTCGAGTTGGCATTGACCGACAGTTCTCCACTCTTCCTTCCATCTCTGATCCACGTATGCACTACCCAGGGGCTTTTACCT
Olig3	AF035446.1	112-212	ACTGTCTCTTGAGACCCCTGAGCATAACTATTGACTCCTGGGAGCGATCACTGACTGCCAGCTGTTGCGACTTGCCCATTTAAAAGTGCATTTACTCACC
FoxD3a (XfD6)	NM_001085557.1	91-191	GCAGCAAGTTCACTACTACTTGCCCTACCGAGCCTCTCTCTATTTCTCTTCTCTGCCCATCGCTGTGGAGCGTAACTGGAATGACCCTGTCAGGCAGCGG
vGlut1	NM_001089635.1	2177-2277	AGTGAATTGAGTTAGATGTACACATTACTGCGTGATTCCCAGGGATACGGTGTAGAAAATATCCATGAGGATGGGGCATGATCAATTCTACATCACTTGG
Gad1	NM_001085801.1	794-894	GGCAGCAGTCCCCAGATTGGTCCTGTTTACTTCAGAACACAGCCACTATTCCATAAAGAAAACTGGCGCGGCATTAGGATTTGGAAGTGAAAATGTGATC
Krox20/egr2	NM_001085779.1	273-373	AGGAGATGGAATGATCAGTGTGGATATGAATAATGACAAGCGGTCGCTGGATTTCTCCTACTCGTCCAACTACCCCTTGGCCCCTAGGACTCAGCCGATC
Eng1-a/b	D14693.1	122-222	CCCTGTGCACAAGAAAGACTCTGTGGTGTGGCCCGCCTGGGTCTATTGCACTCGCTACTCCGACCGACCCTCCTCTGGCCCTAGGACCCGCAAGCTAAAA
Islet1 (isl1)	NM_001110718.1	1102-1202	TACAGAGTGACATTGATCAGCCGGCCTTCCAGCAACTGACCTGTTTCTCACAGGTTAATTTTTCAGAAGGAGGACCTGGCTCTAACTCTACAGGGAGTGA
Insm1	NM_001110719.1	2177-2277	CAAATGACTGTGTCCGCCCATGAGTCGCTTCTACAATGAGATAAATGTATATTGCCCAGTTGCCATCCACTCACTGTTACAGCATTTGTGATGCCCTGAC
Nkx6.1	NM_001099916.1	172-272	AATACATCATTCCCTCTGCAGCTTGAACTGATTTAAACCTCGGCCATCCAACACTACAGCCCAGCGTCGGTAGGATATAGTGATTCACCCTTGGAGTTGT
Nkx6.2	NM_001096886.1	28-128	TGTTTGTCGCCGCTGCATGTGTGGGATCATTACTGCCCTGAAACTTGCGCTGATCGCCGGGAAGTTGCGACAGAAGCCGTTTGCCTCGGGGACTTCTCTC
Pax3	NM_001095524.1	532-632	AAAAGAGACAACCCGGGTATGTTCAGCTGGGAAATTCGCGATAAATTACTTAAAGACGGAGTTTGTGATCGCAATACTGTGCCTTCAGTAAGCTCCATCA
Pax6-a	NM_001085	1551-1651	CTGCCCACAAGTCCATCTGTGAATGGGCGGAGCTATGACACATACACACCTCCCCACATGCAGACACATATGAAC

	944.1		AGCCAGCCAATGGGCACATCTGGCA
Pax6-b	NM_001172195.1	1339-1439	CTTACAGTGCTTTGCCACCTATGCCTAGTTTTACGATGGGCAACAATCTACCTATGCAAGTCTCATTTCCCCTGGAGTGTCAGTCCCAGTTCAAGTACCC
c-myc	NM_001085896.1	523-623	TCTGTCTTCTTCTTCTCCGTGTCCGAGTCAACCACCACCGAGCCCGCTTAAGTCTCCCTCGTGTCATGGGAGCCTGAGTCTGGGAGGGACCCACAGGAGC
Slug	NM_001086880.1	87-187	GGACACTCACTGAGCAAGGACTGGGCGCATTCACTCCACTGTAATTACGGCAAGTGACAAGGGAAGAGGCTGCGAGTATAACACTGCGGGGCCGCTCACT
RBPJ	NM_001090878.1	1537-1637	ACATTTCCGCATTTCGAGAAGGTTGGAGATGGGTTCGTCAGCCAGTGCAAGTGCCTGTTACGTTGGTCCGAAACGACGGTGTAATCTATTCAACCAGCCT
Notch1	NM_001087605.1	468-568	ACTGGGGTGTGCCTATGCGGTAATTTGTATTTCGGTGAAAGGTGCCAGTTCCCCAATCCCTGCACCATAAAGAATCAGTGTATGAACTTTGGAACCTGCG
Dll1 (Delta1)	BC070634.1	628-728	CTGAAGTACTCCTACCGATTTGTGTGTGATGAATACTACTATGGGGAGGGCTGCTCTGACTACTGCCGCCCCAGAGATGATGCTTTCGGCCATTTTTCCT
Delta2	U70843.1	1537-1637	TCTAACTGTGAAAAGAAGATTGATCGCTGTACCAACAGTCCCTGTCTGAATGGAGGTCAATGTCTAGATATGGGCCGAAATGTTTTGTGCAAGTGTCGCC
Jagged1 (Serrate-1)	NM_001090307.1	136-236	GTGCATTCAGGATCGGCGTGCCCTACAACAAGAGCCTTGAAAAGTGTGTGTTGTGTTGCAGTCGTGCATGCTCAAATCGCCTGAGTATATCAGAGGTGCG
Hes5.1 (ESR1)	NM_001095627.1	326-426	CAGAAAATGGAGAAACCCAGATGAAACTGCTTAATCACCTGCAAGCACCCCAAAGGCTCTCAGTTGCCCCTCACACCTATATCCCCAGTGTTTCTGACTC
ESR6e (Hes3.1)	NM_001088503.1	267-367	GCTTTCTGCATACCCAGGAGCACGGACACATTCAAGAAGGAAATAAAAATCTACCGTGGACTGATTCTTGCCTCCCTGCACCCTCTCAAAAATTCTACCA
ESR9.1a	NM_001088237.1	556-656	GATATCCTGCAGACTGGTGGCTTACCTGATGGTTTATTATGACTATGTAATAGAATAACTGGTTACTGTAATGGTGCAACACCAAAGCTATTTTGTAGCT
ESR10	AJ009285.1	824-924	TTGCTTGGGTATAAATGTATTATGGGCTCACATAGGGGAGTCAGAAGTACATGCTGTGTATTGCCACACATTGCGGCATATTTGGGCCTCTCAGAGTCTG
Hes6.1	BC130161.1	1166-1266	TCCTGGCTTTCAGCCATCTAAAGATTGTTGGGATACAACTCTCGCTAACTAGAATGACAAGTTACACTTCAGTAACAGTTTGAGGGCCATGTATCTCTCC
Hes2	NM_001122882.1	799-899	AGTGACCCACATTGTGAACCCAAAGGGTTTAATCTAGTATGCGATTTGCATTATTTTACATTAACCCATGGACTGCCAGAGATGGCCAATGCTACAGTCT
Hes1a(Hairy1)	NM_001087927.1	557-657	GAAGGGGTCAACACAGATGTCCGGACCCGACTCCTGGGGCATCTTGCCAACTGCATGAACCAGATCAATGGCATGAACTACCCTACCCAGCCCCAGATGC
Hes7 (XHR1)	NM_001088706.1	490-590	CGCATTTAGTGTCCAACAGCATCTCCATCAGCCCTACAAAGACTCTGGTTGACAGTCATTTCACTTACCAAACCTTCAAGACCTGGAGACCCTGGGTATG
Xbra-a/b	NM_001090578.1	534-634	AGCCCACTGGATGAAAGATCCTGTCTCTTTTAGCAAAGTCAAACTTACAAACAAAATGAATGGTGGAGGCCAGATTATGTTAAACTCTTTGCACAAGTAT
Arx-a	NM_001085860.1	246-346	GCGCCCACAGCATTCCTTCCCTTGCACATCGGCTAGATCCGGACAAAACTTTGGAAGGGTCCCCTAAGGGCAATGCTCCATTTGAAGGGGATTTGCACCT
PRDM14		650-750	CTGACAGTGCTGGACACTTCCTATGGGACTTTGCCCAAATCTGGAGTTTTCTGCAAGAACCTCATCCCTAAAGGAGCCAAGTTCGGTCCATTTCAAGGCA
Ptf1a-a/b	AY372268.3	149-249	CATTCCTCTAGGGACGCCCTGGACGCAGACGACTTTTTGGAAGACGATGTAGACTTCTTGGCCGGTCAGATCCAAGACTATTACAGAGACAGCCGAGTGC
FGF8	NM_001090435.1	47-147	CTCCGAGCCTCTCAGTCAGCTTCTAGTGTTATTGGCCGGTGGGGTCGGCGCTGCTGGTGCAGACAAGAAGCAAGTCTTACTCATCAACACTTTCATCATC
Numb	BE189039.2	360-460	ACCATGCAATACTGCGCGTCCATTTTCGGTAAAAGTAGAACAGAGACATTTCTCGTGGTTGTGATTGTTTAAAGCAATGTGCTACATACAAGGAAGGTGG
Numbl	GQ214766.1	625-725	AGGCGATGGATCTGTCACTGCTTCATGACTGTTAAAGATACGGGAGAGAGGCTCAGCCATGCTGTTGGATGTGCATTTGCCGCTTGTCTGGAGAGGAAGC
actc1	NM_001086591.1	1126-1226	CTCCATTGTGCACAGGAAGTGCTTCTAAACATTACACACACTCCTCCAAGCAACATATACAGAGTACCTCAAAGTCAAAGAAAACAAGACCTGGACAGTC
ODC	NM_001086698.1	855-955	GGATATAATTGGTGTGAGTTTCCATGTTGGCAGTGGCTGCACTGATCCACAGACTTATGTACAAGCTGTCTCAGATGCACGATGTGTCTTTGACATGGGG
H4	NM_001094457.1	655-755	CCACGCCCCTTCTCCCCATAAAATCAGTTACAGGCTCTCGGGCTCTTTTGCTCTTGCCGGATGGAAATTACTGTTGCTGCTCAGCGTCTCACAGAACTCC
gapdh	NM_001087098.1	773-873	ACCTGCCGCCTGCAGAAGCCGGCCAAGTACGATGACATCAAGGCCGCCATTAAGACTGCATCAGAGGGCCCAATGAAGGGAATCCTGGGATACACACAAG
actb	NM_001088953.1	1179-1279	ATGCTTCTAAAGGACAGACCCTTTCAACATGAACAAATGTACCTGTGCAGGAAGATCACATTGGCATGGCTTTACTCTTTTGTTGGCGCTTGGCTCAGAA
g6pd	NM_001086550.1	862-962	GTGGAGGATACTTTGACGAATTTGGCATCATCCGGGATGTCATGCAAAATCACTTGCTCCAAATGATGTGTTTGATGGCTATGGAGAAGCCGGTCTCCAC
HNF6 gene 2	DC109227.1	141-241	TGTGTCCCAGTTGGCAATGTTATTGGAAGCTTTACTCTTATGAGAGAGGACAGAGGTTTGGGGCCACCAAGTAACTTTTACAGTCACTATCCCAAAGACA
Pdia2 (XPDip)	NM_001090179.1	881-981	TGCTGCCCAGATCCCAAACCACTTGTTGCTGTTTATCAATAAGAGTGACGATTCCCAACTGGTGCTGCTGGAACATTTCCGCAAAGCAGCTCCTGACTTT
Sox9-a/b	NM_001090807.1	441-541	GAAGTTCCCCGTGTGCATCAGAGAAGCGGTCAGCCAGGTGTTGAAGGGATATGATTGGACCCTGGTACCGATGCCAGTCAGAGTTAATGGATCCAGCAAG
Hmx3	NM_001085757.1	356-456	TTAAAGGGGCCCTGGACGGAGCAGCGTTTGCCTTCTCCCCGCTGACAGATTTCACCTTCCCTCGGCTAGAGATCCCGACTCAAAGGTTCGCCCTCCCGGC
Barhl2	NM_001088552.1	1164-1264	CCCGGTGAAACACTATCTATTTACCGAAGCAGCACAGAGTCACCATTGCAGTAATCCAAAAAAAAGGACATCAGAACCGGAGACAGATGAGCTTAGTGAT
Mecom	NM_001095670.1	3934-4034	TATTGTGAATCTTGCAATGTCCAGCGCTCAACAAGAGGTGAAGTCATTAAAGGGCCATTTGAATCACTGATACCACTAATATGTCTTACAGTTCAATGTT
Kirrel2	NM_001086488.1	690-790	CCCAGTCGCCAATGTCCTGCTTGATGTACCCTACAATCTCACCTGTCTTGCTTCCGTCGCTAAGCCTGCTGCAGAGATTACCTGGTTCCGTGATGGAAAG
Cpa1	NM_001095030.1	517-617	CCCAACCGTCCAGCTTTTTGGATTGACACTGGTATCCATTCCCGTGAGTGGGTCACTCAGGCCAGCGGTATCTGGTTTGCCAAGAAGATTGCAACAGATT
PRDM13	BJ064589.1	452-552	TCAGGTCTGCTTTTAAACCAGCTGGACTATCCAAATTACCCAATACTGATTCAGTCAGAGAGGACTCAAAGGCCACCAGTATGGGATTCAGCAAACTTTT
Ptf1a-a/b 5'UTR	NM_001174020.1	4-104	CGAGGAACCGCGGGACCCACTCAGCGCAGTCACCAGGGGGCAGACACCATGGAAACGGTCCTGGAGCAGTTGGCGGGGGCTCGAGTCCTTCCCTTCCCCGT
Ascl1/Xash1 new	NM_001085778.1	630-730	ACCATCTCCCCCAACTATTCCCACGATATGAACTCTATGGCGGGCTCCCCCGTCTCCTCGTACTCCTCAGATGAAGGCTCCTATGATCCGCTGAGCCCGG
RBPJ 3'UTR	NM_001090878.1	2034-2134	TTACAAAAATGCGCAAAAAATAGAAAATGTGGCTTGGGCTGAAACCTTCAGCAAGCTAGAGAAGCATGAAGATAACATAGTTTTTACGGACCAAGGAACT
H4 new	NM_001094457.1	129-229	GGAGAGGGGGAGTCAAGCGCATCTCTGGCCTCATCTATGAGGAGACTCGTGGGGTCCTCAAGGTTTTCCTGGAGAATGTCATCCGGGACGCCGTCACCTA

6.4 Comparison of genes identified by RNA-sequencing with related publications

Table 6.18 Comparison of direct Ptf1a and Ptf1a/Su(H) target genes with Ptf1a target genes identified in the adult mouse pancreas by ChIP-sequencing (Masui et al., 2010)

symbol	Ptf1a-GR vs CC	Ptf1a-GR + SuH-GR vs CC
aldh1b1	703,6	330,9
rpl37	2,9	-
rps19	2,4	-
slc26a2	-	37,9
agrn	-	5,0
swap70	-	3,7
vamp5	-	2,9
nfe2l1	-	2,6
zswim4	-	2,1

Table 6.19 Comparison of direct Ptf1a and Ptf1a/Su(H) target genes with direct Ptf1a target genes identified in the 2-666 pancreatic progenitor cells by ChIP-sequencing (Thompson et al., 2012)

symbol	Ptf1a-GR vs CC	Ptf1a-GR + SuH-GR vs CC
neurod4	39,7	113,5
nr5a2	31,3	72,2
gfi1	19,2	80,9
zc3h12a	17,4	13,9
hes3.3	9,2	15,9
des.1	8,2	5,9
cbfa2t2	7,0	10,0
dll1	6,7	7,4
cox4i2	6,1	5,9
gas6	5,5	3,9
g0s2	5,2	2,2
arl4a	4,5	3,4
hes3.1	3,5	4,5
pou2f3	3,2	3,8
cpa1	-	65,9
atoh8	-	58,5
slc8a2	-	25,0
cdh15	-	24,0
chad	-	16,8
pik3r5	-	14,6
fat4	-	11,8
fjx1	-	10,9
wdr86	-	8,3
ampd3	-	6,3
Rpl30	2,4	-
matn4	-	6,0
gpx3	-	5,8
mn1	-	5,2
mgat3	-	4,8
slit1	-	4,8
nrap	-	4,8
adcy9	-	4,5
cldn5	-	4,3
vash2	-	3,5
kirrel2	-	3,5
slc16a12	-	2,7
sh3rf1	-	2,3
tacc1	-	2,3
pitpnm2	-	2,2

Table 6.20 Comparison of direct Ptf1a target genes with direct Ngn2 target genes identified in animal caps by Affymetrix Microarray analysis (Seo et al., 2007)

symbol	Ptf1a-GR vs CC	Ptf1a-GR + SuH-GR vs CC
dpysl3	15,0	12,0
hes3.3	9,2	15,9
Xl.58208	6,0	8,0
tmem56.2	4,4	-
rbm24	3,4	3,7
tiparp	2,9	4,1
Xl.18615	-	4,6
mafb	-	3,5
mxra7	127,3	147,3
neurod4	39,7	113,5
twist1	19,7	39,0
znf238	11,5	20,3
ebf2	8,9	23,1
cbfa2t2	7,0	10,0
Xl.76708	6,7	7,8
myt1	5,9	10,6
amotl2	5,5	5,2
snai1	4,3	30,3
plk3	3,7	6,0
Xl.71723	3,6	3,1
snrk	3,4	2,6
fstl1	-	11,2
ascl1	-	4,1
zeb2	-	2,7
hes6.1	-	2,7

Table 6.21 Comparison of direct Ptf1a/Su(H) target genes with identified genes downstream of Ptf1a in endodermal explants (Bilogan and Horb, 2012)

	symbol	Ptf1aGR + SuH-GR vs CC
NF32	Xl.72042	4,5
	hes5.1	3,7
	crmp1	3,4
	des.1	2,6
NF36	vcan	3,4
	atp6v0d2	2,6
	sox9	2,4
	unknown	1,6
	myh6	1,6
	cebpd	1,5
	hes4	1,0
NF32/NF36	cpa1	6,0
	il1b	5,2
	thbs3	4,6
	ebf2	4,5
	dpysl3	3,6
	hey1	3,5
	hes5.2	2,3
	cldn5	2,1

6.5 Primary transcriptome sequencing data

The primary sequencing data are provided on CD “Appendix 6.5" attached to the thesis.

Table 6.22 Candidates_Ngn2-GR_6h_Dex_vs_Cc_6h_Dex

Table 6.23 Candidates_Ngn2-GR_25h_Dex_vs_Cc_25h_Dex

Table 6.24 Candidates_Ptf1a-GR_6h_Dex_vs_Cc_6h_Dex

Table 6.25 Candidates_Ptf1a-GR_25h_Dex_vs_Cc_25h_Dex

Table 6.26 Candidates_Ptf1aW224A_W242A-GR_25h_Dex_vs_Cc_25h_Dex

Table 6.27 Candidates_Ptf1aW224A_W242A-GR_6h_Dex_vs_Cc_6h_Dex

Table 6.28 VennView_Comparison of downstream targets of Ptf1a, Ngn2 and Ptf1aW224A_W242A after 6 and 25 h

Table 6.29 Candidates_Ptf1a_vs_CC_CHX_Dex

Table 6.30 Candidates_SuH_vs_CC_CHX_Dex

Table 6.31 Candidates_Ptf1a_SuH_vs_CC_CHX_Dex

Table 6.32 VennView_Comparison of identified direct target genes for Ptf1a and Su(H) alone as well as in combination

Table 6.33 VennView_Comparison of downstream genes of Ptf1a and Ptf1aW224A_W242A after 6 and 25 h and genes identified as direct targets of Ptf1a alone and with Su(H) in combination